ADVANCED MODULATION FORMATS FOR HIGH-BIT-RATE OPTICAL NETWORKS

A Dissertation
Presented to
The Academic Faculty

By

Muhammad Haris

In Partial Fulfillment
of the Requirements for the Degree
Doctor of Philosophy
in
Electrical and Computer Engineering

School of Electrical and computer Engineering
Georgia Institute of Technology
August, 2008

ADVANCED MODULATION FORMATS FOR HIGH-BIT-RATE OPTICAL NETWORKS

Approved by:

Dr. Gee-Kung Chang, Advisor
Professor, School of ECE
Georgia Institute of Technology

Dr. Jianjun Yu, Co-Advisor
NEC Labs, USA
Princeton, NJ

Dr. Chuanyi Ji
Associate Professor, School of ECE
Georgia Institute of Technology

Dr. Stephen E Ralph
Associate Professor, School of ECE
Georgia Institute of Technology

Dr. Yucel Altunbasak
Associate Professor, School of ECE
Georgia Institute of Technology

Dr. Jun Xu
Associate Professor, College of Computing
Georgia Institute of Technology

Date Approved: April 23, 2008

To

My parents Rashid and Nargis

and

My wife Atiqa, son Ahmed and daughter Hania

ACKNOWLEDGMENTS

First, I thank God, the most merciful and compassionate, for giving me wisdom and strength to complete this PhD dissertation.

My deepest appreciation goes to my advisor, Dr. Gee-Kung Chang. I am grateful for his guidance through out my research at Georgia Tech. I could not have imagined having a better advisor and mentor for my Ph.D. Without his support and encouragement, I would never have finished. My co-advisor Dr. Jianjun Yu, who has a great part in shaping my research work and helped me tremendously at every step forward. He has been a source of inspiration for me. I also thank Prof. Chang and Dr. Yu for carefully going through my publication drafts, correcting my presentations, and helping me learn the various skills of academic research. I also thank my committee members Dr. Chuanyi Ji, Dr. Stephen E Ralph, Dr. Yucel Altunbasak and Dr. Jun Xu for their time and insightful comments.

I was fortunate to work with number of people in Optical Networking and Research Group (ONRG) under the supervision of Prof. Gee-Kung Chang. They all helped me, encouraged me and motivated me in one way or another. Thanks to Arshad, Yong-keo, YJ, Zhenseng, DJ, David, Jerome, Chunpeng, Claudio, Yvonne and Money. Finally, I want to thank my family for their full support.

TABLE OF CONTENTS

LIST OF TABLES

LIST OF FIGURES

SUMMARY

The objective of the proposed research is to investigate the performance of advanced modulation formats, specifically modified duobinary return-to zero (MD-RZ) modulation scheme and its long-haul repeaterless transmission over standard single mode fiber (SMF). This research also focuses on phase modulation formats like differential phase shift keying (DPSK) and differential quadrature phase shift keying (DQPSK), specifically free spectral range (FSR) optimization and wavelength offset tolerance in direct detection of these phase modulated systems. Transmission of duobinary modulated signals over SMF has attracted significant attention due to a multitude of factors including high tolerance to chromatic dispersion (CD), ease of implementation, and improved spectral efficiency. These are the key performance indices of an optimal modulation technique, that enables the realization of next generation high data-rate dense wavelength division multiplexed (DWDM) transmission networks. Moreover, repeaterless transmission over SMF is an effective way of reducing network operation and maintenance cost and simplifying system configuration.

In this research we present a novel and cost effective technique to generate a modified duobinary return-to-zero (MD-RZ) signal. This novel technique employs only one dual arm Mach-Zehnder (MZ) modulator, which simplifies the design of MD-RZ transmitter even more as compared to conventional techniques using at least two intensity modulators. Furthermore, an MD-RZ signal with different duty-ratio can be obtained effectively by varying delay between two arms of this MZ modulator. Next, we attained experimental results for single channel 10 Gb/s repeaterless transmission over 300 km of SMF and 8x10 Gb/s WDM repeaterless transmission over 240 km of SMF using these

MD-RZ signals. A numerical comparison is also drawn with other conventional MD-RZ transmitters. MD-RZ transmission characteristics are also studied numerically for 40 Gb/s WDM signals and compared with other two leading constant intensity phase modulated formats, differential phase shift keying (DPSK) and differential quadrature phase shift keying (DQPSK).

We also have presented experimental results for FSR optimization of DQPSK de-modulator for ultra-high data-rate systems in the presence of strong optical filtering. Choice of an optimal FSR beyond 1-bit delay in Mach-Zehnder delay interferometer (MZ-DI) helps relieving some of the degradations due to strong optical filtering. Wavelength offset tolerance is also experimentally measured and numerically investigated for DPSK and DQPSK modulation formats with different transmitter schemes employing intensity or phase modulators to achieve required phase shifts.

CHAPTER 1

INTRODUCTION

The bandwidth-distance product is a key figure-of-merit of lightwave systems. To increase the capacity of lightwave systems, increase in data-rate per channel and tighter channel spacing in dense wavelength division multiplexed (DWDM) systems are the possible solutions. In next-generation lightwave systems, a 40 Gb/s and higher data- rate DWDM systems is inevitable. In such high-speed DWDM systems, linear and nonlinear impairments become worse. These linear impairments include chromatic dispersion (CD) and polarization mode dispersion (PMD); nonlinear impairments include self phase modulation (SPM), cross phase modulation (XPM) and four-wave mixing (FWM).

To minimize both the linear and the nonlinear impairments over the transmission fiber, an optimal modulation format is needed. A modulation format with a narrow optical spectrum can enhance spectral efficiency and tolerate more CD distortion. A modulation format with constant optical power can be less susceptible to SPM and XPM; modulation format with multiple signal levels will carry more information than binary signals and its longer symbol duration will reduce the distortion induced by CD and PMD 0. In addition, in long-haul networks, amplified spontaneous emission (ASE) noise produced by erbium-doped fiber amplifiers (EDFAs) is another factor that requires modulation formats more tolerant to additive ASE noise. These advanced modulation schemes with other key technologies, like low noise optical amplifiers, new advanced optical fibers and forward error correction techniques, are crucial to realize high spectral efficient, high-capacity optical transport networks.

Consequently, on-off keying (OOK), which has been used for a long time in lightwave systems, is no longer an optimal modulation format in the next generation of optical networks. Many optical modulation formats have been considered in the scope of this research. The optical duobinary modulation format turns out to be one of the leading choices in this case, since it has high tolerance to chromatic dispersion (CD), better non-linear tolerance and can go through narrowband optical filtering to put more channels close to each other to improve spectral efficiency. Furthermore, it is easy to implement, since there is a minor change in the transmitter and we can still use the photo diode at the receiver side for direct detection. The overall system setup is simpler compared to other competing formats, like differential phase shift keying (DPSK), and differential quadrature phase shift keying (DQPSK), which require modifications at the transmitter and at the receiver, further increasing system cost and complexity. On the other hand, these constant intensity formats like DPSK and DQPSK, despite their relatively complex transmitter and receiver setups, have proved to be strong candidates for high data-rate and spectral efficient DWDM systems [2]-[4]. These constant intensity formats have inherent 3-dB better receiver sensitivity by using balanced detection. They also reduce the effects of self phase modulation (SPM) and cross phase modulation (XPM) resulting in reduction of signal distortion that accumulates in the optical signal over the fiber link [5].

Chapter two introduces the basic notions of optical fiber communications from the propagation in optical fibers and then lists all the important optical modulation formats. It briefly summarizes the generation and characteristics of various intensity and phase modulated advanced formats. Chapter three focuses our research on intensity modulated systems. In particular, it introduces a novel, cost-effective and simple modified duobinary

return-to-zero (MD-RZ) transmitter setup. This scheme employs only one dual arm Mach-Zehnder (MZ) modulator, compared to at least two intensity modulators used in other schemes. It reduces the transmitter cost and simplifies the overall system architecture. Repeaterless transmission is an effective way to reduce network cost, especially in large metropolitan and long-haul networks where cost is the most critical parameter. Compared to repeated transmission, repeaterless transmission is mostly limited by optical signal-to-noise ratio (OSNR), fiber nonlinearity and fiber dispersion, as well as total gain in the presence of large span loss. We also have demonstrated some experimental results of 10 Gb/s MD-RZ repeaterless transmission over 300 km of single-mode fiber (SMF) and 8x10 Gb/s WDM repeaterless transmission over 240 km of SMF. This novel scheme is further numerically compared with other conventional MD-RZ generation techniques. The transmission performance of MD-RZ transmitter is also compared with DPSK and DQPSK in high data-rate DWDM systems.

Chapter four presents our research results on high-speed phase modulated systems. In the deployment of high spectral-efficient WDM transmission systems, because of narrow band filtering, design of Mach-Zehnder delay interferometer (MZ-DI) in DPSK or DQPSK decoder becomes very important, since choice of optimal free spectral range (FSR) helps us relieve some degradation due to strong optical filtering. In this chapter we present impact of tuning FSR in the presence of strong optical filtering for 100 Gb/s and 50 Gb/s DQPSK signals via experimental and simulation results. Both return-to-zero (RZ) and non-return-to-zero (NRZ) pulse shaping is employed in DQPSK transmitter. We also present wavelength offset tolerance for high-data rate DPSK and DQPSK modulation formats. Any wavelength offset between optical source and MZ-DI will result

in non-optimal interference at its output ports and can cause severe system degradations and receiver power penalties. Phase modulation can be achieved either by using a straight-line phase modulator (PM) or by using a Mach-Zehnder (MZ) intensity modulator (IM). In differential quadrature phase shift keying (DQPSK) transmitters, the phase shifts of π and $\pi/2$ can be achieved by cascading phase modulators or MZ modulators in any combination and sequence. While DPSK signal by a PM has an inherent chirp, MZ modulator can generate chirp-free DPSK signal with perfect π phase shift, since it modulates the phase along the real axis of the complex optical field. It has been verified with experimental results that using an MZ modulator as a phase modulator is useful in imperfect conditions such as low driving voltage, since it only affects residual intensity dips leaving perfect π phase shift intact. In this chapter we measured wavelength offset penalties by simulations and we also performed experiments for DPSK and DQPSK signals when phase and intensity modulators are interchanged.

CHAPTER 2

ORIGIN AND HISTORY OF PROBLEM

The main focus of this chapter is to introduce optical communication systems including basic optical elements, transmission impairments in optical fiber then, summarizing principles of various modulation formats and their characteristics in the scope of this research. A good understanding of optical communication systems and technologies can be found in [6], in addition to some good fundamental textbooks [7] - [9].

2.1 Modulator Technologies

Three basic technologies to modulate the light are commonly used today: directly modulated lasers (DML), electroabsorption modulators (EAM) and mach-zehnder modulators (MZM). A new and innovative way to use these existing modulator technologies usually gives rise to a novel optical modulation format. These modulator technologies can be used with modulation formats to find a novel and cost effective modulation technique in order to resolve the future needs of high spectral efficient and high bit-rate optical DWDM networks.

2.1.1 Directly Modulated Lasers (DMLs)

Direct modulation of lasers is the easiest way to impose data on an optical carrier. The transmitted data is modulated onto the laser drive current, which then switches on and off the light emerging from the laser. This resulting modulation format is binary intensity modulation [2]. Directly Modulated Lasers are widely available up to modulation rates of 2.5 Gb/s, with some limited availability up to 10 Gb/s. In some research demonstrations, up to 40 Gb/s data rates have also been achieved [10]. The main

limitation of DMLs for high data-rate transmission systems is their inherent, highly component-specific chirp, i.e., a residual phase modulation accompanying the desired intensity modulation; this laser chirp broadens the optical spectrum restricting dense WDM channel spacing and can interact with fiber chromatic dispersion and cause increased signal distortions.

2.1.2 Electroabsorption Modulators (EAMs, EMLs)

An electroabsorption modulator is a semiconductor device which controls the intensity of a laser beam via an electric voltage. Its operation principle is based on the Franz-Keldysh effect, i.e., a change of the absorption spectrum caused by an applied electric field, which usually does not involve the excitation of carriers by the electric field. EAMs typically feature relatively low drive voltages and are cost-effective in volume production. They are available for high-speed modulation rates up to 40 Gb/s today, with some research demonstrations up to 80 Gb/s [11]. However, similar to DMLs, they exhibit some residual chirp. They have wavelength dependent absorption characteristics, dynamic extinction ratios typically not exceeding 10 dB, and limited optical power handling capabilities. Their fiber-to-fiber insertion loss is about 10 dB. On-chip integration with laser diodes avoids the high loss at the input fiber-to-chip interface, and leads to compact transmitter packages.

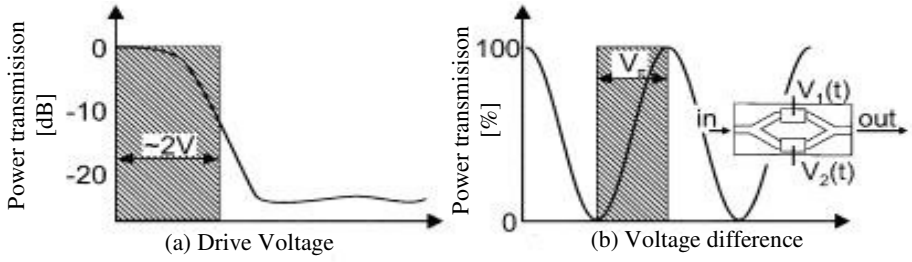

Figure 1. Transmission functions of: (a) EAMs and (b) MZMs

These EMLs, with output powers on the order of 0 dBm, are commonly available today for modulation up to 10 Gb/s. High insertion losses can be eliminated by integration with semiconductor optical amplifiers (SOAs) [2]. Figure 1(a) shows the exponential transmission characteristics of an EAM as a function of drive voltage [2].

2.1.3 Mach–Zehnder Modulators (MZMs)

Unlike electroabsorption modulators, Mach-Zehnder modulators work by the principle of interference. The modulator structure is shown in Figure 1(b). Incoming light is divided into two paths at an input coupler. One path has a phase modulator that let the two optical fields acquire some phase difference relative to each other, controlled by the applied voltages $V_{1,2}$. These two fields interfere at an output coupler. Applied electrical voltage controls destructive or constructive interference thereby producing intensity modulation. Due to their good modulation performance and the possibility of independently modulating intensity and phase of the optical field, many advanced optical modulation formats are based on using these MZMs. They can be driven with different ways to generate a variety of important modulation formats easily. MZMs are most conveniently implemented in $LiNbO_3$ [12].

2.2 Signal Propagation in Optical Fibers

2.2.1 Optical Loss

Optical loss is an important parameter for fiber. When optical signal is transmitted over fiber, its power is lost due to material absorption and Rayleigh scattering. The expression of fiber loss is given as following:

$$P_T = P_0 \exp(-\alpha L) \qquad (1)$$

Where α is called attenuation constant, usually expressed in dB/km; P_o is the optical signal power at the input of a fiber of length L; and P_T is the transmitted power. Modern telecom fibers exhibit attenuation constant below 0.2db/km near 1.55 μ m wavelength band across a bandwidth of many THz. Rayleigh scattering is a fundamental scattering mechanism arising from random density fluctuations frozen into the fused silica during manufacture and it dominates in the short wavelengths. The solid line represents the typical shape observed in the 90's, the dashed line represents the actual shape in Figure 2.

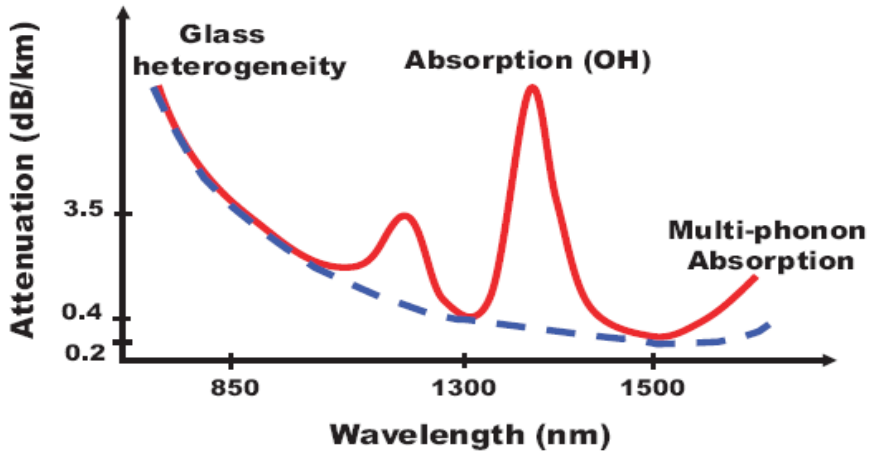

Figure 2. Attenuation of a standard single mode fiber. The solid line represents the typical shape observed in the 90's, the dashed line represents the actual shape

2.2.2 Amplified Spontaneous Emission (ASE)

Amplified spontaneous emission represents an optical source of Gaussian noise. Like the optical amplifier gain, the ASE spectrum is typically constant across the signal spectrum [2]. However, statistical properties of ASE can be modified by nonlinear interactions during fiber propagation. If multiple optical amplifiers are cascaded to periodically compensate for fiber loss, ASE builds up in the system. This noise build-up reflects in

optical signal to noise ratio (OSNR), which degrades with every amplifier along the propagation path. The OSNR is typically defined as the average optical signal power divided by the ASE power, measured in both polarizations and in a 12.5-GHz optical reference bandwidth.

2.2.3 Chromatic Dispersion (CD)

Chromatic dispersion (CD) is a broadening of the input signal as it travels down the length of the fiber. It is important to mention optical phase before any explanations of CD or group delay because of their mathematical relationship. Group delay is defined as the first derivative of optical phase with respect to optical frequency. Chromatic dispersion is the second derivative of optical phase with respect to optical frequency. These quantities are represented as follows:

$$\text{Group Delay} = \frac{\partial \phi}{\partial \omega} \qquad \text{Chromatic Dispersion} = \frac{\partial^2 \phi}{\partial \omega^2} \tag{2}$$

Where ϕ = optical phase and ω = optical frequency

The dispersion-induced spectrum broadening would be very important even without nonlinearity. The effects of dispersion can be accounted for by expanding the mode propagation constant β in a Tayler series about the center frequency ω_o 0 :

$$\beta(\omega) = n(\omega)\frac{\omega}{c} = \beta_o + \beta_1(\omega - \omega_o) + \frac{1}{2}\beta_2(\omega - \omega_o)^2 + \cdots\cdots \tag{3}$$

$$\textit{Where } \beta_m = \left[\frac{\partial^m \beta}{\partial \omega^m}\right]_{\omega=\omega_o} \quad (m = 0,1,2\ldots)$$

Another parameter concerning the dispersion of fiber is more often used, which is often referred to as dispersion parameter *D*. The relationship between *D* and $\beta 1$, $\beta 2$ is shown as following:

$$D = \frac{\partial \beta_1}{\partial \lambda} = -\frac{2\pi c}{\lambda^2}\beta_2 \approx -\frac{\lambda}{c}\frac{\partial^2 n}{\partial \lambda^2} \tag{4}$$

From Equation (4), we can see that D has opposite sign with respect to β_2. Figure 3 shows the measured variation of dispersion parameter D with wavelength for a single-mode fiber. In the regime where wavelength $\lambda < \lambda_D$, $\beta_2 > 0$ (or $D < 0$), the fiber is said to exhibit normal dispersion. In the normal-dispersion regime, high-frequency components of optical signal travel slower than low-frequency components.

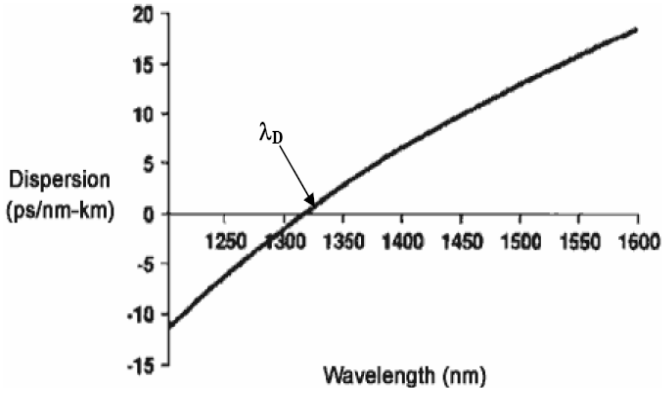

Figure 3. Measured variation of dispersion parameter D with wavelength for a single-mode fiber

Soliton transmission is possible in the anomalous regime through a balance between the dispersion and nonlinear effects. Dispersion plays an important role in signal transmission over fibers. The interaction between dispersion and nonlinearity is an important issue in lightwave system design. There exist some other fibers whose characteristics have been modified to have a dispersion profile different to pure silica (Figure 4).We have fibers with:

- Zero dispersion (DSF, *Dispersion Shifted Fiber*) or small dispersion (NZ-DSF, *Non-Zero Dispersion Shifted Fiber*) around 1.55μm. The main advantage of

NZ-DSF is due to reduction of the nonlinear effects that require phase matching like FWM (*four-wave mixing*).

- Constant dispersion over a large window (DFF, Dispersion Flattened Fiber).

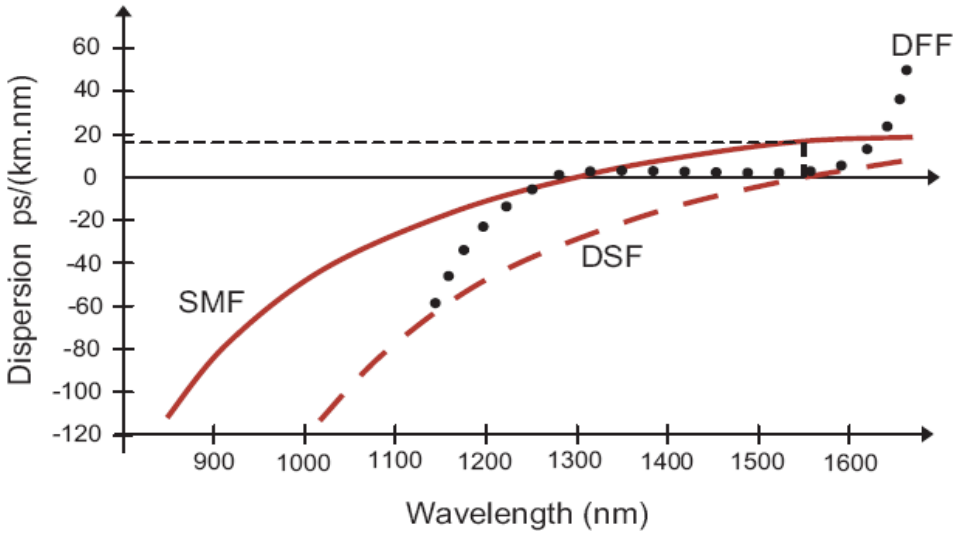

Figure 4. Dispersion profile of various type of fiber. SMF: single mode fiber, DSF: dispersion shifted fiber, DFF: dispersion flattened fiber

2.2.4 Nonlinear effects

Although silica glass used as material for making optical fibers has very small nonlinear coefficients, the nonlinear effects in optical fibers are generally not negligible. This is because the optical intensity of a propagating signal is high despite the fact that the signal power is rather low (several milliwatts to tens of milliwatts). The small cross section of an optical fiber causes the intensity to be very high, which in effect is sufficient to induce significant effects of nonlinearity. Furthermore, for optically amplified systems, the distance between regeneration is large, so the nonlinear effects may accumulate over long distances. The nonlinear effects can be divided into two cases based on their origins: stimulated scatterings and optical Kerr effects. The latter is the result of intensity dependence of the refractive index of an optical fiber leading to a phase constant that is a

function of the optical intensity, whereas the former is a result of scattering leading to an intensity dependent attenuation constant. There are two stimulated scattering phenomena in an optical fiber: Raman scattering and Brillouin scattering. The intensity dependence of refractive index results in self-phase modulation (SPM), cross-phase modulation (XPM), and four-wave mixing (FWM). Another difference between stimulated scatterings and the effects of nonlinear refractive index is that the former is associated with threshold powers at which their effects become significant. All of these effects are summarized below.

- Self-Phase Modulation (SPM), Cross-Phase Modulation (XPM)

SPM (Self-phase modulation) and XPM (Cross-phase modulation) are the two most important nonlinear effects which originate from the intensity dependence of the refractive index. SPM refers to the self-induced phase shift experienced by an optical field during its propagation in optical fibers. XPM refers to the nonlinear phase shift of an optical field induced by a co-propagating field at a different wavelength. When two optical fields at frequencies ω_1 and ω_2, polarized along the *x* axis, co-propagate simultaneously inside the fiber:

$$E = \frac{1}{2} x\left[E_1 \exp\left(-i\omega_1 t\right) + E_2 \exp\left(-i\omega_2 t\right) + c.c\right] \qquad (5)$$

Nonlinear phase shift for the field at ω_1 induced by SPM and XPM can be expressed as:

$$\phi_{NL} = n_2 k_o L\left(\left|E_1\right|^2 + 2\left|E_2\right|^2\right) \qquad (6)$$

Where n_2 is the nonlinear-index coefficient, $k_0 = 2\pi/\lambda$ and *L* is the fiber length. On the right-hand side of the Equation (6), the first term is the SPM-induced nonlinear phase shift;

and the second term is the XPM-induced nonlinear phase shift. From this equation we can say that for equally intense optical fields, the contribution of XPM to the nonlinear phase shift is twice compared with that of SPM. Figure 5 show a pulse (top curve) propagating through a nonlinear medium undergoes a self-frequency shift (bottom curve) due to self-phase modulation. The front of the pulse is shifted to lower frequencies, the back to higher frequencies. In the centre of the pulse the frequency shift is approximately linear.

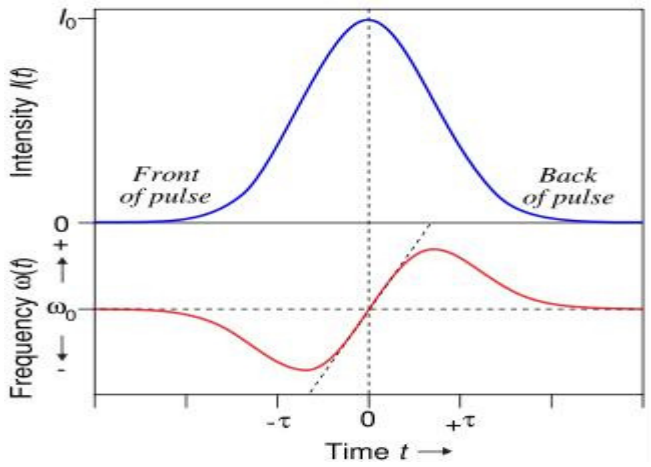

Figure 5. Phenomenon of Self Phase Modulation (SPM)

- Four Wave mixing (FWM)

When a high-power optical signal is launched into a fiber, the linearity of the optical response is lost. Four-wave mixing (FWM) is a type of optical Kerr effect, and it occurs when light of two or more different wavelengths is present in a fiber. We can say that FWM occurs when light from three different wavelengths is launched into a fiber, giving rise to a new wave, the wavelength of which does not coincide with any of the others. When two pump photons are annihilated, two photons are created: the first one at the signal frequency, the other one at a complementary frequency called idler as shown in

Figure 6a. In a WDM context, this resulting power transfer impairs the transmission since it produces a crosstalk between the channels [13]. Nevertheless, this process requires a phase-matching condition that is not spontaneously satisfied when the local chromatic dispersion is non zero. For this reason, FWM will not be the dominant nonlinear effect in our study (Figure 6b). However, it is exploited in various applications such as frequency conversion, de-multiplexing or parametric amplification. Finally, phase conjugation is an inherent property of FWM which is particularly useful [14]-[16].

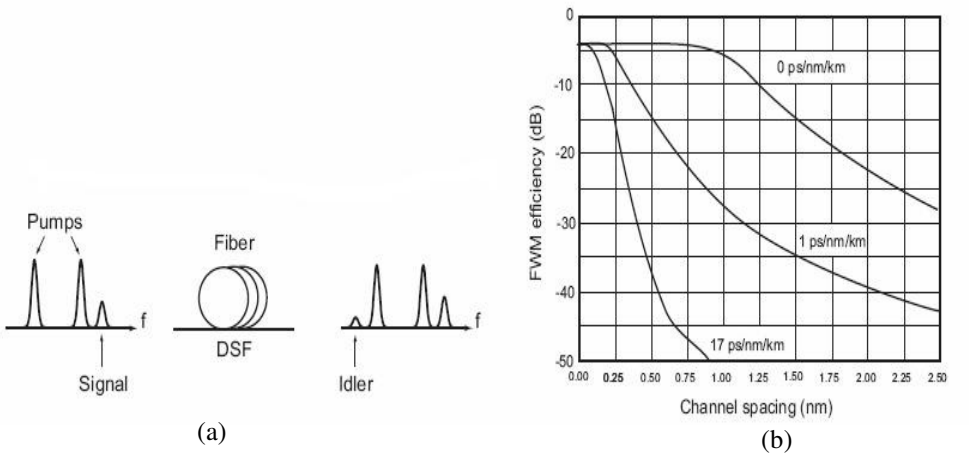

Figure 6. (a) FWM effect in the spectral domain after the propagation of the signal and the two pumps in DSF fiber (b) FWM efficiency as a function of the channel spacing for various dispersion values

- Stimulated Brillouin scattering:

Brillouin scattering arises from the inter-action of light with propagating density waves or acoustic phonons. In this case, the Stokes wave is generated opposite to the direction of pump at a frequency which is 11 GHz lower. This means that the fiber output power no longer varies linearly with the incident power but reaches a threshold beyond which the excess is entirely reflected[1]. This retro-scattering has a narrow bandwidth (up to 10 MHz around 1.55 μm) which only concerns intense continuous sources[2]. In our work, as

the pulse width is inferior to 1 ns, the required power to get a significant scattering is not confined in this band, therefore we neglect this effect.

- Stimulated Raman scattering (SRS):

Raman scattering arises from the interaction of light with the vibrational modes of the constituent molecules in the scattering medium; equivalently this can be considered as the scattering of light from optical phonons. In this case, the generated Stokes wave is produced at a frequency 13 THz lower than the pump frequency. If the bandwidth of this effect is greater (around 7 THz), it will only impact the propagation if the spectrum of the pulses greater than 13 THz: for intense pulses shorter than 1 ps – in this case the blue part of the signal acts as a pump for its red part – or if the spectrum contains wavelengths spaced by this interval.

- Polarization Mode Dispersion

Polarization mode dispersion (PMD) occurs when different planes of light inside a fiber travel at slightly different speeds, making it impossible to transmit data reliably at high speeds. PMD is the one of the mail impairment for higher data-rate (above 40 Gb/s) optical networks. However, PMD is not just a problem at 40 Gb/s; it is also evident in 10 Gb/s optical networks as well. When light travels down a single mode fiber toward the receiver, it has two polarization modes that follow the path of two axes. They move toward the receiver at right angles to each other. When the core of the fiber that bounds the light is asymmetrical, the light traveling along one polarization axis moves slower or faster than the light polarized along the other axis. This effect can spread the pulse enough to make it overlap with other pulses or change its own shape to make it undetectable at the receiver.

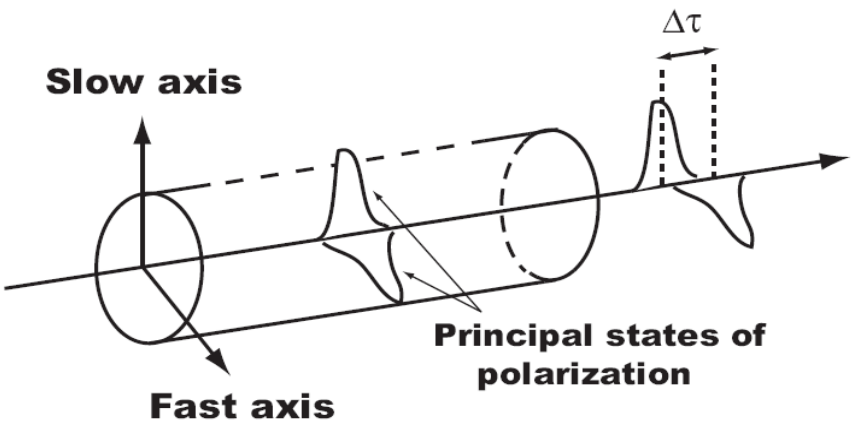

Figure 7. PMD effect on an optical pulse

A pulse will propagate though those two axes with different group velocities. The differential group delay (DGD) between the two modes (Figure 7) results in a time broadening at the detection. In opposition to chromatic dispersion, stable and perfectly known, PMD has a random evolution in time. One can show that the average DGD increases with the square root of the fiber length [17]. The specifications of some commercial fibers are presented in Table 1.

Table 1. Parameters of commercial fibers at 1550 nm according to [18]

Fiber	Manufacturer	D $ps/(km.nm)$	S $ps/(km.nm)^2$	α_0 dB/km	A_{eff} μm^2	PMD $ps/\sqrt{km}$
TrueWave™ RS	Lucent	4.5	0.045	0.22	55	< 0.1
LEAF™	Corning	4.2	0.09	0.22	72	< 0.1
TeraLight™ Ultra	Alcatel	8	0.052	< 0.22	63	< 0.04
Standard	Lucent, Corning Furukawa	16.9	0.055	0.23	87	< 0.1
Under-sea	Lucent	−3.1	0.05	0.215	50	< 0.1
Deeplight™	Pirelli	−2.2	< 0.12	< 0.23	70	< 0.1
Teralight™ Metro	Alcatel	8	0.058	< 0.25	63	< 0.08
DCF	Lucent	−100	−0.22	0.5	20	< 0.25
WB-DCF	Lucent	−95	−0.33	0.5	19	< 0.25
HS-DCF	Lucent	−100	−0.67	0.68	15	< 0.25

2.2.5 Optical Amplification

Until now, we have just focused on the description and the modeling of the physical phenomena occurring in the fiber when an intense electric field is propagating. In this paragraph, we summarize different technical solutions focusing on amplification that allowed to get rid off some physical constraints and limitations.

- *Erbium-doped fiber amplifier (EDFA)*

In the case of an erbium-doped fiber amplifier (EDFA), the energy from the pump operating at one of the absorption wavelengths of the erbium ion (980 – 1480 nm) is absorbed. The excited erbium ions are stimulated by any signal around 1.5 µm that is injected in the fiber. The stimulated ion emits one photon which has the same state than the one which returns to the fundamental state. At the same time, a spontaneous emission (SE) is generated in the fiber with or without the presence of any signal. This non desired contribution is amplified by the same mechanism as the signal and gives rise to the amplified spontaneous emission (ASE) noise, which can be a problems for increased spans of fiber. Figure 8 shows a simple schematic of fiber doped amplifier.

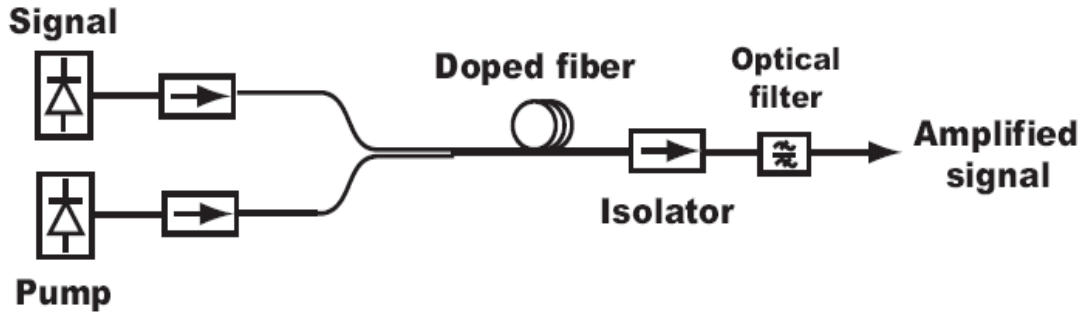

Figure 8. Scheme of a fiber-doped amplifier

- *Raman amplification*

The previous amplification technique requires the doping of a fiber, used as the gain medium. Another solution exists in which the gain is obtained in the fiber where the signal propagates. The stimulated Raman scattering (SRS) is the physical phenomenon at the origin of the amplification. Thus, the transmission fiber can be used as a amplification medium, and so a fiber with gain is created. The optical signal is injected in the fiber with the pump, typically at a 100 nm shorter wavelength and gradually amplified along the fiber (Figure 9). Energy transfer occurs when the pump photon gives up energy to create a new photon at signal wavelength plus some residual energy, which is absorbed as phonons.

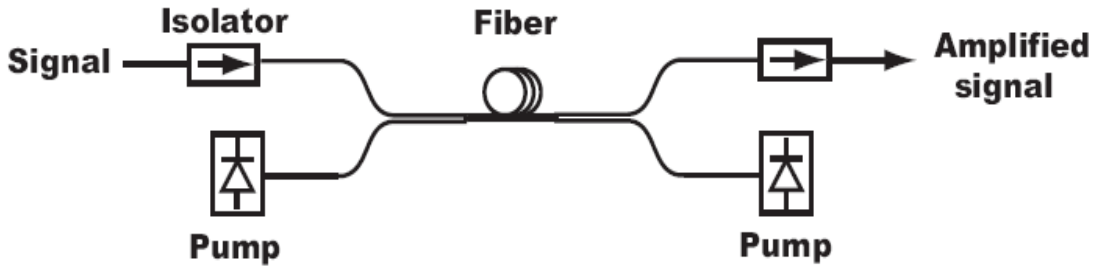

Figure 9. Scheme of a Raman amplifier

Although this effect has been known and studied for more than 30 years, the high pump power needed to get a 10-15 dB gain delayed its practical use. Arrival of EDFA also put hold further research on this technology. Nevertheless, Raman amplification is successfully used with ultra-long haul undersea systems [19]. At this time more powerful laser diodes are now available at lower cost, which make use of this technology more practical. Ability to amplify the signal in low noise conditions is extremely important for optical transmission systems. Distributed along the fiber, the Raman gain considerably improves the OSNR since at the end of a fiber span. This improvement is typically

represented by an equivalent noise factor which would be the same as the amplifier located at the end, producing the same gain and the same contribution of spontaneous emission. So Raman amplifiers have a lower equivalent noise factor than EDFAs which are in principle limited to values higher than 3-dB. The margin gained on the OSNR could go up to 6 dB and could potentially be used to increase the total transmission length. Figure 10 shows Raman gain coefficient against frequency difference between signal and pump. Gain increase linearly with frequency difference peaking when the signal is 13 THz lower frequency than the pump then dropping rapidly.

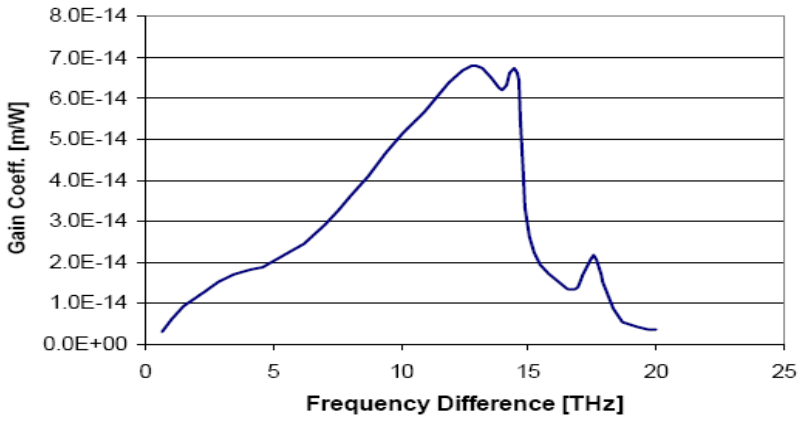

Figure 10. Raman gain coefficient versus frequency difference between signal and pump

- *Hybrid amplification*

For gain higher than 20 dB, the equivalent noise factor improvement of Raman amplification is limited by the double Rayleigh retro-scattering. It imposes a limit on the usable Raman gain which is no more sufficient to compensate for the fiber losses. This is the case for terrestrial transmissions when the losses due to the dispersion compensation and the add-drop multiplexing are taken into account. A low gain EDFA is usually added to the Raman amplifier to overcome these limitations. The noise factor resulting from this

hybrid amplification is entirely determined by the Raman amplifier placed first. Optical amplification is not only limited to the techniques previously presented. Parametric amplification is an important example regarding the interest it provokes.

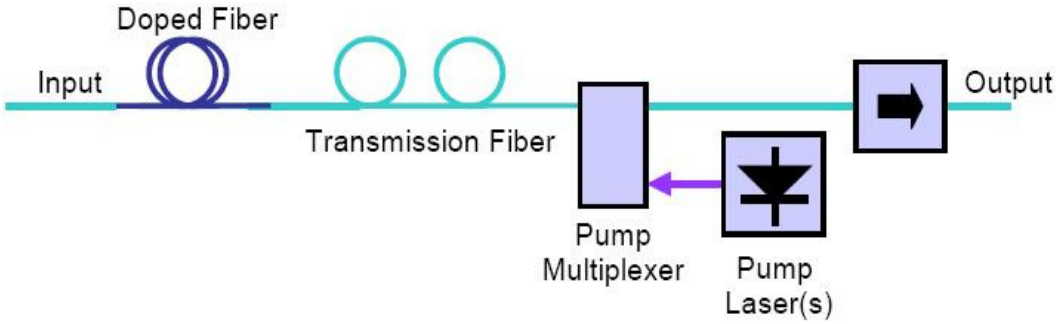

Figure 11. Hybrid Raman doped-fiber amplifier

Figure 11 shows one of the many possible configuration for hybrid Raman amplifier where doped fiber is pumped remotely via transmission fiber. Figure 12 gives an idea of the bands covered by different technologies.

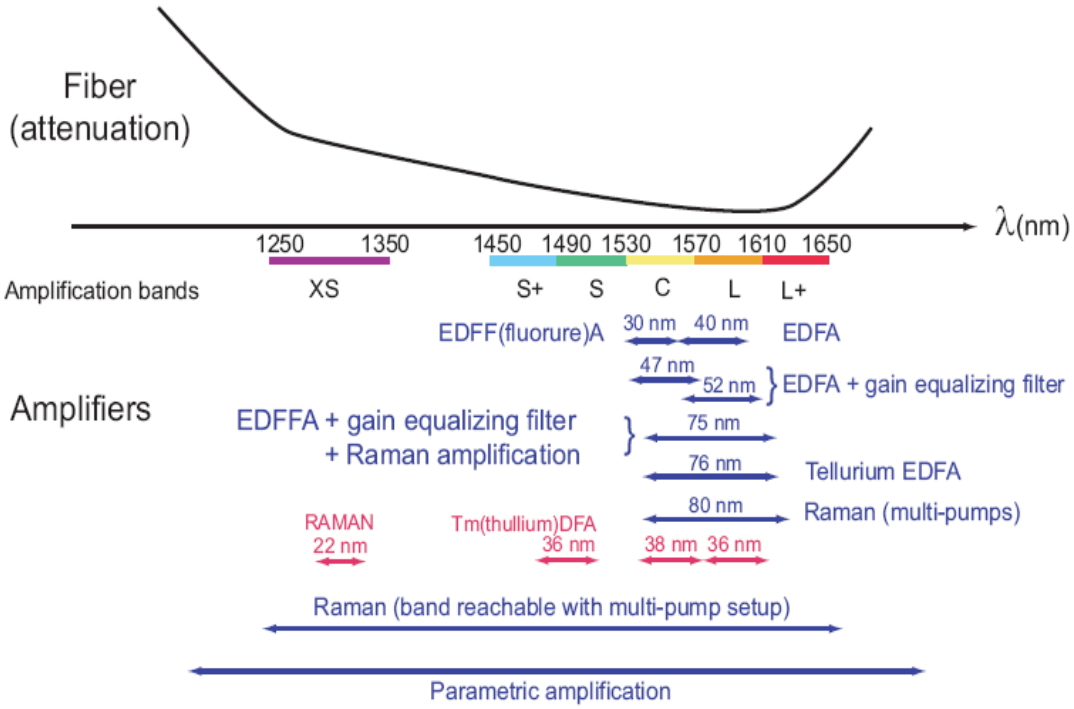

Figure 12. Amplification bands covered by various amplification technologies ([20], [21])

2.3 Intensity Modulation Formats

Optical filed has three physical attributes which can be used to transmit information, intensity being one of them; phase and polarization are the other two. Realizing cost-effective and spectral efficient optical transport system requires overcoming the transmission distance limitation due to both linear and nonlinear optical fiber impairments such as group velocity dispersion (GVD), polarization-mode dispersion (PMD) self-phase modulation, cross-phase modulation (XPM), four-wave mixing (FWM) etc. The decrease in optical signal-to-noise ratio (OSNR) due to the increase in signal bandwidth requires an increase in the optical signal launched power, which further strengthens the impact of fiber nonlinear effects. To overcome these problems for 40 Gb/s and higher per channel transmission, key transmission technologies such as modulation and detection format [22]- [28], distributed Raman amplification (DRA[29]-[31], and dispersion compensation in terms of GVD and PMD, including dispersion-slope management [32] have been proposed.

2.3.1 Non-return-to-zero On-Off Keying (NRZ-OOK)

Non-return-to-zero on-off-keying (NRZ-OOK) has been the dominant modulation format for fiber-optical communication systems. There are several reasons for using NRZ in the early days of fiber-optical communication: First, it requires a low electrical bandwidth for the transmitters and receivers (compared to return-to-zero); second, it is not sensitive to laser phase noise (compared to phase shift keying); and last, it has the simplest configuration for the transmitter and receiver. Considering recent advancements in optical communication field, NRZ modulation format may not be the best choice for future high capacity optical networking systems. However, it has been widely deployed

in field and due to its simplicity, and its historic dominance, NRZ would be a good reference for the comparison.

The block diagram of a NRZ transmitter is shown in Figure 13, where electrical signal is modulated with an external intensity modulator 0. The intensity modulator can be either Mach-Zehnder or electro-absorption modulator, which converts an electrical signal to optical signal at the same data rate. When using an MZM, modulator is usually biased its quadrature point and is driven from minimum to maximum transmission with switching voltage V_π. A simple photodiode is used at the receiver to detect a NRZ optical signal, which converts optical power of signal into electrical current. This is called direct detection. In general, NRZ modulated optical signal has the most compact spectrum compared to that with other modulate formats. However, this does imply that NRZ optical signal has superior resistance to residual chromatic dispersion in an amplified fiber system with dispersion compensation. Also this does not reflect that NRZ is more tolerant to XPM and FWM in DWDM systems because of its strong carrier component in the optical spectrum [33].

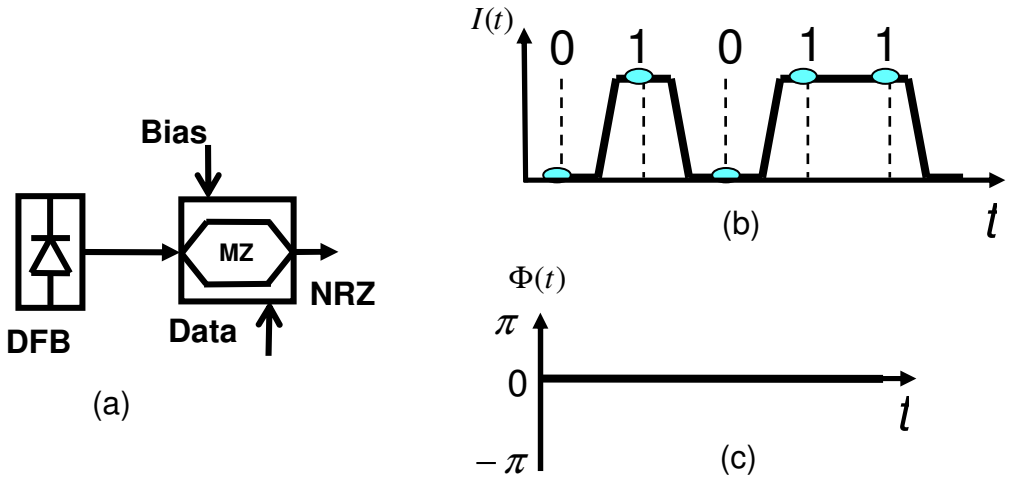

Figure 13. NRZ modulation scheme: (a) Block diagrams of NRZ transmitter (b) waveform for intensity *I(t)* and (c) phase *Φ(t)*

In addition, NRZ optical signal has been found to be less resistive to GVD-SPM effect in transmission compared to its RZ signals. A simple explanation is that different data patterns in a PRBS NRZ data stream require different optimum residual dispersion for the best eye opening. For example, an isolated digital "1" would generate more self-phase modulation (SPM) effect than continuous digital "1"s. Since SPM can be treated as an equivalent signal frequency chirp, it modifies the optimum value of the dispersion compensation in the system. The difference in the optimum dispersion compensation between an isolated digital "1" and continuous digital "1"s makes it impossible to optimize the residual dispersion in the system and thus makes the system performance vulnerable to the data patent-dependent fiber nonlinear effect 00. This effect is especially obvious in long-haul distance fiber-optic systems.

2.3.2 Return-to-zero On-Off Keying (RZ-OOK)

RZ means "return-to-zero", so the width of optical signal is smaller than its bit period. Usually a clock signal with the same data-rate as electrical signal is used to carve RZ

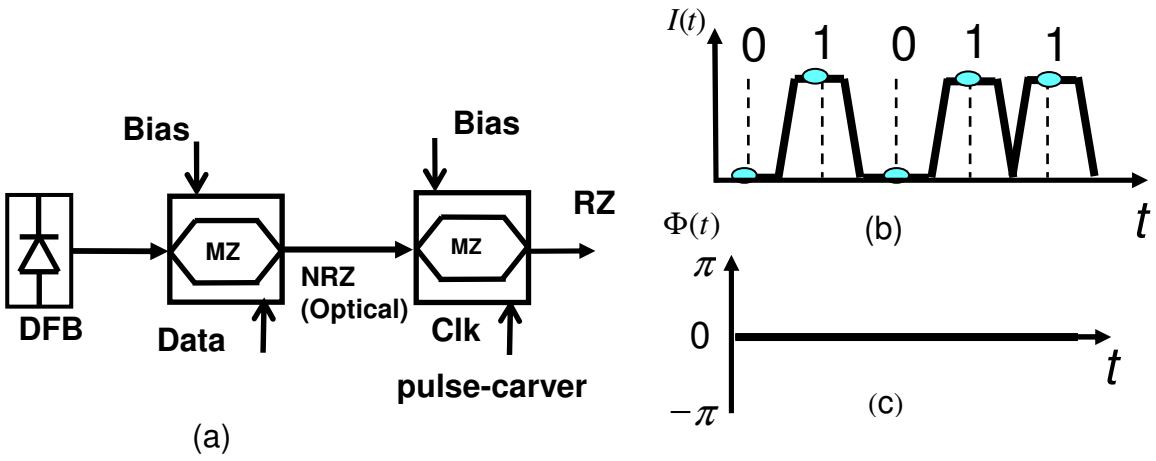

Figure 14. RZ modulation scheme: (a) Block diagrams of RZ transmitter (b) Waveform for intensity *I(t)* and (c) phase *Φ(t)*

shape of optical signals. Figure 14 presents the block diagram of a typical RZ transmitter

Initially, NRZ optical signal is generated by an external intensity modulator; then, it is modulated by a synchronized pulse train with the same data-rate as the electrical signal by cascading another intensity modulator. We can also generate RZ waveforms first and then modulate onto an optical carrier. RZ optical signal has been found to be more tolerant to nonlinearity than NRZ optical signal. If the average optical power launched into the fiber is kept constant, an optical RZ pulse with a 50% duty cycle will have twice the peak power of an NRZ pulse. This increase in power occurs because optical amplifiers are run in the saturation mode, resulting in a gain that scales with average input power. The photodiode is a square-law detector, i.e., the photocurrent is proportional to optical power. Hence the received electrical power (proportional to the square of the photocurrent) is proportional to the square of the optical power. Therefore, the electrical power of an RZ pulse with a 50% duty cycle will be twice that of an NRZ pulse.

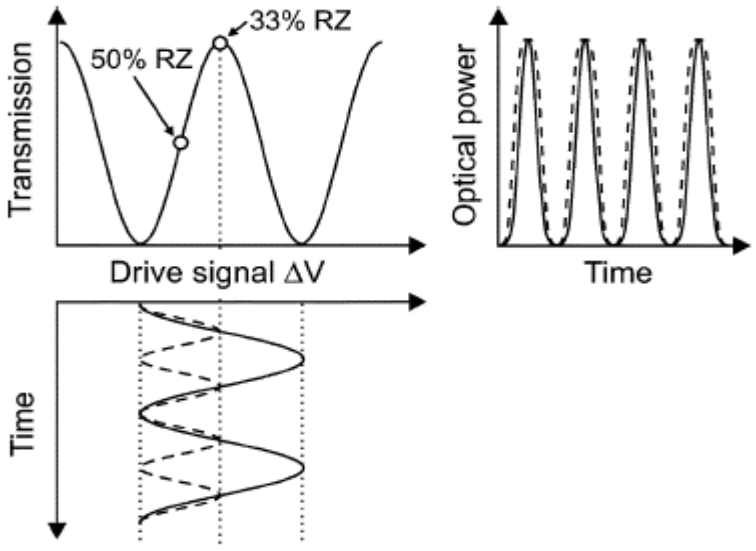

Figure 15. Bias setting of pulse carver for 33% RZ and 50% RZ

RZ formats usually require a slightly more complex transmitter structure, but are generally more robust to ISI [34]-[37]. Figure 15 shows bias settings for pulse carver modulator to generate 33% and 50% RZ duty cycle. By driving an MZ modulator at half the data rate between its transmission minima produces a RZ pulse with duty-cycle of 33%. In order to produce RZ pulse with 50% duty-cycle, pulse carver modulator is driven at data rate between transmission maxima and minima (Figure 15). The reason for its better tolerance to fiber nonlinear effects than NRZ can be explained due to its regular data pattern of optical signal. Because of characteristic of 'return-to-zero' of RZ optical signals, an isolated digital bit '1' and continuous digital "1"s would require the same amount of optimal dispersion compensation for the best eye opening. So if we have optimal dispersion compensation in the system, RZ format exhibits better tolerance to nonlinearity than NRZ. RZ pulse has a wider spectrum because of its narrower pulse width. This would make RZ pulse shaping less spectrum efficient in a WDM system.

2.3.3 Carrier-Suppressed Return-to-Zero (CSRZ)

CSRZ [38] is a pseudo-multilevel modulation format. It is characterized by reversing the sign of the optical field at each bit transition. In contrast to the correlative coding formats like duobinary, the sign reversals occur at every bit transition, and are completely independent of the information-carrying part of the signal. Figure 16(a) shows typical CSRZ transmitter setup. CSRZ (67% RZ) can easily be generated by driving an MZM pulse carver sinusoidally at half the data rate between its transmission maxima, as presented in Figure 16(b) [2]. Phase inversions between adjacent bits are achieved because optical field transfer function of the MZM changes its sign at the transmission minimum. Thus, on average, the optical field of half the 1-bits has positive sign, while

the other half has negative sign, resulting in a zero-mean optical field envelope [2]. As a consequence, the carrier at the optical center frequency is diminished. Since the optical phase in a CSRZ signal is periodic at half the data rate, the CSRZ spectrum exhibits characteristic tones at $\pm R/2$.

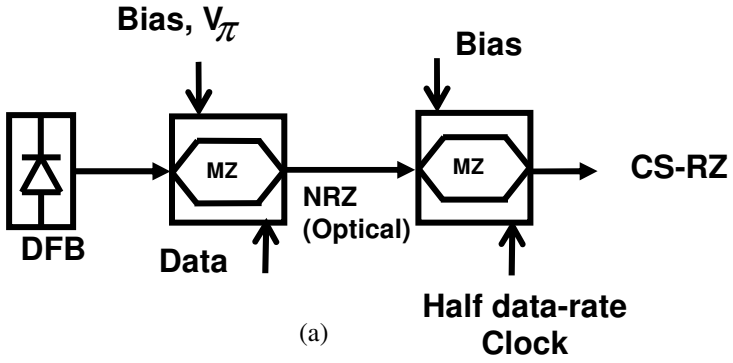

(a)

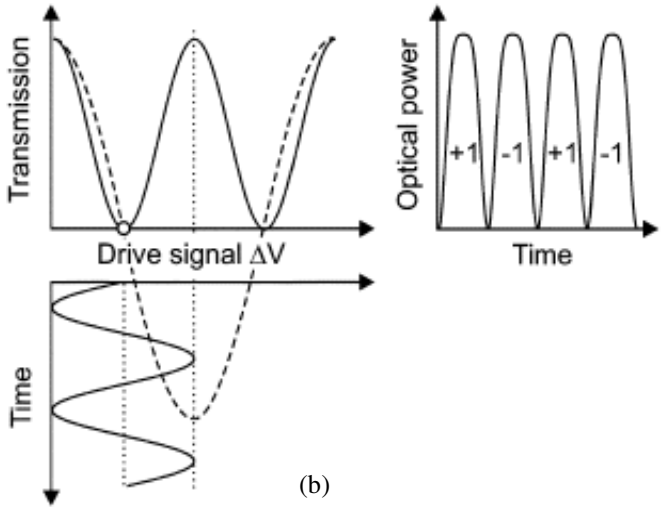

(b)

Figure 16. (a) CS-RZ transmitter setup, (b) Bias setting of pulse carver for 67% duty-cycle CSRZ

2.3.4 Duobinary (DB) and Modified Duobinary (MDB)

Optical duobinary (DB) scheme belong to a class of correlative coding formats. It has also been named as phase shaped binary transmission (PSBT) [39] and phased amplitude-shift signaling (PASS) [40]. Duobinary modulation is a scheme to transmit R bits/s using

less than R/2 Hz of bandwidth. Main advantage of DB is their high dispersion tolerance and narrowband optical filtering. Conventional DB transmitters use a differential precoder at the input. Although it is possible to use decoder at the receiver but precoding at the transmitter is used in order to avoid error propagation. Precoded sequence is converted to three-level electrical signals by using low pass electrical filter. This low-pass filter (LPF) can also be implemented by a delay-and-add circuit, which typically results into a better back-to-back sensitivity while carefully selected low-pass filter enhance CD tolerance at the expense of this sensitivity. Figure 17 shows a typical duobinary precoder and encoder.

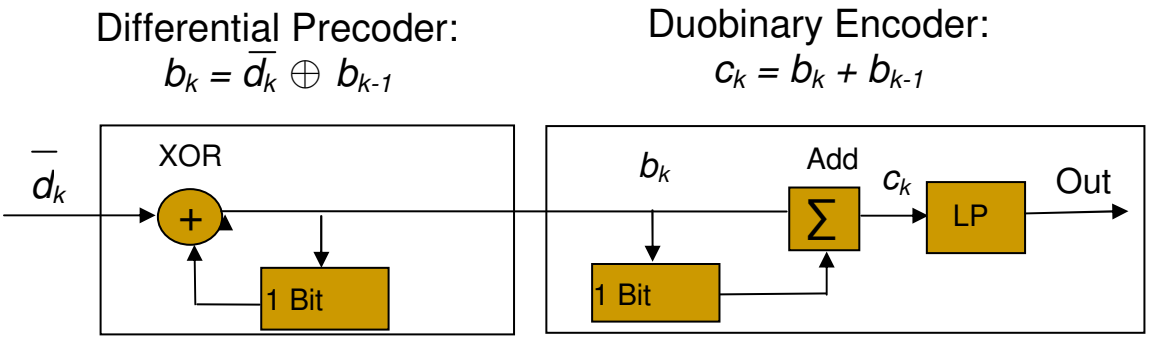

Figure 17. Duobinary Precoder and Encoder

However, with higher bit rate, it is difficult to implement the 1-bit delay in the feedback path. An alternate way of implementing the same differential encoder without using the 1-bit delay is shown in Figure 18. When the data is 'high', the counter changes the state, which is equivalent to adding a 1 modulo 2. When the data is 'low', the counter state remains the same, which is equivalent to adding a 0 modulo 2.

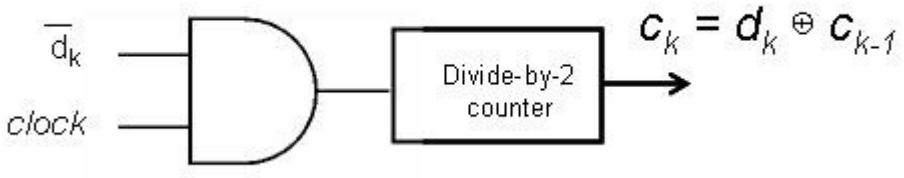

Figure 18. An alternate implementation of duobinary precoder

The cutoff frequency of the LPF equals a quarter of the bit rate. This is also called duobinary filter. The LPF acts as an analog converter, which simultaneously converts signals from binary to duobinary and trims high-frequency components in the duobinary signal spectrum. Finally, we modulate light with this three level duobinary signal. Here we use MZM biased at its null point. With 0 input no light is transmitted but +1 and -1 are transmitted as +E and –E electrical filed respectively. Thus three level electrical signal is converted to two level optical signal (see Figure 19).

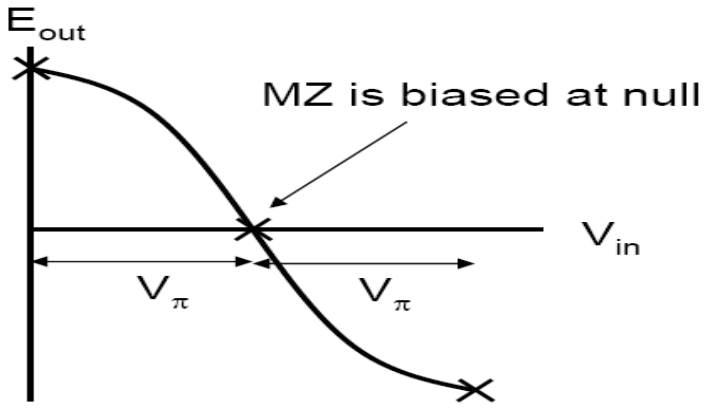

Figure 19. Biasing of MZM modulator

An important property of a correlated signal like DB is that all possible sequences of the three values can not occur. For example, in NRZ a data sequence of {1 0 1} is mapped to {+E 0 +E}, in encoded DB signal {1 0 1} can not occur, instead {1 0 -1} do occur, which is mapped to {+E 0 –E} in optical domain. The effect of dispersion in these two cases is

shown in Figure 20, which clearly indicates the mitigation of dispersion in case of DB signal [41].

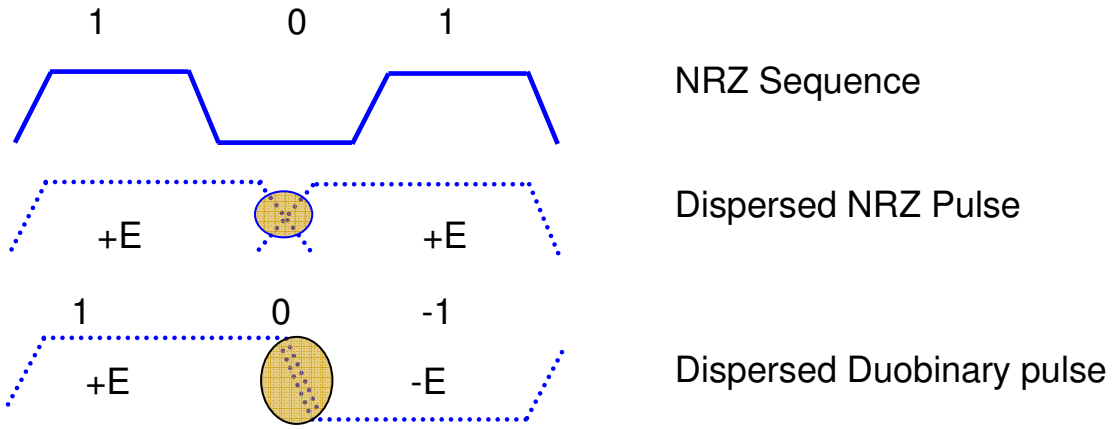

Figure 20. Dispersed NRZ and Duobinary pulse

Table 2 presents an example of transformation of data in a duobinary system [41]. You can see that "1"s separated by odd number of "0"s has opposite phase shifts.

Table 2. An example of transformation of data in a duobinary system

K	-1	0	1	2	3	4	5	6	7
d_k		0	1	0	1	1	0	0	1
$\overline{d_k}$		1	0	1	0	0	1	1	0
Bit to Voltage	0	1	1	0	0	0	1	0	0
Mapper	-1	1	1	-1	-1	-1	1	-1	-1
Duobinary		0	1	0	-1	-1	0	0	-1
Encoder		0	+E	0	-E	-E	0	0	-E
Electric Field		0	$\|E\|^2$	0	$\|E\|^2$	$\|E\|^2$	0	0	$\|E\|^2$
Optical Power		0		0			0	0	
Received Bits									

Modified duobinary (MDB) format, on the other hand, is inherently asymmetric. This modulation format is characterized by phase inversion in the pulses triggered by the

presence of a logical “one” in the previous bit slot. Duobinary spectrum has DC content while modified duobinary does not have any DC content. MD-RZ has opposite phase in adjacent “1”s and due to this fact self-phase modulation in single channel, cross-phase modulation and intra-channel four-wave mixing in WDM transmission systems can be reduced. A typical modified duobinary transmitter is shown in

Figure 21. Another name used in research publications for this modulation format is alternate mark inversion (AMI).

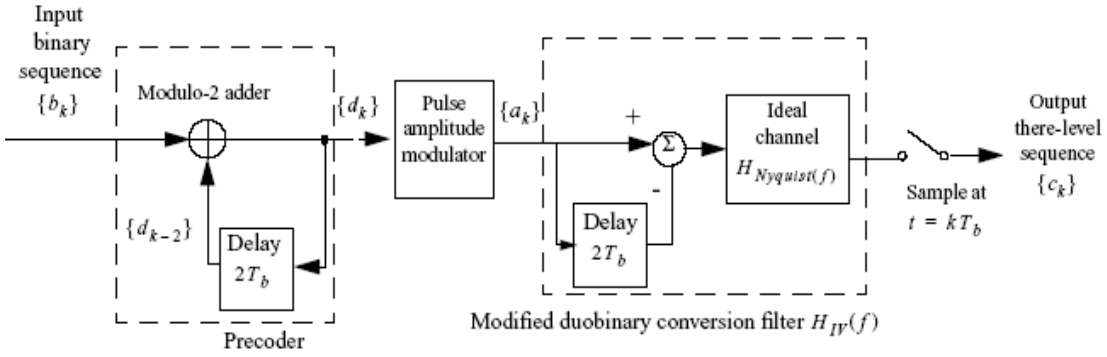

Figure 21. A typical modified duobinary coder setup

2.4 Differential Phase Modulation Formats

With optical intensity modulation, digital signal is represented by instantaneous optical power levels. Digital signal can also be represented by the phase of an optical carrier and this is commonly referred to as optical phase-shift-keying (PSK).

2.4.1 Non-return-to-zero Differential Phase Shift Keying (NRZ-DPSK)

Recent advancements of single-frequency laser sources and the application of active optical phase-locking make this format feasible in practical optical systems. Specifically,

differential-phase-shift-keying (DPSK) is the most often used format. Figure 22(a) shows the block diagram of a typical NRZ-DSPK transmitter 0. Like duobinary, the data signal is first differentially encoded at the transmitter, which avoids error propagation that may occur by differential decoding at the receiver. In a DPSK encoder, the NRZ data is combined with its one-bit delay version by a XOR gate. This DPSK encoded electrical signal is then used to drive a phase modulator (PM) or an MZM to generate a DPSK optical signal. A digital "1" is represented by a π phase change between the consecutive data bits while digital "0" is presented by no phase change between the consecutive data bits in the optical carrier. Signal intensity is always constant in NRZ-DPSK.

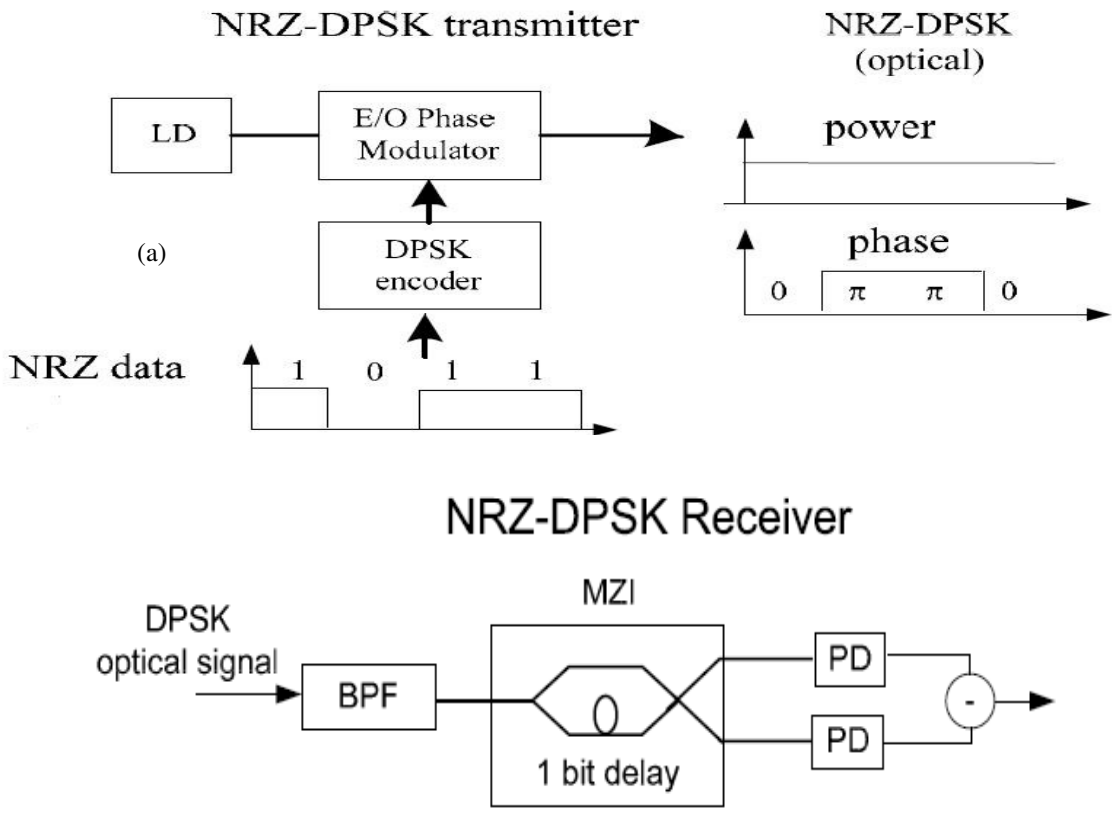

Figure 22. Block diagrams of NRZ-DPSK: (a) Transmitter and (b) Balanced receiver

As shown in Figure 22(b), a one-bit-delay Mach-Zehnder Interferometer (MZI) is usually used as a DPSK optical receiver. MZI is used to correlate each bit with its neighbor and

make the phase-to-intensity conversion. There are two outputs of MZI, called constructive port or destructive port respectively. For constructive port, when the two consecutive bits are in-phase, they are added constructively in the MZI and results in a high signal level; otherwise, if there is a π phase difference between the two bits, they cancel each other in the MZI and results in a low signal level.

In a practical DPSK receiver, both constructive port and destructive port of MZI are used, which is called balanced receiver. The main advantage from using DPSK instead of OOK comes from a 3-dB receiver sensitivity improvement, which can be understood from the fact that the symbol spacing for DPSK is increased by $\sqrt{2}$ compared to OOK for fixed average optical power. This increased symbol distance makes DPSK accept $\sqrt{2}$ larger standard deviation of the optical field noise than OOK for equal BER, which translates into a 3-dB reduction in OSNR. Direct detection using one of MZ-DI port can also be used to detect DPSK signals (Figure 23).

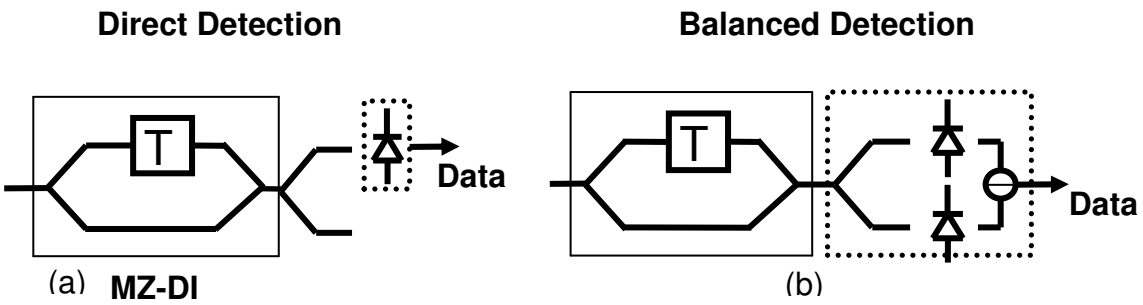

Figure 23. DPSK receiver: (a) Direct detection (b) Balanced detection

Because of its constant optical power the performance of NRZ-DPSK is less susceptible by optical power modulation-related nonlinear effect such as SPM and XPM. However, when the chromatic dispersion is considered, this is not entirely true. Phase modulations can be converted into intensity modulation through group velocity dispersion (GVD), and

then SPM and XPM may contribute to waveform distortion to some extent. In a long distance DPSK system with optical amplifiers, nonlinear phase noise is usually the limiting factor for phase-shift-keying optical signals.

2.4.2 Return-to-Zero Differential Phase Shift Keying (RZ-DPSK)

In order to improve system tolerance to nonlinear distortion and to achieve a longer transmission distance, return-to-zero DPSK (RZ-DPSK) is a strong candidate. Similar to NRZ-DPSK modulation format, the binary data is encoded as either a "0" or a "π" phase shift between adjacent bits. Due to RZ pulse shape width of the optical pulse is narrower than the bit slot. Typically, one more modulator is cascaded with NRZ transmitter to carver NRZ pulse to RZ pulse shape. Figure 24 shows the block diagram of a RZ-DPSK transmitter 0. First, an electro-optic phase modulator generates a conventional NRZ-DPSK optical signal, and then, this optical signals is modulated by a same data-rate clock signal with the second

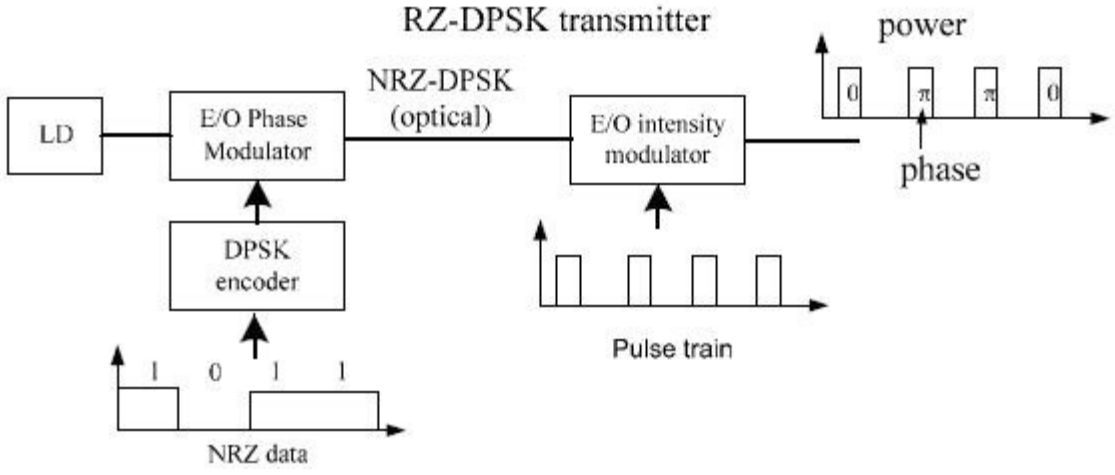

Figure 24. Block diagrams of RZ-DPSK transmitter

modulator. Sometimes RZ-DPSK is also referred to as intensity modulated DPSK (IM-DPSK) because of its additional bit-synchronized intensity modulation. In this

modulation format unlike NRZ-DPSK, optical power of the signal is no longer constant; this will introduce the sensitivity to power-related nonlinearity like SPM. Due to the narrow optical signal pulse width, the optical spectrum of RZ-DPSK is wider than a conventional NRZ-DPSK. Similar to RZ-OOK, RZ-DPSK is more tolerant to data-pattern dependent SPM-GVD effect with optimal dispersion compensation because of its regular RZ waveform.

2.4.3 Differential Quadrature Phase shift Keying (DQPSK)

DQPSK is a true multilevel modulation format that has received good attention in optical communications research lately. It transmits the four phase shifts {0, + π/2, -π/2, π} at a symbol rate of half the aggregate bit-rate. As in the case of DPSK, a DQPSK transmitter is most conveniently implemented by two parallel MZMs operated as phase modulators.

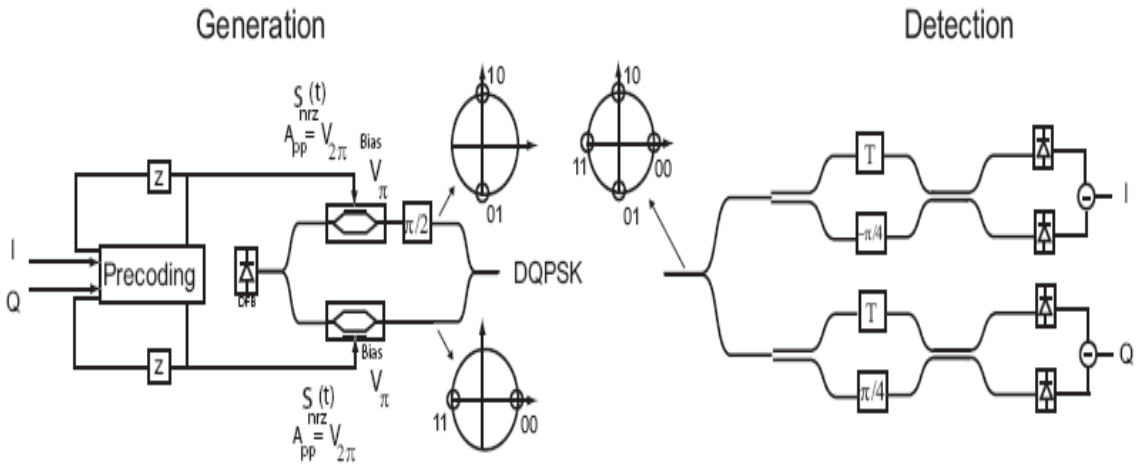

Figure 25. A typical DQPSK modulation scheme

Figure 25 shows the corresponding transmitter setup, consisting of a continuously operating laser source, a splitter to divide the light into two paths of equal intensity, two MZMs operated as phase modulators, an optical π/2 phase shifter in one of the paths, and

a combiner to produce a single output signal. A serial DQPSK transmitter setup is also possible [2].

The symbol constellations of the upper and lower paths as well as at the modulator output are also shown, together with the symbol transitions. Using this transmitter structure, we take advantage of the near perfect π phase shifts produced by MZMs, independent of drive signal overshoot and ringing. Second, this transmitter structure requires only binary electronic drive signals, which are much easier to generate at high speeds than multilevel drive waveforms.

Optionally, a pulse carver can be added to the structure to produce RZ-DQPSK. Note that the shape of the DQPSK optical spectrum is identical to that of DPSK, but the DQPSK spectrum is compressed in frequency by a factor of two due to the halved symbol rate for transmission at fixed bit-rate. The compressed spectrum is beneficial for achieving high spectral efficiencies in WDM systems, as well as for increased tolerance to CD, the longer symbol duration compared to binary modulation formats makes DQPSK more robust to PMD. Like at the transmitter, one also strives to work with binary electrical signals at the DQPSK receiver due to implementation benefits in high-speed electronics. At the receiver, the DQPSK signal is thus first split into two equal parts, and we use balanced receivers with differently biased delay interferometers in parallel to simultaneously demodulate the two binary data streams contained in the DQPSK signal. MZ-DI delay is equal to the symbol duration for DQPSK demodulation, which is twice the bit duration.

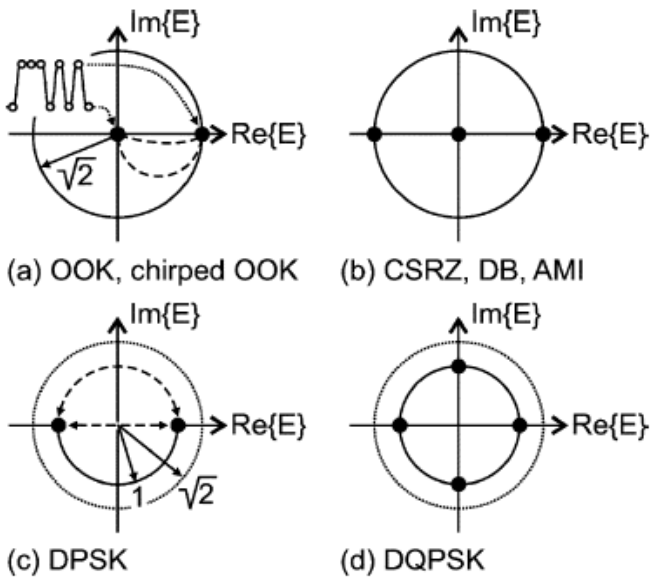

Figure 26. Optical symbol diagrams for modulation formats [2]

Figure 26 shows the four important symbol diagrams encountered in optical communications, comprising almost all formats. Symbol diagrams show the complex optical field values of data symbols, used either for data transport or for improving specific format properties. All these diagrams are plotted on the same scale, normalized to unity average optical power. In Figure 26(a), dashed lines show examples for transitions between symbols for chirped formats; in Figure 26(c), dashed double-arrows represent different phase modulator implementations, using a straight line phase modulator or Mach-Zehnder modulator. The symbol diagram in Figure 26(

Figure 26b) represents CSRZ as well as DB and AMI. Figure 26(c) and 26(d) represent DPSK and DQPSK, respectively. The two phase modulation formats are shown for the same average optical power as the intensity modulation formats of Figure 26

Figure 26(a) and (b).

CHAPTER 3

MODIFIED DUOBINARY RZ (MD-RZ) SIGNAL GENERATION, TRANSMISSION AND CHARACTERISTICS

In this chapter, we demonstrate a simple and cost effective technique to generate the modified duobinary RZ (MD-RZ) signal by using only one single dual-arm Mach-Zehnder $LiNbO_3$ modulator. We also present experimental results for single channel and WDM repeaterless transmission of MD-RZ signal over SMF. In the end, numerical comparison is drawn with other MD-RZ generation schemes.

3.1 A novel architecture to generate 10 Gb/s Modified Duobinary return-to-zero (MD-RZ) signals

3.1.1 Motivation

Duobinary data encoding has received much attention because of its advantages in dispersion tolerance and reducing nonlinear effects in optical communication systems [42]- [44] . Relative to non-return-to-zero (NRZ) format optical signals, return-to-zero (RZ) format optical signals can tolerate high input power, and have small inter-symbol interference and high receiver sensitivity [45]. Recently it has been shown [42], that modified duobinary RZ (MD-RZ) signals show more advantages compared to regular RZ, duobinary RZ, and alternating phase RZ signals because the MD-RZ has an opposite-phase in the adjacent “1”s, which leads to the fact that self-phase modulation in single channel, cross-phase modulation and intra-channel four-wave mixing in WDM transmission systems can be reduced. In a conventional scheme, generation of the duo-

binary RZ usually needs two modulators; one is used to generate duobinary signals and the other is cascaded to this modulator for carving NRZ signals to generate RZ signals [42], [44] .

3.1.2 Proposed Scheme and Setup

Duobinary and modified duobinary RZ signal is conventionally generated by the use of two cascaded modulators. One modulator is used to carve RZ pulse shape and second modulator is driven by data signals after low pass filtering to produce duobinary modulation (Figure 27). A regular photo detector is then used at the receiver for detection of these duobinary signals.

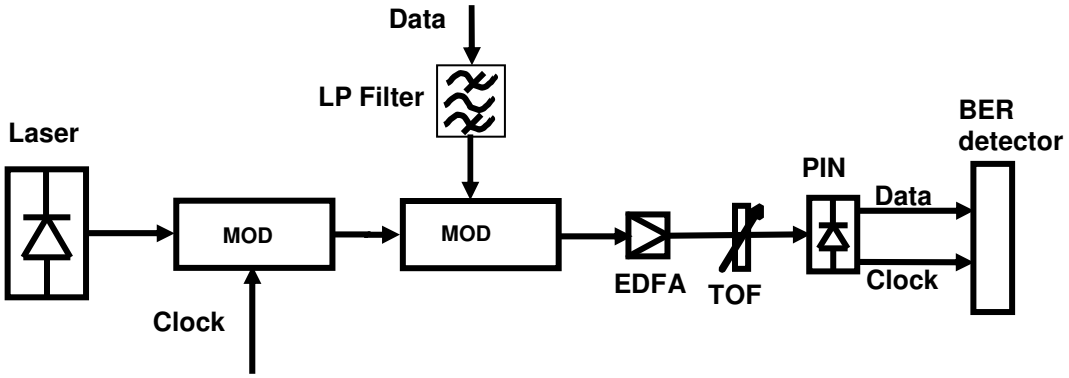

Figure 27. Conventional duobinary transmitter

The proposed setup for MD-RZ generation is shown in

Figure 28. The binary NRZ signal, generated by a pattern generator with the data rate of 10 Gb/s drives a dual-arm Mach-Zehnder modulator to generate modified duo-binary RZ signal. The driven electrical signal is inserted in

Figure 28. We can see that the rise time and fall time from 10% to 90% amplitude of the electrical signal are both approximately 25ps. The word length of the pseudorandom bit sequence (PRBS) of the electrical signal is 2^{31}-1. In real systems, precoder is required in

duobinary transmitter as explained in previous section [43], since PRBS pattern is not altered after the pre-coder, but only gets delayed and depending on the word-length, in some cases pattern is inverted. Therefore we do not have to use pre-coder or decoder in this experiment. The dual-arm Mach-Zehnder modulator has a half-wave voltage of 3.8V at 10GHz [46]. The data from the 10Gbit/s pattern generator is divided into two equal parts. One is delayed and amplified to drive the Mach-Zehnder modulator. The other is directly amplified to drive the second arm of the modulator. The amplitude of the amplified electrical signal after the electrical amplifier is 3.8V; which is equal to the half-wave voltage of the modulator. The MZ modulator is biased such that there is the minimal output power when the data is turned off. The generated duobinary optical signal is received by an APD receiver with 8GHz bandwidth.

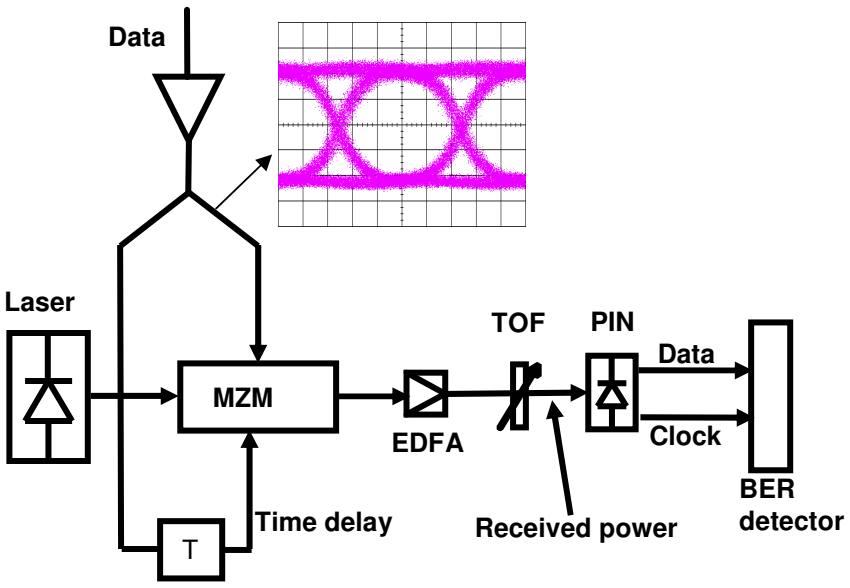

Figure 28. Experimental setup for modified duobinary RZ generation

Figure 29 shows the principle for the MD-RZ signal generation. We can see that consecutive ones in the symbol sequence alternate between the two opposite-phase levels [43]. Depending on the time delay between the two arms, MD-RZ signal with different

duty ratio can be obtained. In principle, any duty cycle MD-RZ signals can be generated by using this method; however the pulse-width or duty cycle is limited by the rise/fall time of the data and the bandwidth of the electrical amplifiers and the MZ modulator. In this experiment, the rise and fall time of the data are both 25ps and the bandwidth of the electrical amplifiers and the MZ modulator is larger than 30GHz. When the time delay is 1 bit or 100ps, a MD-NRZ signal is generated and the duty cycle is one.

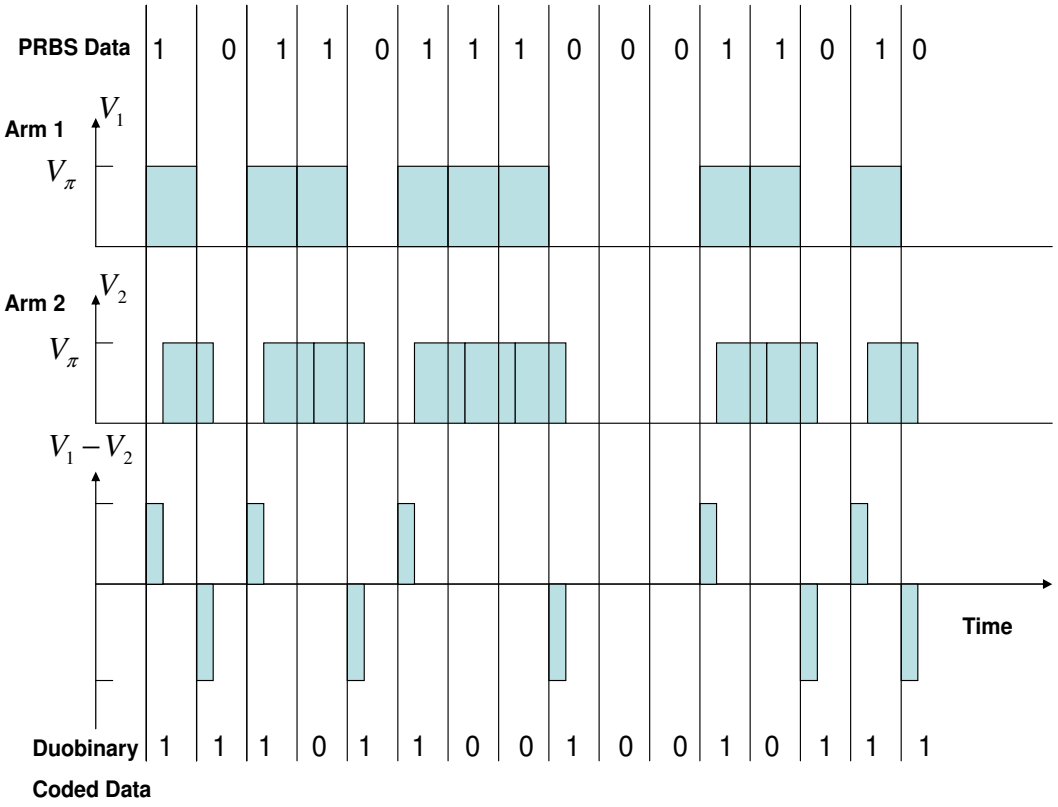

Figure 29. Principle of modified duobinary RZ generation

3.1.3 Results and Discussion

Figure 30 presents eye diagrams achieved by varying the delay between two arms of $LiNbO_3$ modulator. 100ps delay gets a MD-NRZ signal, while 50ps delay produces a MD-RZ signal with 50% duty ratio. The eye diagrams are measured by an oscilloscope

with 20GHz bandwidth. We can see that the smaller the time delay between the two-arm driven electrical signals, the smaller the duty cycle and the wider the spectrum. Because the rise and fall time of the electrical signal is 25ps, the shortest pulse-width of the optical signal is approximately 25ps. Figure 31 shows optical spectra of these signals with varying duty ratios.

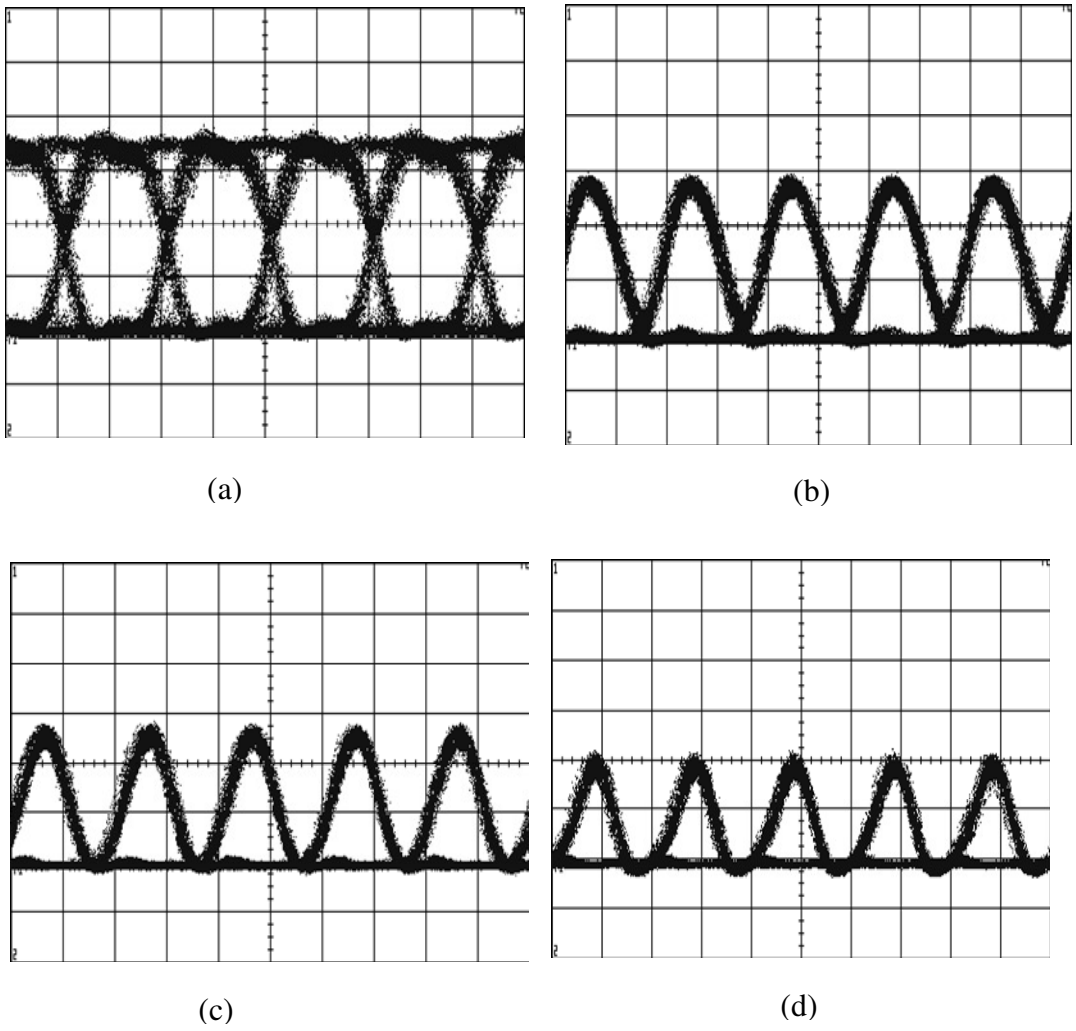

Figure 30. Measured typical eye diagrams with different time delays between two-arm electrical signals (50ps/div), (a) 100ps, (b) 50ps, (c) 40ps, and (d) 20ps

The bit error rate (BER) is also measured and shown in

Figure 32(a). Relative to NRZ signal, RZ has high receiver sensitivity and

Figure 32 shows the fact. The receiver for both NRZ and RZ modulation is a photo detector based on square-law (intensity) detection. In principle, NRZ and RZ should obtain the same quantum-limited receiver sensitivity. However, in practice RZ is found to be less susceptible to inter-symbol interference (ISI), and typically achieves 1- 2 dB better performance compared to NRZ. The RZ pulse shape also benefits from a soliton-like effect in optical fiber, suffering less distortion due to fiber nonlinearity compared to NRZ. For these reasons, RZ modulation is currently favored in ultra-long haul submarine systems where the use of more costly transmitters and receivers is justified.

When the signal is MD-NRZ, which is obtained by setting the delay equal to 100ps between two arms of the MZ modulator, the power sensitivity at a BER of 10^{-10} is -25.8dBm; however when the signal is MD-RZ and the time delay between two arm electrical signals is 40ps, the power sensitivity at a BER of 10^{-10} is -27.4dBm. There is an improvement of 1.6dB in power sensitivity is when MD-RZ signals are detected as compared to MD-NRZ signals [47].

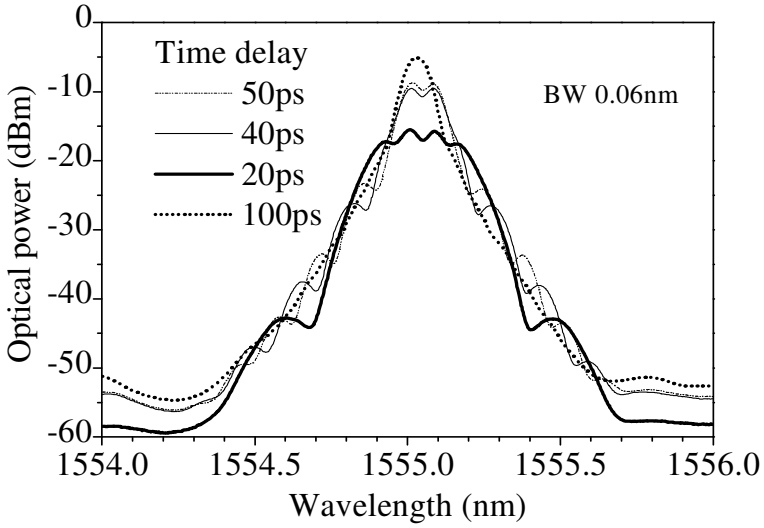

Figure 31. Measured typical optical spectra with different time delays between two-arm electrical signals

As the MZ modulator is driven asymmetrically, the modulated signal will be chirped. Experimental results show that the chirp is always negative no matter what kind of shape (NRZ or RZ) is obtained. Although the negative chirp benefits signal to transmit in the standard single mode fiber (SMF), the wide spectrum of the MD-RZ signal limits the maximum transmission distance over SMF.

Figure 32(b) shows eye diagram after the MD-RZ signal with a duty cycle of 0.5, when it is transmitted over 40km of SMF; the eye is distorted because of dispersion. The power penalty is also measured at BER of 10^{-9} to be 3.2dB; however the power penalty is only 0.1dB when the input signal is a chirp-free and regular RZ signal with the same extinction ratio and duty cycle as the MD-RZ signal [47]. This results show that the MD-NRZ or MD-RZ signal generated by this method might not be suitable for the signal transmission without dispersion compensation. However, for long distance transmission, the dispersion is always compensated in each amplifier span. Hence, it can prove to be useful in repeaterless fully compensated links. We demonstrated this fact by experimental results in next section.

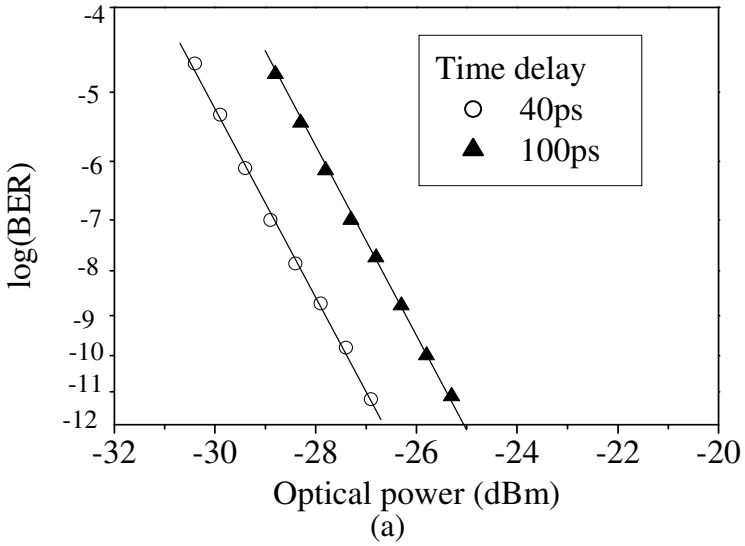

(a)

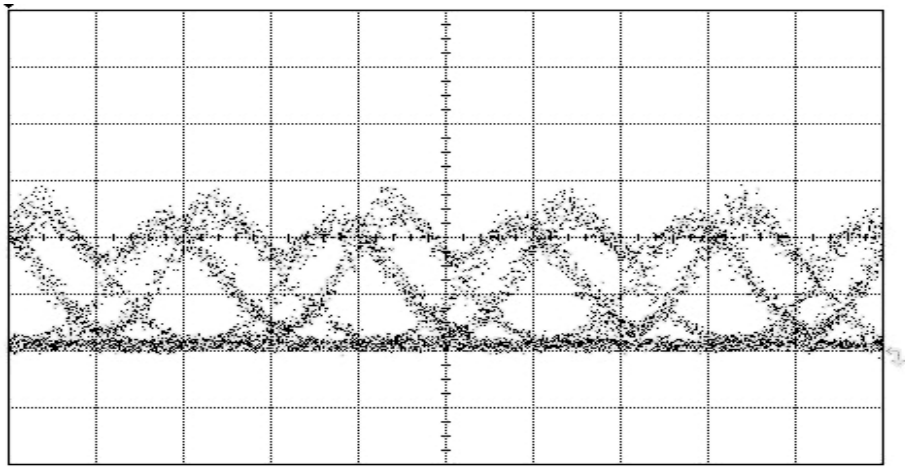

(b)

Figure 32. (a) Measured BER when modified duobinary signal operates at RZ and NRZ format. (b) Measured eye diagram when MD-RZ with a duty cycle of 0.5 is transmitted over 40km of SMF

In above section, we have demonstrated a method to generate modified duobinary return-to-zero (MD-RZ) signals by using only one single push-pull type MZ modulator. The duty cycle of the MD-RZ signals can be adjusted from 1 to 0.25 by changing the time delay of the two-arm driven electrical signals and the duty cycle is limited by the rise/fall time of the electrical signal and the bandwidth of the modulator and electrical amplifiers.

3.2 Performance of the proposed MD-RZ Transmitter

This section will cover the performance characteristics of proposed MD-RZ transmitter setup and its comparison with other MD-RZ generation techniques. Repeaterless transmission experiments have been performed for single channel and WDM MD-RZ signals over SMF. Repeaterless transmission can reduce network cost and simplify transmission systems [48], [49]. Repeaterless transmission is mainly limited to fiber non-linear effects such as self-phase modulation (SPM) and stimulated Brillouin scattering (SBS).

3.2.1 Repeaterless Transmission of 10Gbit/s MD-RZ Signal over 300km SMF-28

We experimentally demonstrate a repeaterless transmission of MD-RZ signal over 300km using backward Raman pump amplifier. This demonstration does not employ effective-area enlarged single-mode fiber (EE-SMF) and remote erbium-doped fiber amplifier (EDFA) set in the middle of the transmission line [50]. By using above mentioned techniques transmission distance can be increased beyond 300km. Significance of our experiment becomes more important as transmission media is conventional single mode fiber (SMF), which is widely deployed in the optical networks.

3.2.1.1 Experimental Setup

The experimental setup is shown in Figure 33. Modified duobinary return-to-zero (MD-RZ) signal is generated by driving a dual-arm $LiNbO_3$ modulator. PRBS word length of the electrical signals to drive the LN modulator is 2^{31}-1. Ten Gb/s binary data from the pattern generator is divided into two equal paths by an electrical coupler. One is delayed

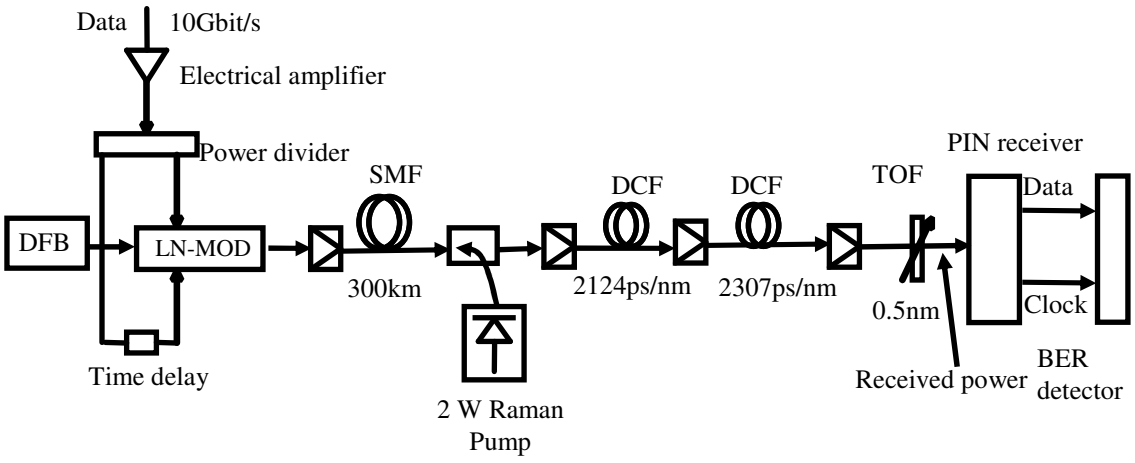

Figure 33. Experimental Setup for MD-RZ repeaterless transmission over 300km of SMF-28

by an electrical delay line and amplified to drive one arm of the modulator. The other is amplified and directly drives the second arm of the modulator. The amplitude of these divided electrical signals is equal to half-wave voltage of the LN-MOD. Electrical delay line can be adjusted to set the duty cycle of the MD-RZ signal. By setting the delay between two arms equal to 50 ps, a MD-RZ signal with 0.5 duty cycle can be generated. Modulator is biased such that it delivers minimum output power in the absence of data.MD-RZ signal with a duty cycle of 0.5 and a centre wavelength of 1550.47nm is amplified to 20.7 dBm by an EDFA before it is transmitted over 300km of standard single mode fiber with dispersion of approximately 17ps/nm/km and a total loss of 61.9 dB. A counter-propagation 2W Raman pump at 1450nm is used as a Raman amplifier. Optical signal-to-noise ratio (OSNR) of MD-RZ signal after the Raman pump is 17.5 dB. Total Raman on-off gain is approximately 12 dB. After the transmission, accumulated dispersion of fiber is partially compensated by two dispersion compensation fiber modules providing 4431ps/nm total compensation. Input power to these dispersion compensation fiber (DCF) modules was fixed at 0 dBm with EDFAs to minimize nonlinear effects in DCF. Dispersion under-compensation for this system is employed because some dispersion in standard SMF is compensated by SPM if the signal is chirp free or has very small chirp. An optical filter with a 3 dB bandwidth of 0.5nm was used in the receiver to suppress ASE noise from EDFAs. The signal is detected by a PIN receiver with a 3-dB bandwidth of 7GHz. Clock recovery is also realized in the PIN receiver.

3.2.1.2 Results and Discussion

Eye diagrams of MD-RZ signal for back-to-back transmission and after 300km transmission are shown as inset (i) and (ii) in Figure 34 respectively. Bit error rate (BER)

plot is also measured and shown as inset (iii). For back-to-back measurements attenuators are used to emulate fiber loss. Power penalty after 300km transmission over SMF is 2.7 dB for BER = 10^{-9}.

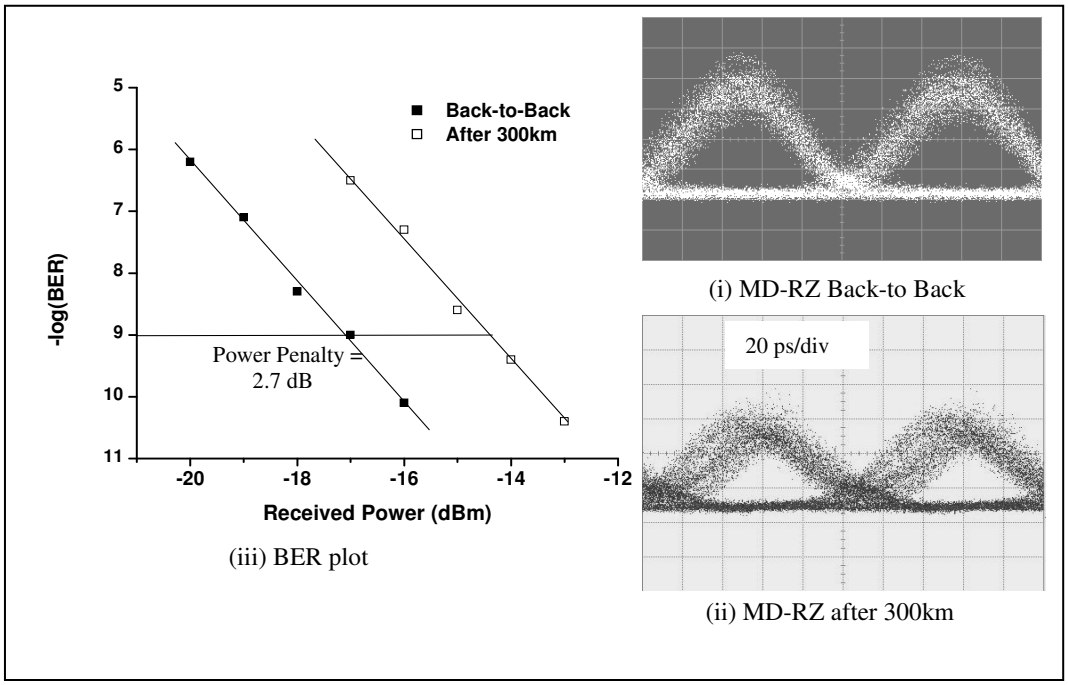

Figure 34. (i) MD-RZ back-to-back eye diagram (ii) MD-RZ eye after 300km transmission over SMF (iii) Measured BER against received power for back-to-back and 300km repeaterless transmission

In this section we have successfully demonstrated repeaterless MD-RZ signal transmission over 300km of single mode fiber. This MD-RZ signal is generated by our novel and cost effective technique employing only one dual arm $LiNbO_3$ modulator. A counter-propagating Raman pump is used to provide extra gain. Total on-off Raman gain is 12dB and power penalty for this transmission is 2.7 dB. Results indicate that MD-RZ signal generated by our novel technique can tolerate higher input power and can be transmitted on long SMF-28 without repeaters [51].

3.2.2 8 x 10 Gb/s WDM repeaterless transmission over 240 km of SMF

Wavelength division multiplexing (WDM) is a very attractive solution to realize high capacity transmission systems. WDM repeaterless transmission becomes significant for long-haul networks especially if it is over conventional SMF. Here we demonstrate eight equally spaced wavelengths in the C-band simultaneously modulated by a dual-arm MZ modulator to generate 10 Gb/s MD-RZ signals and its repeaterless transmission over 240km of conventional SMF. The carrier wavelengths of eight channels ranged from 1554.56 to 1560.13.4nm with l00 GH channel spacing. The experimental setup for MD-RZ WDM experiment is shown in Figure 35.

3.2.2.1 Experimental Setup

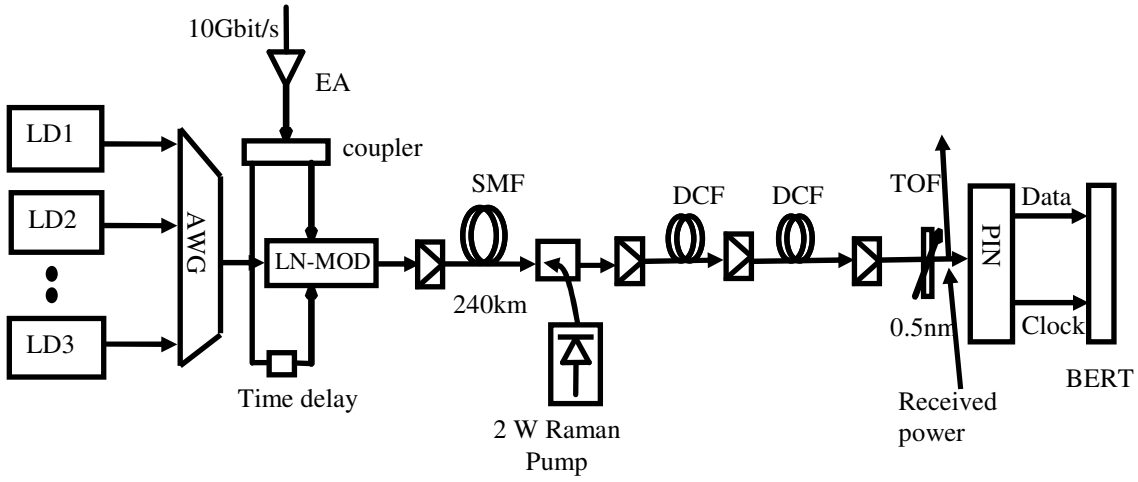

Figure 35. Experimental Setup for WDM MD-RZ repeaterless transmission over 240km of SMF

Eight equally spaced wavelengths separated by 100 GHz, were multiplexed using an arrayed waveguide grating (AWG) and simultaneously modulated with a dual-drive $LiNbO_3$ modulator to generate eight MD-RZ channels. PRBS word length of the electrical signals to drive the LN modulator is 2^{31}-1. 10-Gbit/s binary data from the

pattern generator is divided into two equal paths by an electrical coupler. One is delayed by an electrical delay line and amplified to drive one arm of the modulator. The other is amplified and directly drives the second arm of the modulator. The amplitude of these divided electrical signals is equal to half-wave voltage of the LN-MOD. Electrical delay line can be adjusted to set the duty cycle of the MD-RZ signal. By setting the delay between two arms equal to 50 ps, a MD-RZ signal with 0.5 duty cycle is generated.

Total input power into the fiber is set to 20.4 dBm by an EDFA. Fiber dispersion is approximately 17 ps/nm/km. Received power after the transmission is approximately -40 dBm per channel. A counter-propagation 2W Raman pump is used as a Raman amplifier at the end of transmission fiber and it uses last portion of fiber as gain medium. Total Raman on-off gain per channel is approximately 11 dB.

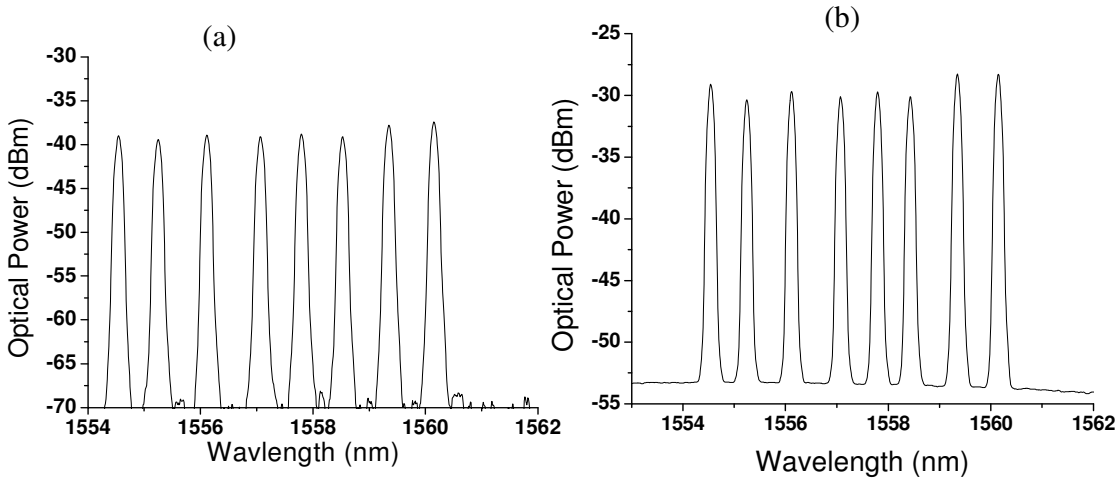

Figure 36. Optical spectra (RW: 0.1nm): (a) before amplification and (b) after Raman amplification

Figure 36 shows optical spectrum for all eight channels before and after Raman amplification. After transmission, the accumulated dispersion of the transmission fiber is partially compensated by two dispersion compensation fiber modules. Input power to these DCF modules is fixed at 0 dBm to avoid nonlinear effects in DCF. Dispersion

under-compensation for this system is employed because some dispersion in standard SMF is compensated by SPM.

3.2.2.2 Results and Discussion

As an example, eye diagrams of channel 4 for back-to-back transmission and after 240km transmission are shown as inset (i) and (ii) in Figure 37 respectively. BER plots for back-to-back transmission, and repeaterless transmission for channel 4 and channel 5 over 240km of fiber are also measured and shown.

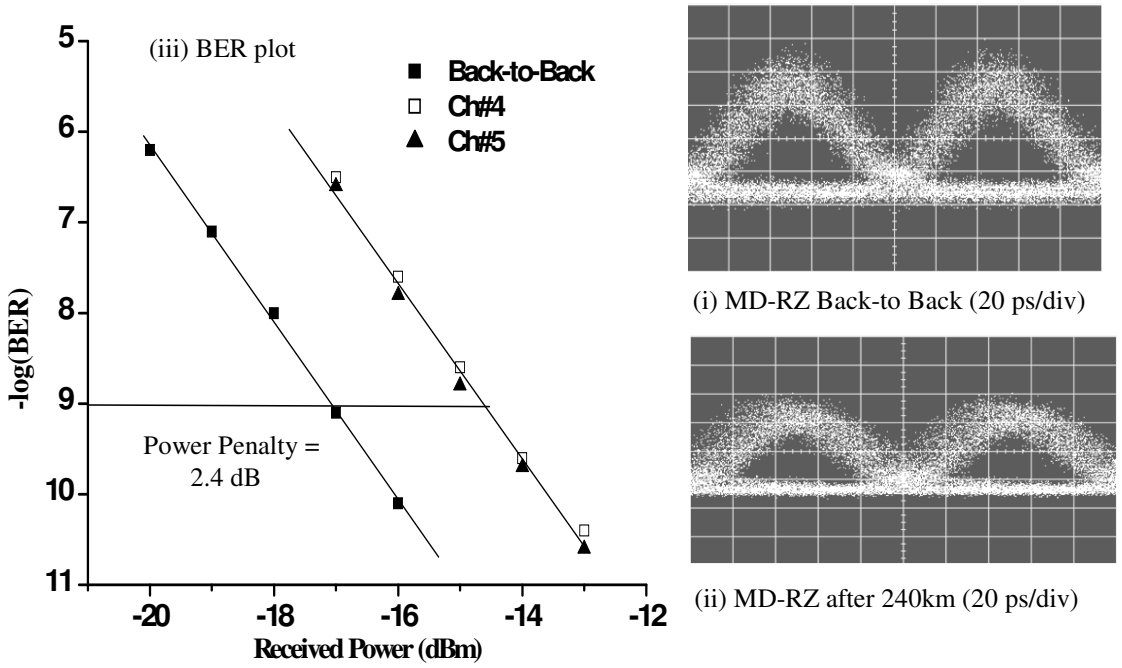

Figure 37. (i) MD-RZ back-to-back eye diagram (ii) MD-RZ eye diagram after 240km transmission over SMF (iii) Measured BER for back-to-back transmission and 240km repeaterless transmission

For back-to-back measurements attenuators are used to emulate fiber loss. Power penalty after 240km transmission over SMF-28 is approximately 2.4dB for BER = 10^{-9}. No BER floor is observed for channel 4 and channel 5. This experiment employs conventional SMF which is widely deployed in field and hence more practical than using enhanced area or dispersion shifted fiber [52], [53]. We also did not use passive remotely pumped

optical amplifier within the fiber or FEC limits. Above mentioned techniques may result in longer distance but have practical limitations and complex setup. In this section we have successfully demonstrated repeaterless transmission of eight WDM MD-RZ equally spaced channels at 100GHz over 240km SMF-28. These MD-RZ signals were simultaneously modulated by our novel and cost effective technique employing only one dual arm $LiNbO_3$ modulator. A counter-propagating Raman pump is used to provide extra gain. Total on-off Raman gain is 11dB/channel and power penalty is 2.4 dB for the worst channel. All received channels exhibit optical SNR more than 20 dB [54].

3.3 Numerical Analysis of Advanced Optical Modulation Formats

In this section we compare the performance of the modified duo-binary RZ (MD-RZ) signals generated by three different techniques. Our numerical results show that MDRZ signal generated by our novel technique employing one dual arm Mach-Zehnder modulator tolerate higher input power, dispersion and can be transmitted over longer single mode fiber.

3.3.1 Comparison of MD-RZ transmitter schemes

Generally, duo-binary RZ signal can be generated by two cascaded intensity modulators (Figure 38) [42] or a phase modulator followed by a delay-line interferometer [55]. In previous sections we have already proposed and experimentally demonstrated a novel technique to generate a modified duo-binary return-to-zero (MDRZ) signal using a single dual arm Mach-Zehnder modulator and its repeaterless transmission for single channel and WDM signals over conventional 300km and 240 SMF respectively.

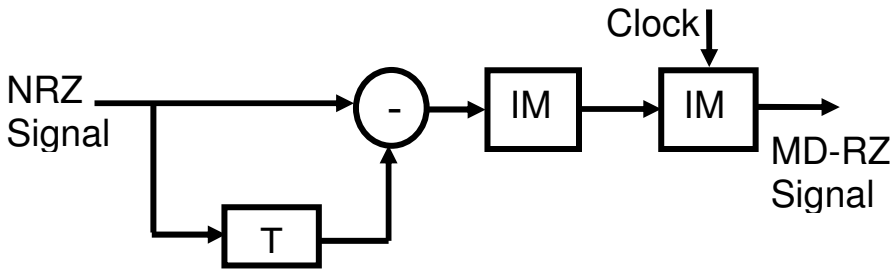

Figure 38. Conventional MD-RZ transmitter

Our scheme has a simple configuration and MDRZ signal with different duty cycles can be generated just by changing the delay of the electrical signals added on two arms of the modulator. In this section we will numerically compare their performances of all three methods and show that our technique performs better. Experimental data and simulation results using VPI Transmissionmaker are presented in this section. All the simulations are performed for the data bit-rate of 10 Gb/s**,** and dispersion compensation fiber (DCF) is set to provide full compensation. Table 3 presents some of the common parameters for the simulation environment.

Table 3. Common simulation parameters

Data Rate	10 Gb/s
PRBS	2^{31}-1
SMF Loss	0.2 dB/km
DCF Loss	0.4 dB/km
SMF dispersion	17 ps/nm/km
DCF dispersion	-100 ps/nm/km
NF	4.5 dB

MDRZ-1 is the signal generated by a phase modulator, MDRZ-2 by two intensity modulators and MDRZ-3 by our novel scheme employing one dual-arm $LiNbO_3$ modulator. The performance of an optical communication system can be estimated with the Q factor which represents the signal to noise ratio (SNR) at the input of the receiver decision circuits. Q factor can be defined as

$$Q = \frac{|\mu_1 - \mu_0|}{\sigma_1 + \sigma_0} \tag{7}$$

μ_1 and μ_0 are the mean values for logical "1s" and "0s", σ_1 and σ_0 are their corresponding standard deviation.

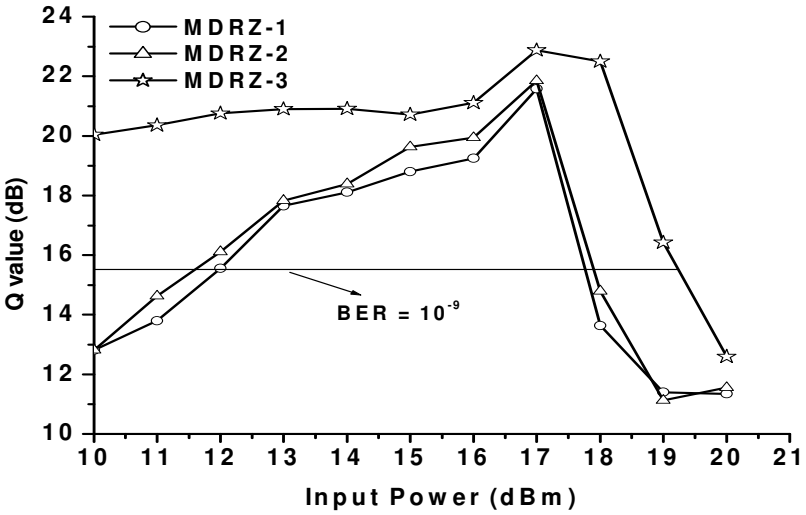

Figure 39. Q value as a function of input power

We set SMF-28 length to be 220km and Q values are plotted against input power. Numerical simulation results are plotted in Figure 39. As the input power is increased nonlinearities mainly SPM and SBS take over and one can observe a sharp decrease in Q value after 17 dBm. MDRZ-3 performs better than the other two, and even at 19 dBm BER is still better than 10^{-9}. Overall MDRZ-3 can tolerate high input power. Next,

maximum transmission distance is plotted against input power for BER value of $10^{-9.}$ Results are shown in Figure 40.

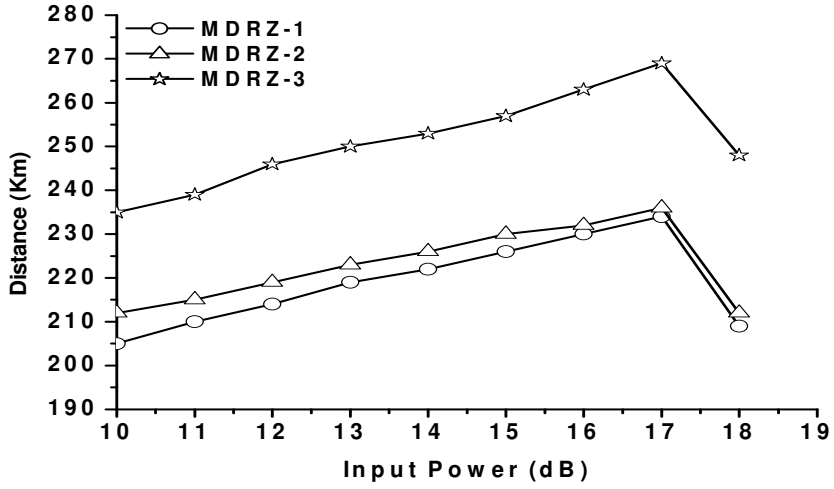

Figure 40. Maximum transmitted distance as a function of input power for BER 10^{-9}

MDRZ-3 shows improvement up to 35km in transmission length for various input power levels. At 17dBm, the maximum transmission length of our scheme is approximately 265km,while the maximum transmission distance is only 230km when the other two techniques are employed. There is no much difference in performance between MDRZ-1 and MDRZ-2.

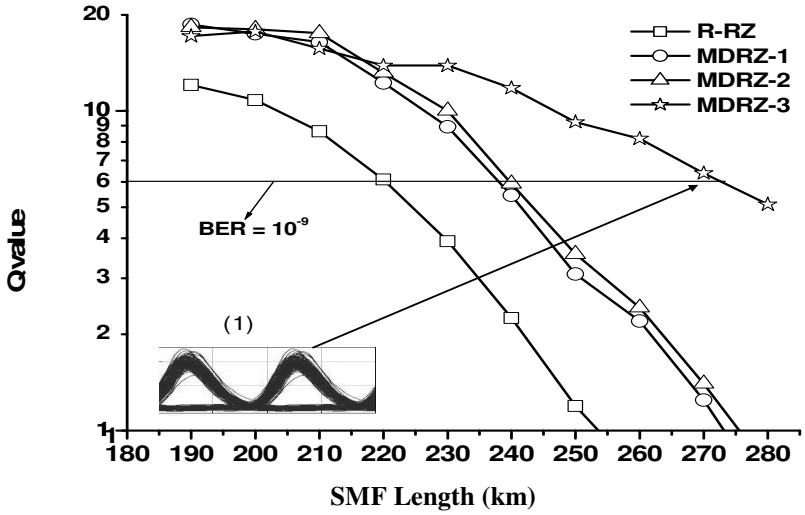

Figure 41. Repeaterless transmission distance

Long repeaterless transmission is an important task which in affect reduces network cost and simplifies transmission systems. The input power into the SMF is kept at 17dBm and Q values are plotted against distance. All three techniques exhibit similar performance for shorter distance. However MDRZ-3 differentiates with the other two and shows marked improvement in maximum transmission distance. For BER of 10^{-9}, MDRZ-3 approximately covers 270km and other two methods only transmit over 240km. Resulting plot is drawn in Figure 41 .

We have numerically and experimental demonstrated that MDRZ signals generated by our technique employing low cost dual-arm $LiNbO_3$ modulator exhibit high tolerance to nonlinear effects and high SBS threshold. Repeaterless transmission of MDRZ signals over 300km of SMF is achieved with this technique [56].

CHAPTER 4

PHASE-SHIFT KEYING MODULATION FORMATS

The differential phase shift keying (DPSK) and differential quadrature phase-shift-keying (DQPSK) modulation formats are recently gained much attention for ultra high speed and high spectral efficiency (SE) WDM transmission systems due to their inherent 3-dB better receiver sensitivity. Design of Mach-Zehnder delay interferometer is of significant importance in direct detection of these phase coded formats. In this chapter, we present how optimization of free spectral range helps these modulation schemes in the presence of narrow-band optical filters. We also experimentally demonstrate wavelength offset tolerance for different designs of high data-rate DPSK and DQPSK transmitters.

4.1 Impact of Free Spectral Range Optimization on RZ/NRZ DQPSK Modulation Format with Strong Optical Filtering

4.1.1 Motivation

In the deployment of high spectral-efficient WDM transmission systems, narrow optical filtering effects on such modulation formats are of key importance because these signals pass through various narrow optical filters at different stages. In this regard, design of Mach-Zehnder delay interferometer (MZ-DI) in DQPSK decoder becomes very important since choice of optimal FSR helps us relieve some degradation due to strong optical filtering, and we can realize high bit rate and high spectral efficient WDM DQPSK transmission systems. In this paper, we present impact of tuning FSR in the presence of strong optical filtering for 100 Gb/s and 50 Gb/s DQPSK signals via experimental and simulation results. Both return-to-zero (RZ) and non-return-to-zero

(NRZ) pulse shaping is employed in DQPSK transmitter. Numerical simulations were performed with a commercial software tool VPI Transmission maker. Similar study has been performed for DPSK format recently [57]- [59]

4.1.2 Experimental Setup

Figure 42 shows the schematic of the experimental setup. In the transmitter, the first dual-drive Mach-Zehnder modulator (MZM) was driven by a full symbol-rate clock (biased at 1.5 Vπ) to generate 50% RZ pulse. We use the second MZM in a push-pull configuration, and the following phase modulator to generate DQPSK-modulated signal, where the required 50 Gb/s electrical NRZ signals (for 100Gb/s optical DQPSK signal generation) was obtained by using electrical multiplexing technique. In the receiver, we use an EDFA as pre-amplifier followed by a 1.4 nm optical filter, a tunable DQPSK delay-interferometer and a balanced detector. Bit error rate (BER) of the considered tributary versus the optical power entering into the receiver (i.e. the received power) was measured by using the 12.5 Gb/s BERT.

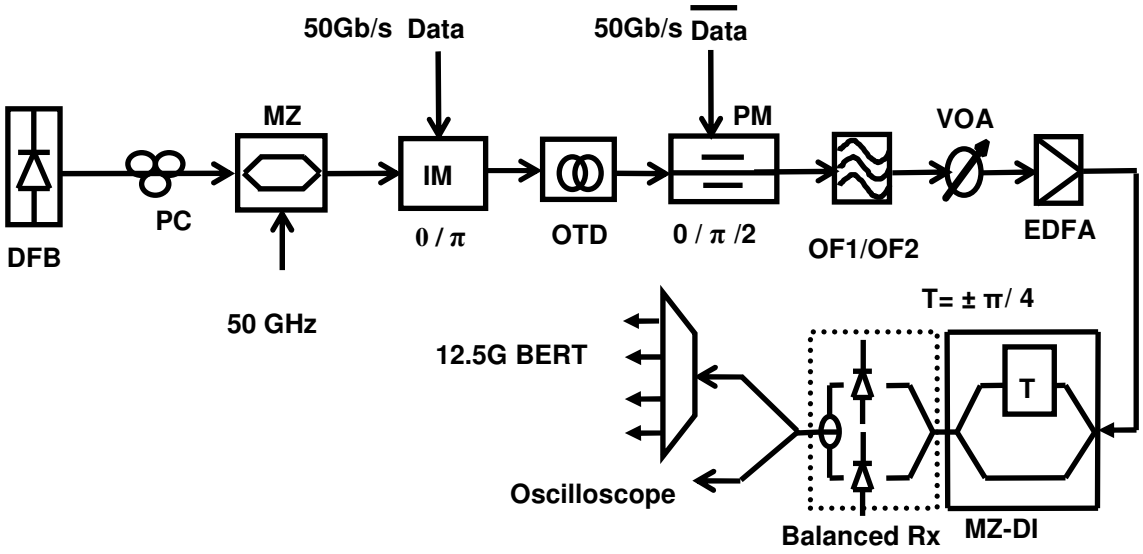

Figure 42. Experimental setup for RZ-DQPSK transmitter and receiver

4.1.3 Results and Discussion

Figure 43 shows the measured BER at one tributary of the 100 Gb/s RZ-DQPSK signal with different DI FSR and in-line filter configurations using 2^7-1 PRBS pattern. The measured 3 dB bandwidth for OF1and OF2 are 90 GHz and 62.5GHz, respectively. We can observe that the performance with 55 GHz FSR (0.55 bit rate) is substantially better than the case with 44.5 GHz FSR (0.445 bit rate) for all the three conditions (more than 6 dB difference at 10^{-3} with OF2). This clearly shows that increasing FSR will substantially help the transmission even in the presence of narrow band optical filters, which in turn can help us achieve more SE high bit-rate WDM systems.

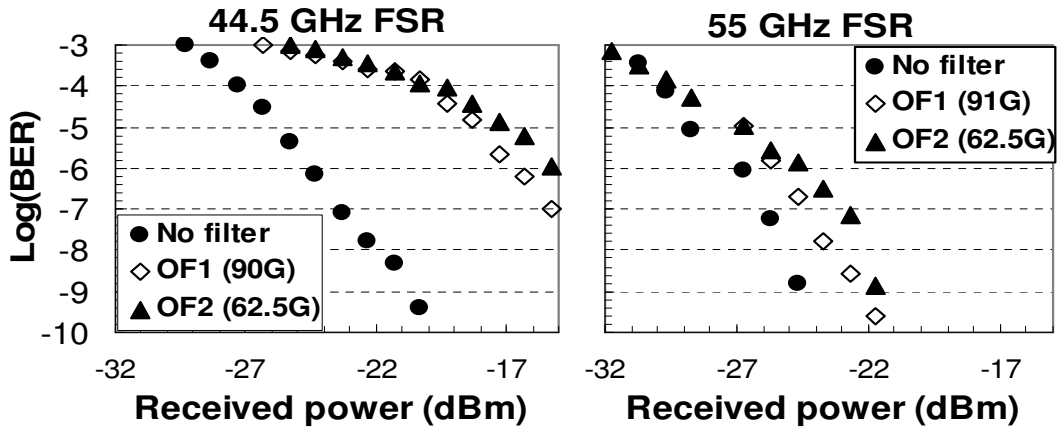

Figure 43. Measured BER at one tributary of the 100 Gb/s RZ-DQPSK signal under different conditions

In order to further verify we also performed simulations using VPI Transmission maker. 100 Gb/s and 50 Gb/s DQPSK signal with both RZ (50% duty cycle) and NRZ pulse shaping were employed. A PRBS length of 2^{30}-1 was used. The OSNR was set to 20dB (0.1nm resolution bandwidth). We used various narrow band fifth-order Gaussian optical filters with 3-dB bandwidths ranging from 0.35R to 0.55R before balanced receiver for

detection. We calculated BER versus FSR/R for these optical filters. BER is converted into Q (dB) by relationship:

$$Q = 20\log\left[\sqrt{2} \times erfc^{-1}(2BER)\right] \qquad (8)$$

Relative Q penalty is calculated by normalizing by its own optimal Q value and then plotted against FSR/R ratio for each filter for better visualization.

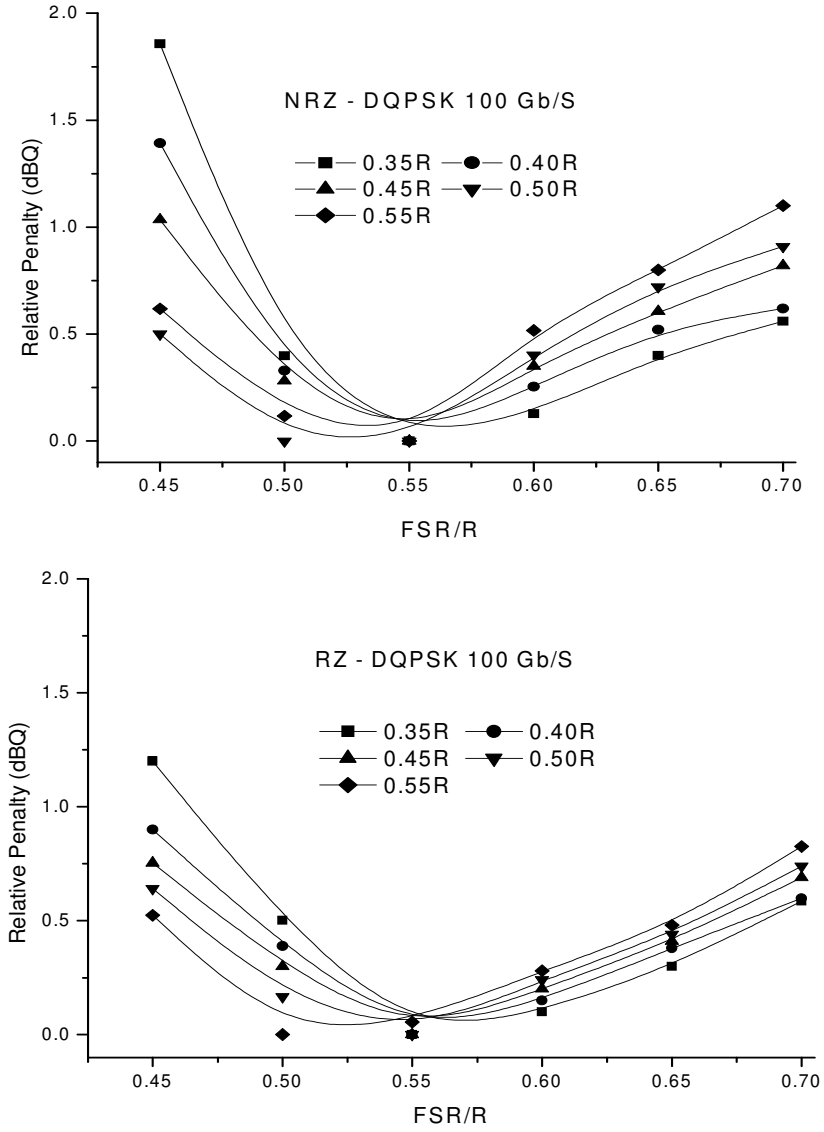

Figure 44. Relative Q penalty vs. FSR/R for a) 100Gb/s NRZ-DQPSK, b) 100Gb/s RZ-DQPSK

Figure 44(a) and (b) show relative Q penalty as a function of FSR/R for 100 Gb/s RZ/NRZ DQPSK signals, which clearly exhibits that for narrow optical filters optimal FSR/R ratio is greater than half-bit FSR (nearly 5% increase from exact half-bit FSR). Relative Q penalty between optimal FSR and exactly half-bit FSR is about 0.5dB for the narrowest filter (0.35R), and it decreases as we increase the filter bandwidth. For filters with bandwidths greater than 0.55R and beyond, optimal FSR converges to half-bit FSR as expected.

If MZ-DI is considered as a filter (Figure 45), its bandwidth scales with FSR, larger FSR results in increased width of DI which helps in relieving the degradation due to narrow optical filters [58].

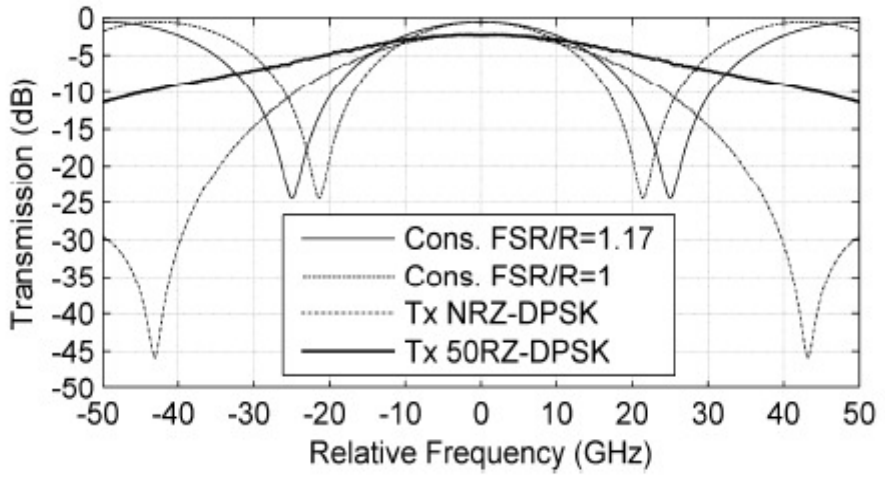

Figure 45. Transmission plot for the constructive port for MZ-DI with FSR/R=1 and 1.17 at 42.8 Gbps

There is a sharp increase in penalty for FSR smaller than half-bit in plots and this penalty is greater for NRZ pulse shape than RZ pulse shape. This concludes that FSR optimization helps NRZ pulse shape more than RZ pulse shape. This is consistent with RZ/NRZ DPSK results presented in [57]. MZ-DI set to less than 1 bit delay (higher FSR) results in partial interference between a bit with itself rather than neighboring bit. With

RZ pulse shape, energy is more concentrated in the middle of the bit period and for NRZ pulse energy is evenly distributed for the whole bit period, so RZ pulse shape is inherently tolerant to inter symbol interference (ISI). Due to this, moving away from optimal FSR in case of NRZ pulse shape, results in more penalty than RZ pulse shape.

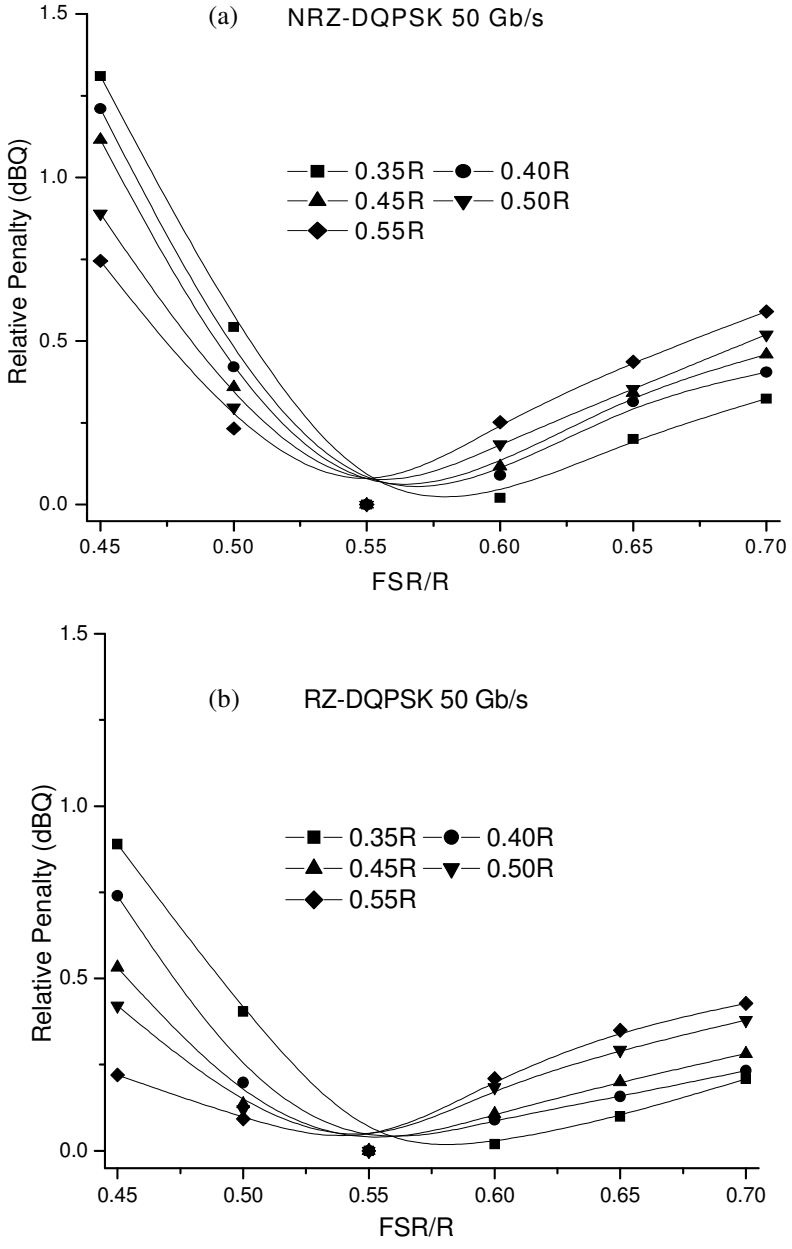

Figure 46. Relative Q penalty vs. FSR/R, a) 50Gb/s NRZ-DQPSK, b) 50Gb/s RZ-DQPSK

Figure 46 (a) and (b) show relative Q penalty as a function of FSR/R for 50 Gb/s RZ/NRZ DQPSK signals. Similar observations can be made from this plot as well.

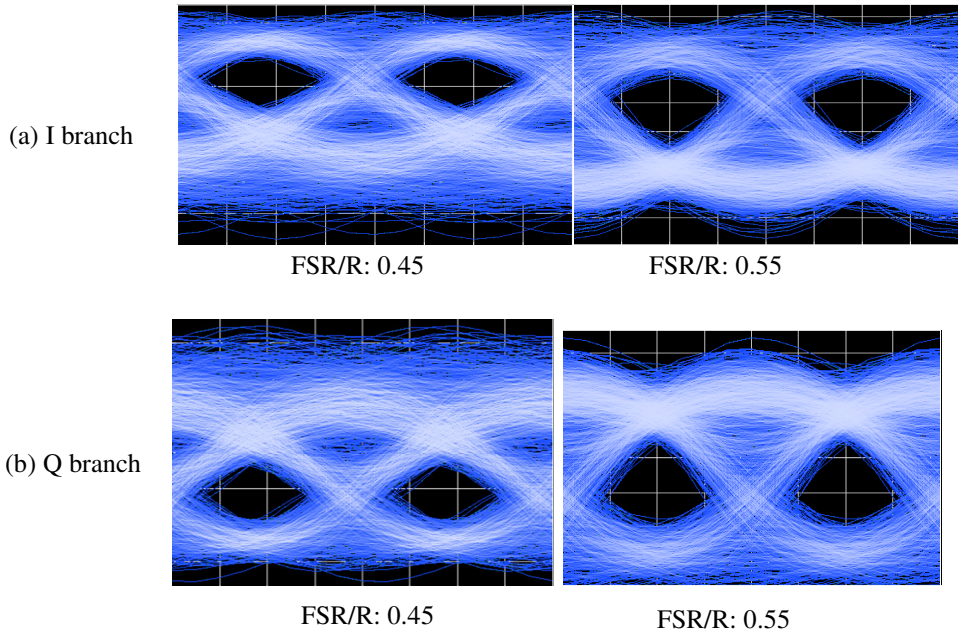

Figure 47. Simulated Eye diagrams for 100 Gb/s RZ-DQPSK with 0.40R optical filter a) I Branch, b) Q Branch

Simulated eye diagrams are presented in Figure 47 for both I and Q branch of 100 Gb/s RZ-DQPSK signal for FSR/R ratio of 0.45 and 0.55 with 0.4R optical filter used before reception. In case of larger FSR/R ratio (0.55) eye opening is obviously better for both the I and Q branch DQPSK signals.

With both experiments and simulations employing high data-rate (100 Gb/s, 50Gb/s) RZ/NRZ DQPSK signals, we show that the significant performance improvement can be achieved by tuning FSR of the DQPSK demodulator beyond half-bit rate when strong optical filters are present in the system. This FSR optimization of high data-rate signals helps NRZ pulse shapes more than RZ pulse shapes due to inherent tolerance of RZ pulse

shape to Inter Symbol Interference (ISI).

4.2 Investigation of Robustness to Wavelength Offset for DPSK and DQPSK Transmitter System

4.2.1 Motivation

Differential phase shift keying (DPSK) has recently been studied intensively due to its advantages of increasing transmission capacity and minimizing the system degradations due to fiber impairments in dense-wavelength-division-multiplexed (DWDM) networks [60]. Mach-Zehnder delay interferometer (MZ-DI) plays an important role in direct detection of these phase modulated signals. Any wavelength offset between optical source and MZ-DI will result in non-optimal interference at its output ports and can cause severe system degradations and receiver power penalties. Phase modulation can be achieved either by using a straight-line phase modulator (PM) or by using a Mach-Zehnder (MZ) intensity modulator (IM). In differential quadrature phase shift keying (DQPSK) transmitters, the phase shifts of π and $\pi/2$ can be achieved by cascading phase modulators or MZ modulators in any combination and sequence [61]. While DPSK signal by a PM has inherent chirp, MZ modulator can generate chirp-free DPSK signal with perfect π phase shift since it modulates the phase along the real axis of the complex optical field. It has been verified with experiments that using an MZM as phase modulator is useful in imperfect conditions such as low driving voltage since it only affects residual intensity dips leaving perfect π phase shift intact [2]. In this article, we analyzed and experimentally measured wavelength offset penalties for DPSK and DQPSK signal when phase and intensity modulators are interchanged.

4.2.2 Experimental Setup

Figure 48 shows experimental setup to measure wavelength offset tolerance for 40Gb/s DPSK signals generated by a PM and a MZ modulator. The output of a DFB laser was modulated by 40 Gb/s electrical NRZ signals. The 40Gbit/s electrical signals were generated from a 40Gbit/s pattern generator. Pseudorandom bit sequence (PRBS) length of data was set to 2^{15}-1.

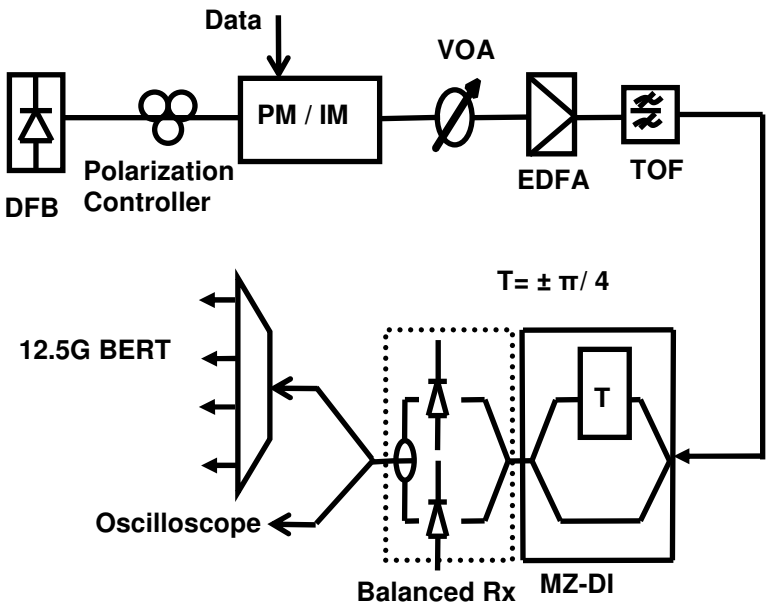

Figure 48. Experimental setup for DPSK transmitter and receiver

DPSK receiver consists of a pre-amplifier, a tunable optical filter with 3-dB bandwidth of 0.6nm, a MZ-DI with 1 bit delay and a balanced receiver. An electrical de-multiplexer is used to de-multiplex 40 Gb/s to 10Gbit/s signal for BER measurements. Phase modulation was achieved by using either a PM or MZ modulator resulting in two different DPSK transmitter setups.

The serial DQPSK transmitter setup as presented in Figure 49 consists of a MZ modulator driven by 12.5 GHz clock to produce career-suppressed RZ pulse shape from

DFB laser output. Then DQPSK coding is achieved either by cascading two phase modulators or by cascading a PM and a MZ modulator. As a result we have two different DQPSK transmitter setups. Two complementary 25 Gb/s NRZ data signals with a PRBS length of 2^7-1 are used to drive both cascaded modulators in order to achieve aggregate bit rate of 50Gb/s (25Gbaud). Modulation depth of one modulator is set to π and modulation depth of other modulator is set to $\pi/2$ by adjusting bias point and driving voltage.

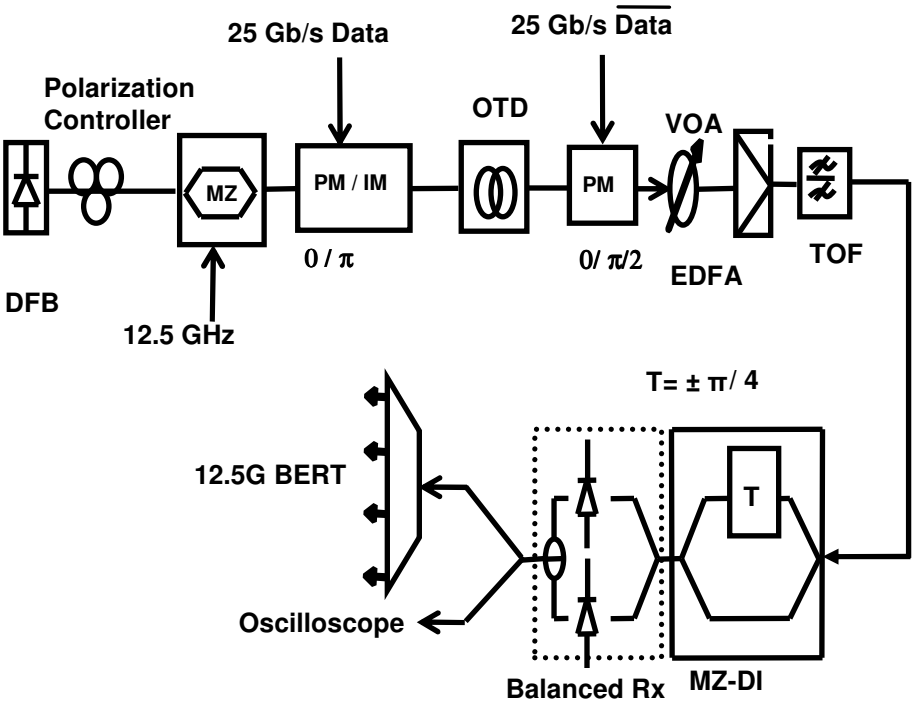

Figure 49. Experimental setup for DQPSK transmitter and receiver

50 Gb/s RZ-DQPSK signal generated in this manner is detected by a DQPSK receiver composed of a pre-amplifier, a tunable optical filter and MZ-DI with free spectral range (FSR) ratio of 25 GHz. A balanced receiver is used in the end for the detection. In order to avoid using a DQPSK pre-coder, we recorded 127 bit sequence and programmed to bit error rate tester (BERT) to measure bit error rate (BER) ratios for de-multiplexed signals.

BER of the considered tributary versus the optical power entering into the receiver (i.e. the received power) was measured by using the BERT. A general view of experimental setup is shown in Figure 50 and Figure 51.

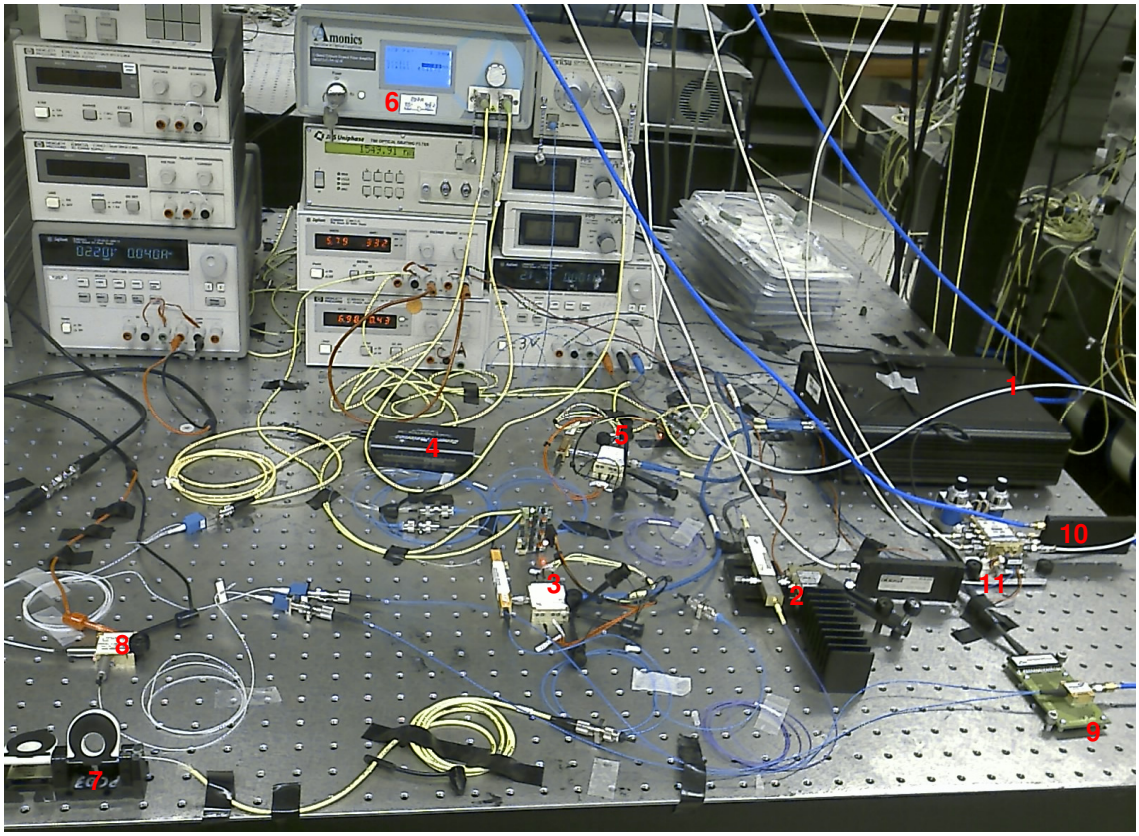

Figure 50. A general view of experimental setup

- 1 Centellax 40 Gb/s PRBS generator
- 2 Lucent dual-arm MZ modulator
- 3 EOSPACE 40Gb/s phase modulator
- 4 Variable optical delay line (General Photonics)
- 5 EOSPACE 40Gb/s intensity modulator
- 6 EDFA

- 7 Polarization Controller
- 8 DQPSK demodulator (Optoplex)
- 9 Balanced receiver (U^2t Photonics)
- 10 SHF De-Mux (50 Gb/s to 12.5 Gb/s)
- 11 Electrical delay line

For both DPSK and DQPSK setups, we changed the wavelength offset between incoming optical signal and MZ-DI by tuning DFB laser. A mismatch is created at MZ-DI outputs which resulted in performance penalty. We recorded these penalties and BER for all configurations of DPSK and DQPSK transmitters.

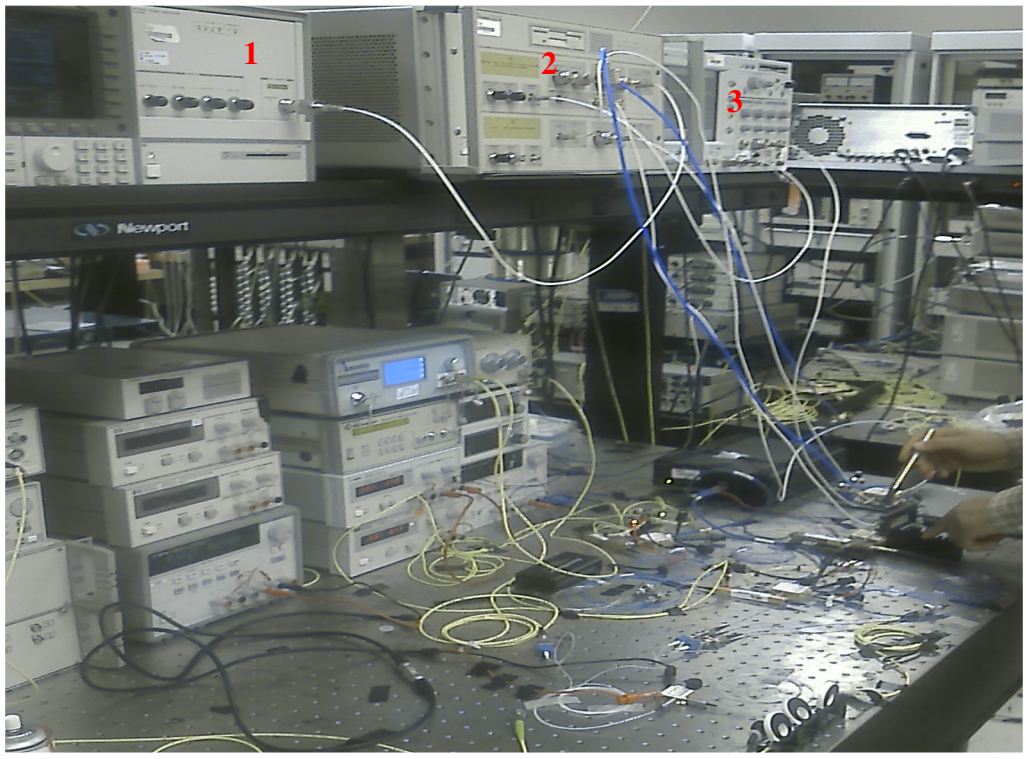

Figure 51. Another view of experimental setup

- 1 HP 703040A Pattern generator (1-20GHz)
- 2 Agilent 70843C Error performance analyzer (0.1-12.5 Gb/s)
- 3 Agilent 8610A Oscilloscope

In case of DPSK reception, DPSK receiver needs an optical decoder. The DPSK decoding method is achieved by comparing the phase of two sequential bits. An incoming DPSK optical signal is first split into two beams with equal intensities, in which one beam is delayed in space by an optical path difference that introduces a time delay corresponding to one bit. The two beams in the two paths are then coherently recombined to interfere each other constructively or destructively. The interference intensity is measured and becomes the intensity-keyed signal. A typical optical system for such a purpose is Mach-Zehnder interferometer, forming an optical DPSK Demodulator. Time delay between two arms of MZ interferometer depends on the data rate ($1/B$). In optical DQPSK, information is encoded in the differential optical phase between successive bits. Since each symbol transmits 2 bits of information, the symbol rate is equal to half the total bit rate B. DQPSK transmitter consists of a digital precoder and optical encoder and then DQPSK receiver would need a decoder. In DQPSK receiver decoding is performed optically, using an optical delay-and-add structure to provide decoding sensitive to differential optical phase shifts without needing a coherent local oscillator. The decoder structure usually comprises of a pair of Mach-Zehnder interferometers, each with an optical delay τ equal to the symbol period $2/B$. The differential optical phase between MZ interferometer arms is set to $\pi/4$ and $-\pi/4$ for upper and lower branches respectively. Balanced optical detectors are employed for each interferometer.

4.2.3 Results and Discussion

Figure 52 shows recorded power penalties at BER of 10^{-9} for 40Gb/s DPSK signals generated by a PM and MZ modulator. The balanced receiver sensitivity for DPSK signals was -22.5dBm at BER of 10^{-9}. Measured results show that DPSK signals produced by a MZ modulator are more robust to wavelength offset as compared to DPSK signals generated by a PM. Performance penalty difference is close to 2.5dB at wavelength offset of 0.04nm.

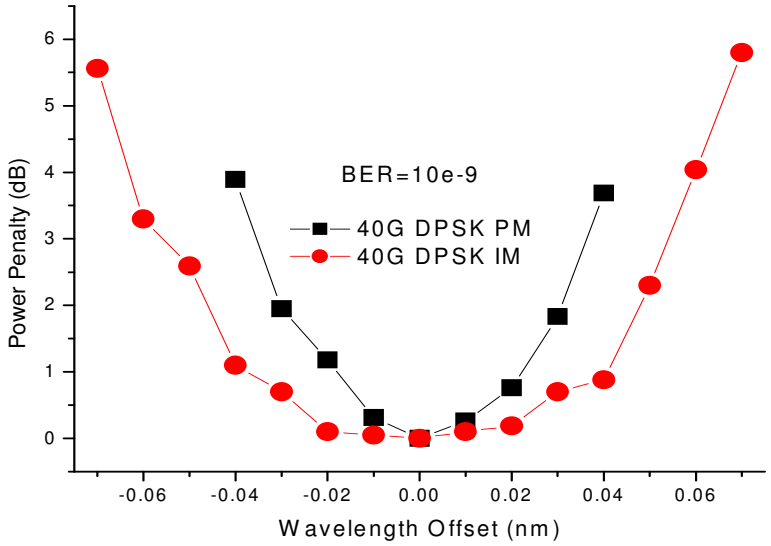

Figure 52. Measured power penalties vs. wavelength offset for 40 Gb/s DPSK signals

Figure 53 shows eye diagrams at wavelength offset of 0.04nm. It is clear that 40 Gb/s DPSK-IM still has open eye at same offset as compared to DPSK-PM. Eye for DPSK signals generated by a PM closes faster relative to DPSK signals by an IM. Any transmitter imperfection in case of MZ modulator being used as a PM only affects the residual intensity dips and chirp free DPSK signal with perfect π phase shift can be generated.

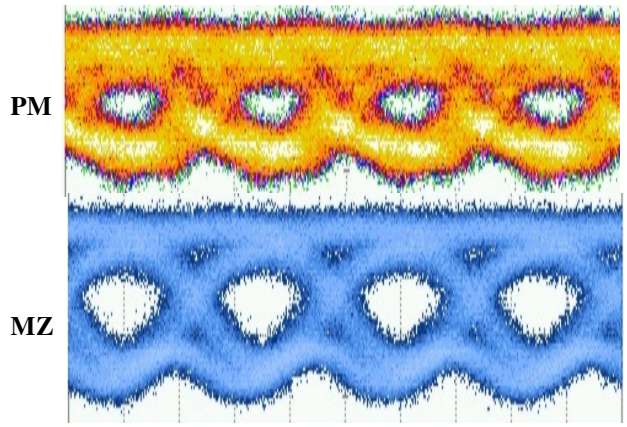

Figure 53. Eye diagrams (10ps/div) for 40 Gb/s DPSK signal at 0.04nm offset generated by a PM and a MZ modulator

DQPSK signals are inherently more sensitive to wavelength offset penalties as compared to DPSK signals. First, for the same bit rate MZ-DI delay has twice the delay for DQPSK signals resulting in twice the penalty due to phase mismatch. Secondly, DQPSK signals use four symbol constellations as compared to two symbols in DPSK signals. These higher numbers of optical phases in DQPSK format make it more sensitive to phase errors [62].

Figure 54 (a) shows measured power penalties at BER of 10^{-9} for one tributary plotted against wavelength offset for 50 Gb/s RZ-DQPSK signals. Receiver sensitivity for RZ-DQPSK signals using balanced receiver is recorded at -26.6dBm at BER of 10^{-9}. Measured results exhibit increased power penalty in case of DQPSK setup comprising two cascaded phase modulators. We can observe 0.5dB improvement at wavelength offset of 0.03nm for IM-PM setup. This reduced penalty can be attributed to the replacement of phase modulator with IM in DQPSK transmitter. Figure 54 (b) shows eye diagrams at 0.03nm offset and it is seen that diagrams measured in DQPSK setup consisting of a cascaded PM and IM is relatively open.

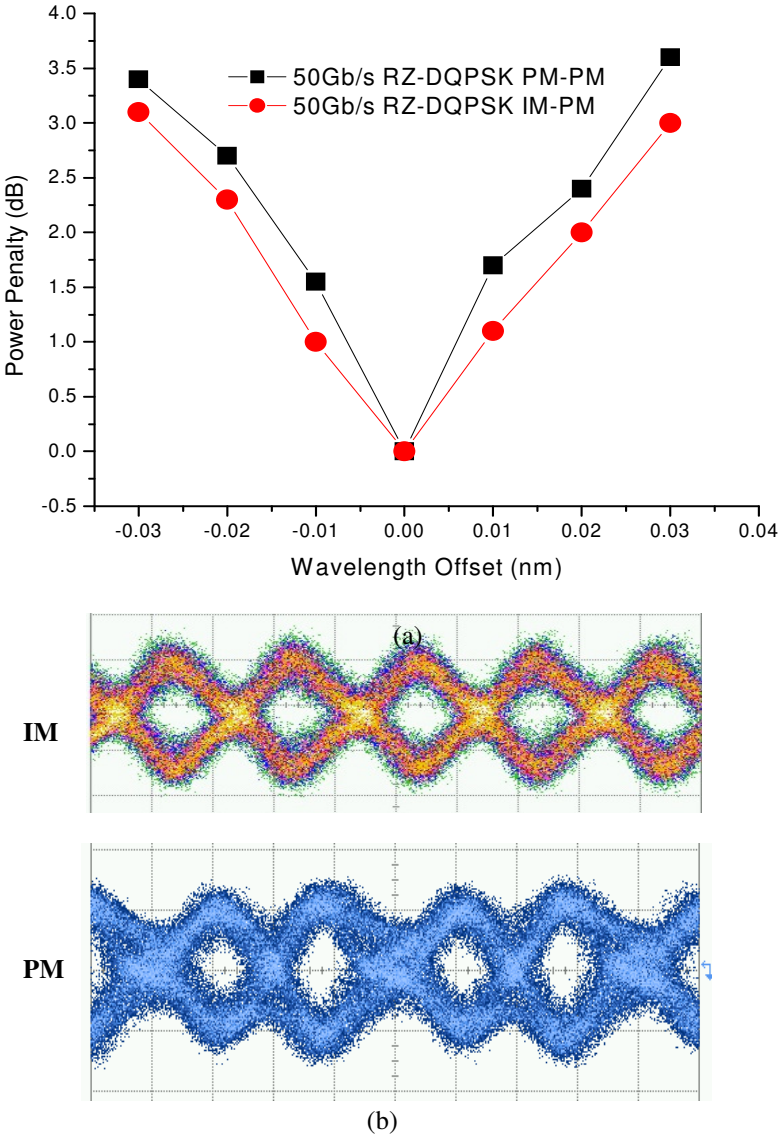

Figure 54. a) Measured power penalties vs. wavelength offset for 50Gb/s RZ-DQPSK signals b) Eye diagrams (20ps/div) at 0.03nm offset generated by a PM and a MZ modulator

Reduction in receiver penalties is much less as compared to DPSK signals, which are inherently more tolerant to frequency and wavelength offset penalties. If an IM is used to achieve both π and $\pi/2$ phase shift in DQPSK transmitter replacing both phase modulators, these penalties can be further reduced.

We have experimentally demonstrated wavelength offset tolerance between optical source and Mach-Zehnder delay interferometer in direct detection of phase modulated systems. Various transmitter designs for DPSK and DQPSK signals are tested by employing phase and intensity modulators to achieve required phase modulation. Our experimental results show that receiver penalties can be relieved if MZ modulator is used instead of phase modulator. These penalties are greatly reduced in case of DPSK signals; 2.5dB decrease in power penalty is measured at 0.04nm offset when using intensity modulator as phase modulator. DQPSK format being inherently more sensitive to frequency and wavelength offset exhibit relatively less improvement, 0.5dB at 0.03nm offset, when one of the phase modulator is replaced by an intensity modulator.

4.3 Performance Degradations of DPSK RZ/NRZ Signals Due to Transmitter and Receiver Imperfections

4.3.1 Motivation and background

In the modulation scheme of DPSK, the "0"s and "1"s are represented by the phase (0 or π). In the receiver, a delay interferometer (DI), whose differential delay is equal to one bit period, converts phase modulation to intensity modulation. The one bit period delay is used to guarantee the maximal interference between neighboring bits. But in the real systems, the difference between the phases of "1" or "0"s may not be a perfect "π" at the transmitter, also the differential delay is not exact one bit period. This section is aimed at the investigating the RZ/NRZ-DPSK transmission performance when the modulator at the transmitter is over or under driven and the delay of Mach-Zehnder Delay Interferometer (MZ-DI) at the receiver is not optimal.

4.3.2 Simulation Setup

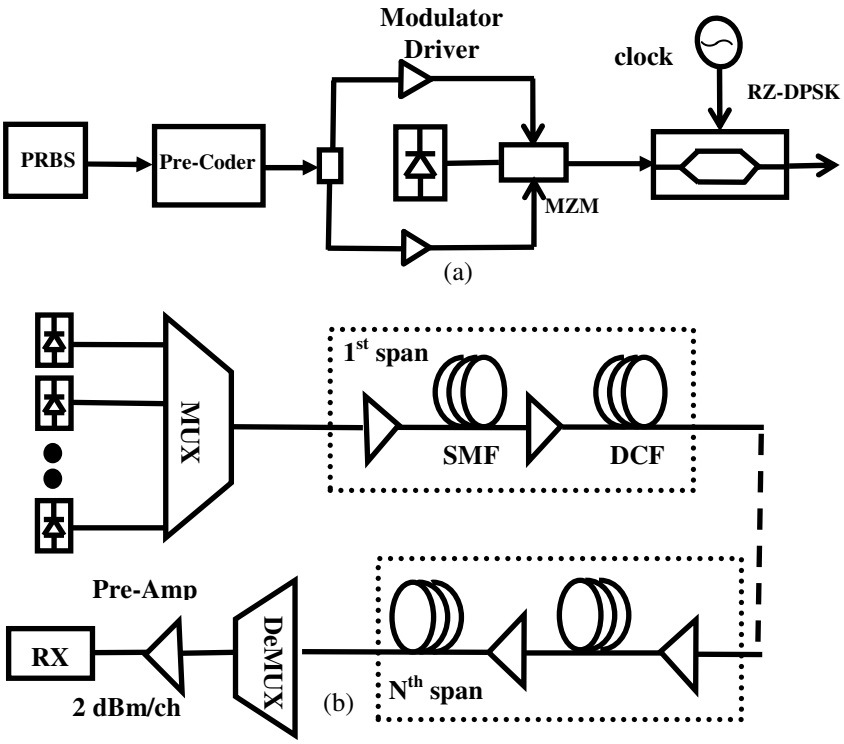

Figure 55. (a) RZ/NRZ- DPSK transmitter setup (b) system setup for 8 x 40 Gb/s over N x 100 km of SMF-28 transmission

The investigated system setup is shown in Figure 55. The transmitter consists of one laser source followed by a dual-drive external $LiNbO_3$ modulator. The modulator performs phase modulation and is driven at twice the switching voltage by a NRZ data stream in a push-pull configuration and biased at the transmission null point. Eight channels are considered with data rate of 40 Gb/s per channel and 50 GHz channel spacing. The multiplexer and de-multiplexer both consist of third order band-pass Bessel filter with 3-dB bandwidth of 50 GHz. Each span has 100km of SMF which is compensated by dispersion compensation fiber (DCF). The optical power launched into SMF is kept at 0dBm per channel and noise figure of EDFA is 4dB. Loss of SMF and DCF is 0.25 and 0.45dB/km.

4.3.3 Results and Discussion

Figure 56 shows RZ-DPSK signal performance with varying modulation factor for all three duty cycle ratios when the signals are transmitted over 100 to 500 km of SMF-28. It is clear that a small variation of switching voltage results in performance degradation, but all three duty cycle ratio signals undergo similar distortion once the modulation factor is varied from 0.5 to 1.5. BER is 10^{-9} when Q value is 6.

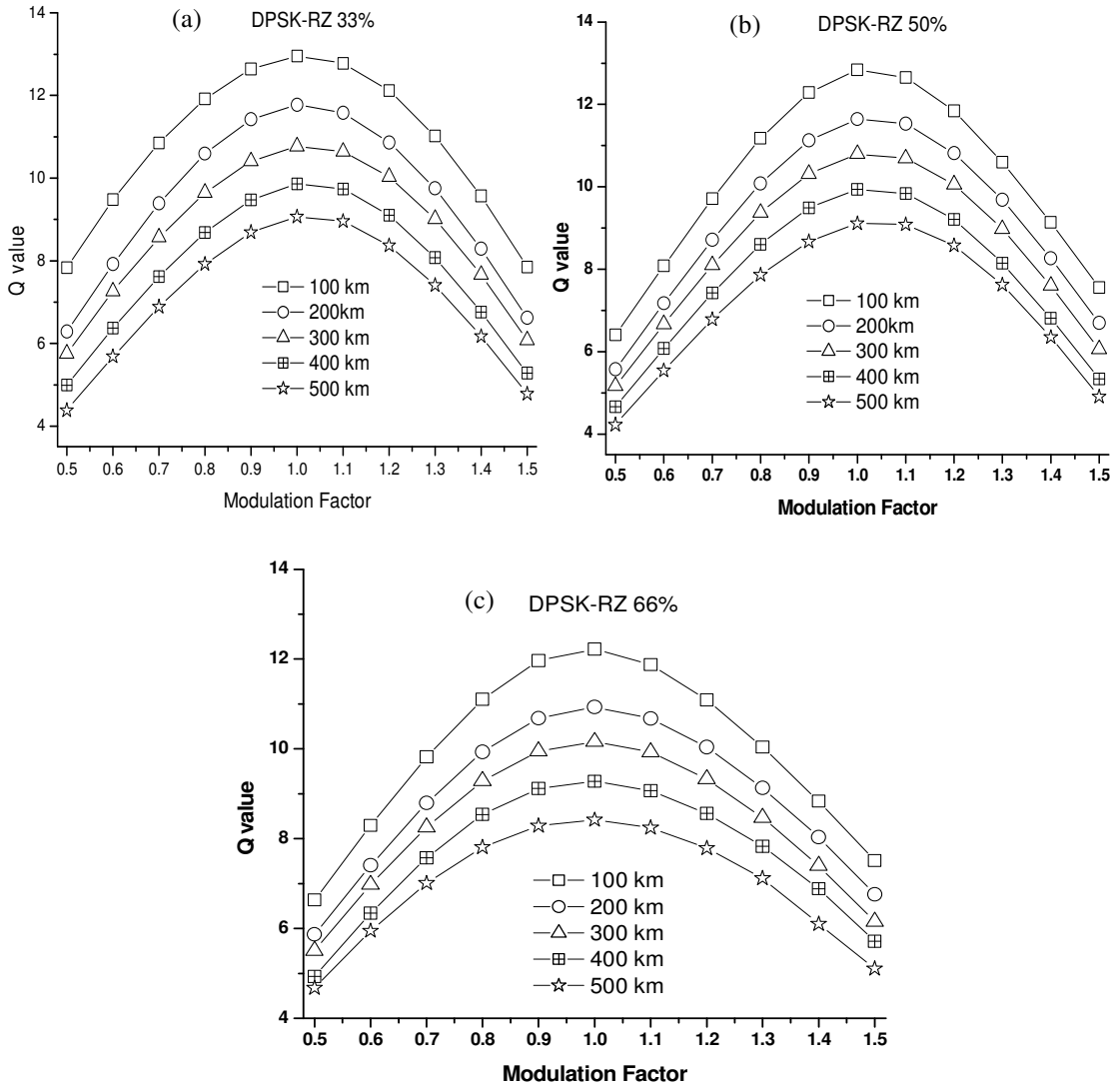

Figure 56. Q value versus modulation factor for 8 x 40 Gb/s RZ-DPSK signals with 100-500km SMF-28 length: a) 33% RZ-DPSK (b) 50% RZ-DPSK (c) 66% RZ-DPSK

A DPSK receiver consists of an optical delay interferometer (DI) and a balanced receiver. The DI is a Mach-Zehnder filter with l one-bit delay, and converts the incoming phase-shift-keying signals into two complementary amplitude-shift-keying signals. In reality, due to temperature variations or ageing, MZ-DI delay might not be optimal before reconstruction and may cause performance degradation. Figure 57 presents the performance penalties caused by inappropriate MZ-DI delay at the receiver. Results are plotted for all three duty cycle ratios when the signals are transmitted over one to five spans of SMF-28. 33% RZ-DPSK shows the best overall results under these conditions. It is obvious that greater the duty ratio results in the worst of the degradation. 66% RZ-DPSK is affected the most and BER of 10^{-9} can not be achieved even for shorter distances once Mach Zehnder delay interferometer (MZDI) is set for delays of 0.3 to 0.6 bit. We used VPI Transmissionmaker, a commercial software to develop this simulation model and analyze the results.

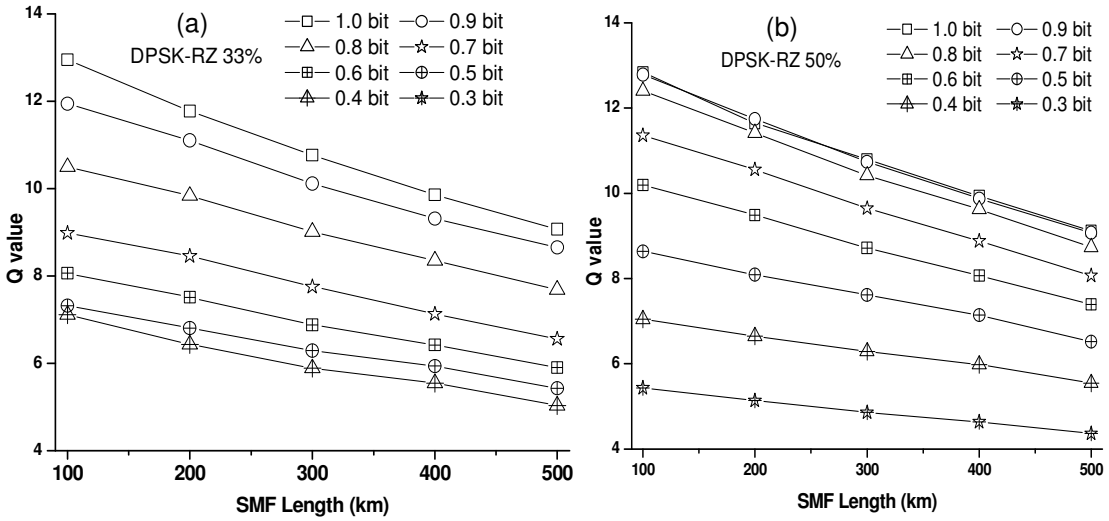

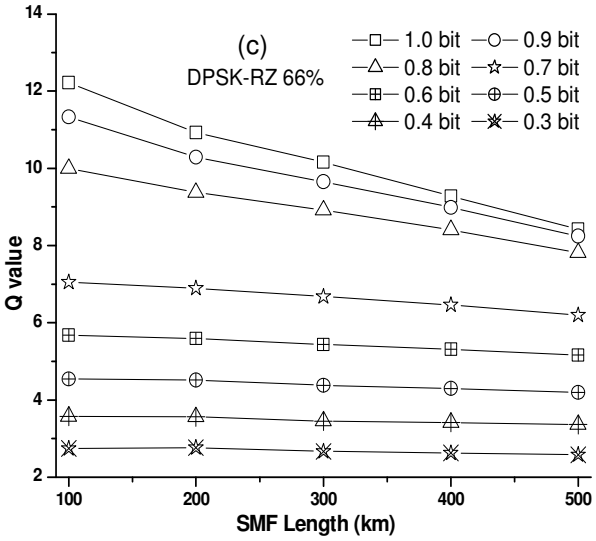

Figure 57. Q value versus SMF length for 8 x 40 Gb/s RZ-DPSK signals with different MZ-DI delay and duty-cycle: a) 33% RZ-DPSK (b) 50% RZ-DPSK (c) 66% RZ-DPSK

We also performed simulations using NRZ pulse shape for DPSK signals. Similar performance comparison is also drawn for 8 x 40 Gb/s NRZ-DPSK signals. Q value is plotted against modulation factor in Figure 58(a) and in (b) we can observe Q value against SMF length for varying MZ-DI delay at the receiver.

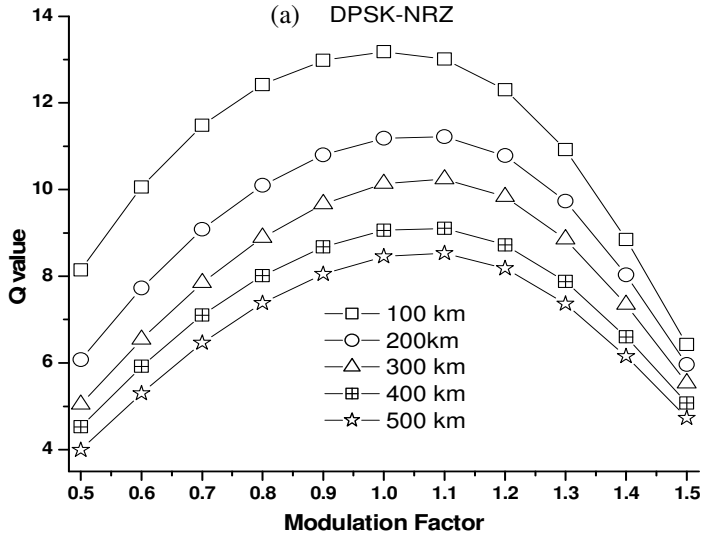

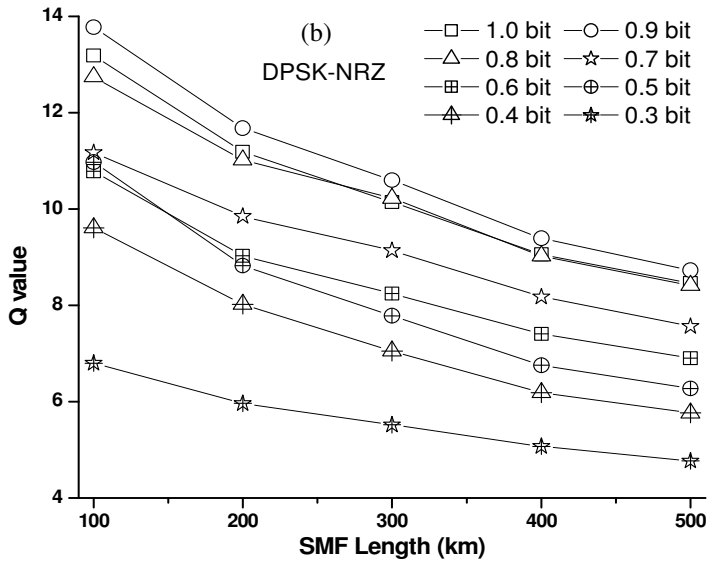

Figure 58. (a) Q value versus modulation factor for 8 x 40 Gb/s NRZ-DPSK signals (b) Q value versus SMF length with different MZ-DI delay values

NRZ signal seems more robust in case of inaccurate MZ-DI delay as compared to RZ pulse shaping for shorter fiber lengths as it can be seen in Figure 58(b), but for long SMF over 500km its performance is similar to 50% RZ-DPSK. In above section, numerical simulation for 8 x 40 Gb/s DPSK RZ/NRZ signals with 0.8 b/s/HZ spectral efficiency has been demonstrated and their tolerance towards impairments caused due to improper driving voltage and MZ-DI delay was investigated for different duty cycle ratios. Results show that DPSK-RZ and DPSK-NRZ show similar performance limitations overall as far as driving voltage is concerned, but NRZ pulse signals are more robust to degradations caused by small MZ-DI delay values as compared to RZ pulse signals.

4.4 Optimal RZ Modulation Format for 40 Gb/s Transmission Systems

4.4.1 Motivation and Background

In this section the impact of chromatic dispersion, nonlinear effects and filtering effect

has been investigated for 40 Gb/s return-to-zero modulation formats including differential phase-shift keying (DPSK), differential quadrature phase-shift keying (DQPSK) and modified duobinary (MD) signals for single channel and WDM systems. Return-to-zero (RZ) signals are preferred over non-return-to-zero (NRZ) signals because they benefit from soliton-like effects in optical fiber and are less susceptible to fiber nonlinearities and have higher SBS threshold. For various reasons optical duo-binary and differential phase shift keying have emerged as leading formats for both single channel and WDM transmission systems.

4.4.2 Simulation Setup

We have drawn comparison among RZ-DQPSK, RZ-DPSK and MD-RZ signals by numerical simulation. System performance is evaluated by eye opening penalty (EOP). Here

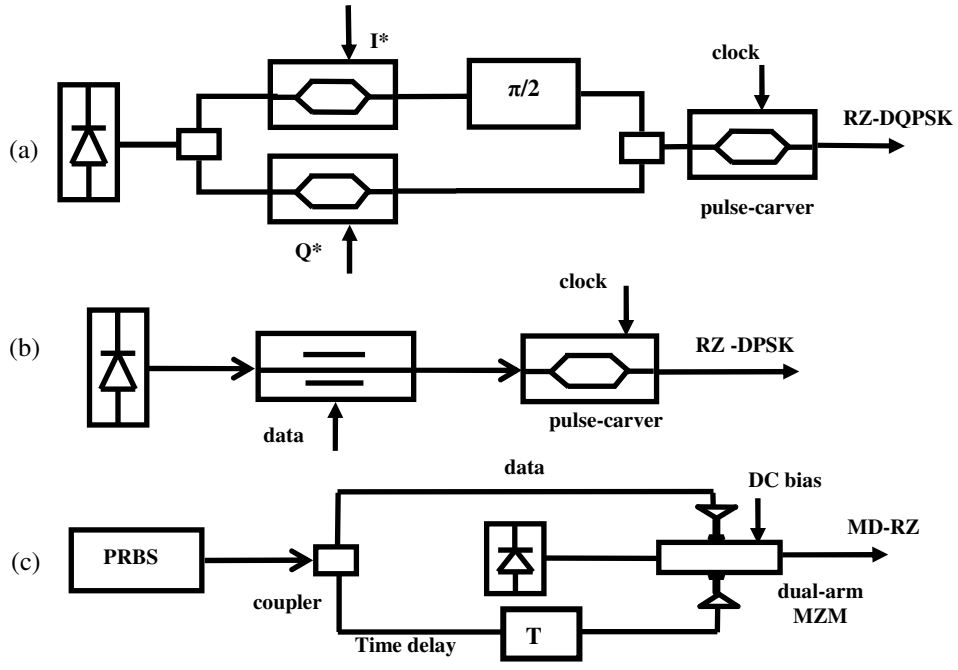

Figure 59. Configuration of transmitter setup a) RZ-DQPSK (b) RZ-DPSK c) MD-RZ

EOP is calculated with respect to back-to-back transmission by using commercial software VPI Transmission maker. Figure 59 shows typical transmitter setup for all three modulation formats. RZ-DQPSK signal is generated by parallel combination of two Mach-Zehnder modulators [63]. RZ-DPSK employs one phase modulator and then RZ pulse carver. MD-RZ is generated by our novel technique using only one dual arm $LiNbO_3$ modulator. The simulation system setup is shown in Figure 60.

Balanced detection is used for phase modulated signals, while direct detection is used for duobinary signals. Eight channels are considered with a bit rate of 40 Gb/s and a channel spacing of 100 GHz. The transmitter and receiver both consist of third order band-pass Bessel filter with 3-dB bandwidth of 60 GHz. Each span has 100km of SMF-28 which is compensated by dispersion compensation fiber (DCF).

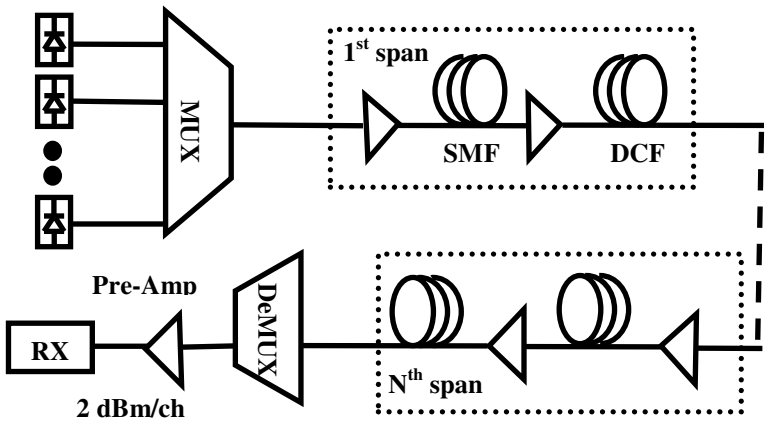

Figure 60. System setup for 8 x 40 Gb/s over NX100 km of SMF-28 transmission

4.4.3 Results and Discussion

Figure 61 shows residual dispersion tolerance plotted against EOP for both single and WDM transmission. DCF length is varied in each span to provide cumulative dispersion

for 5 spans with a total length of 500km SMF-28. It is clearly shown that RZ-DQPSK exhibits much better performance than RZ-DPSK and MD-RZ when either over or under compensation. The reason is that DQPSK carries two bits of information per symbol employing four states of optical phase. Dispersion tolerances with a 2-dB EOP are 60, 70 and 200ps/nm, respectively, for single channel, and 40, 60 and 170ps/nm, respectively, for 8x40 Gb/s MD-RZ, RZ-DPSK, RZ-DQPSK signals.

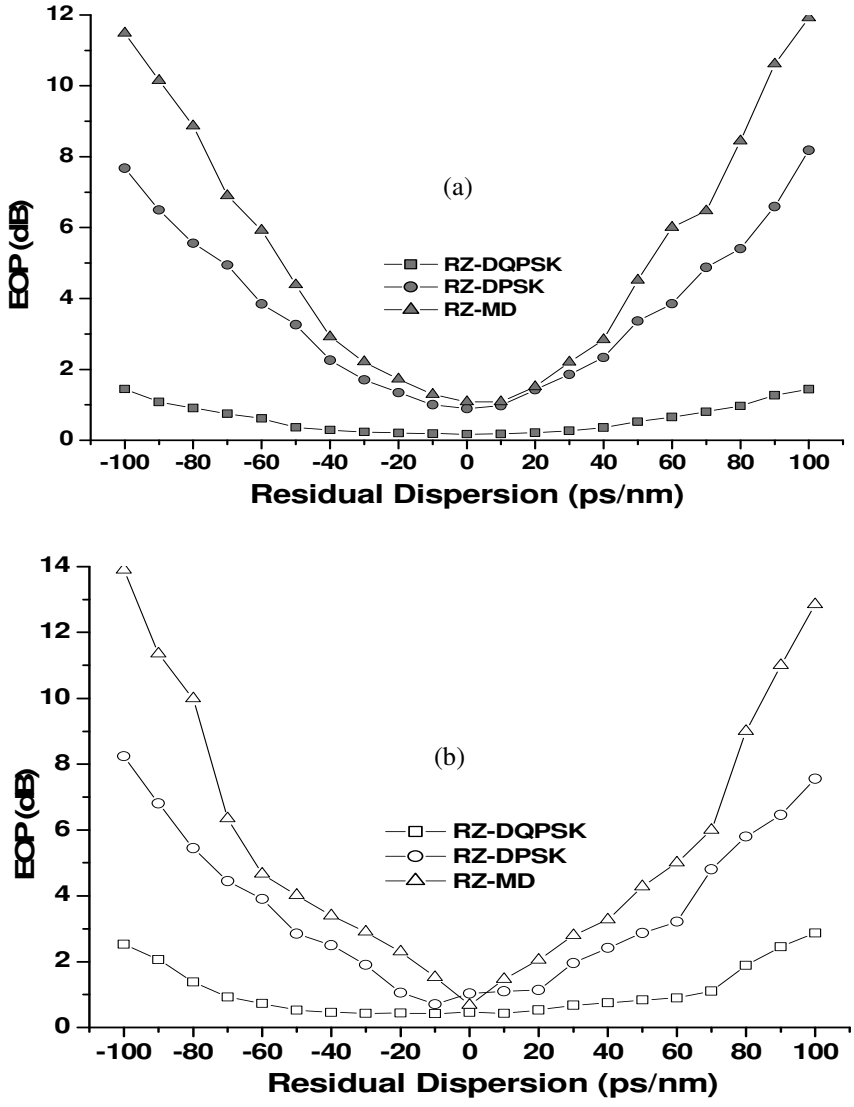

Figure 61. Simulated residual dispersion dependence of EOP after 500km (a) Single channel (b) 8x40Gb/s (ch#4)

The simulated EOP with respect to back-to-back transmission versus the number of fiber spans for 40 Gb/s data rate are presented in Figure 62. For single channel RZ-DQPSK can be transmitted over 2000km for a BER of 10^{-9}, while RZ-DPSK and MD-RZ can only transmit over 1700 and 1400km, respectively. For 8x40Gb/s RZ-DQPSK, RZ-DPSK and MD-RZ signals, they can be transmitted over 1800, 1600 and 1300 km, at a BER of 10^{-9} (Figure 62).

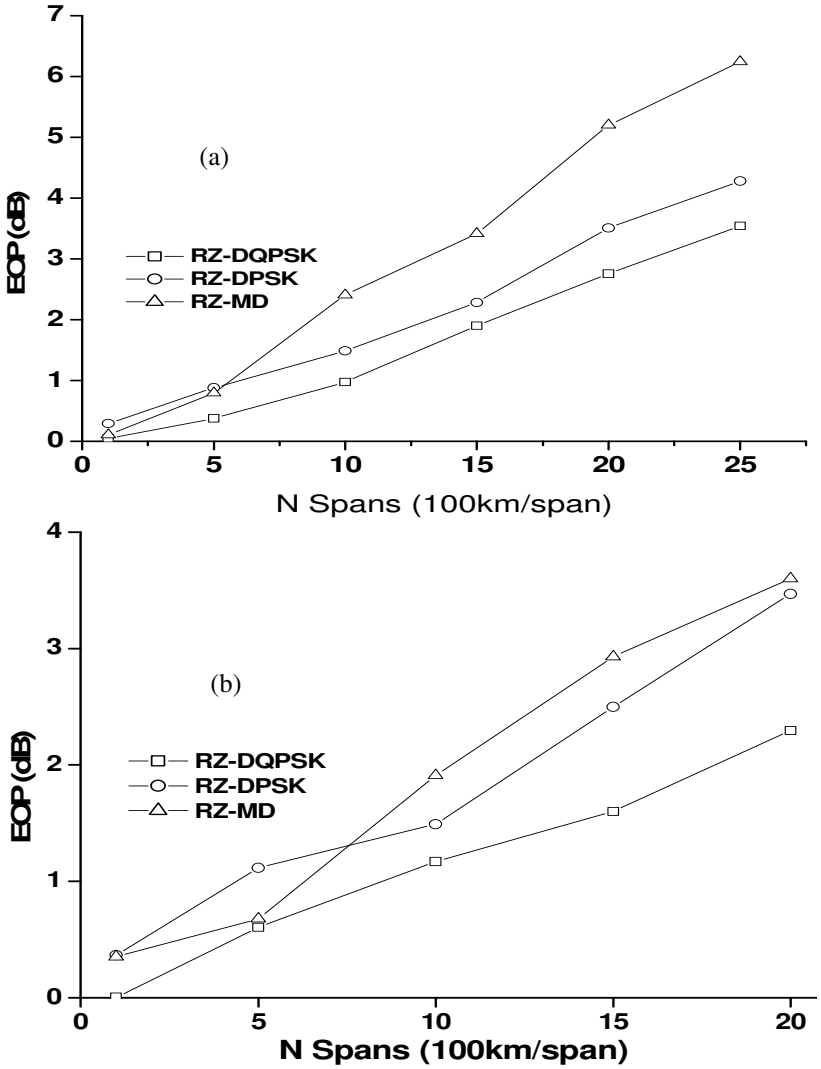

Figure 62. Simulated EOP versus number of fiber spans Single channel (b) 8x40Gb/s (ch#4)

DQPSK definitely provides the longest transmission distance benefiting from half of the data rate. The narrow spectrum improves the transmission performance in DQPSK and

duobinary case, but MD-RZ signal is adversely affected by ISI in WDM transmission system. In next setup EOP is plotted against 3-dB bandwidth of 3rd order band-pass Bessel filter. Fiber length is 500km and is fully compensated by DCF. DQPSK is a non-binary modulation scheme and can attain very narrow spectrum by encoding multiple bits per symbol. Also, duobinary encoding improves spectral efficiency for duobinary signals. It is clear from Figure 63(b) that below 30 or after 80 GHz RZ-DPSK signals suffer from greater EOP due to adjacent signals.

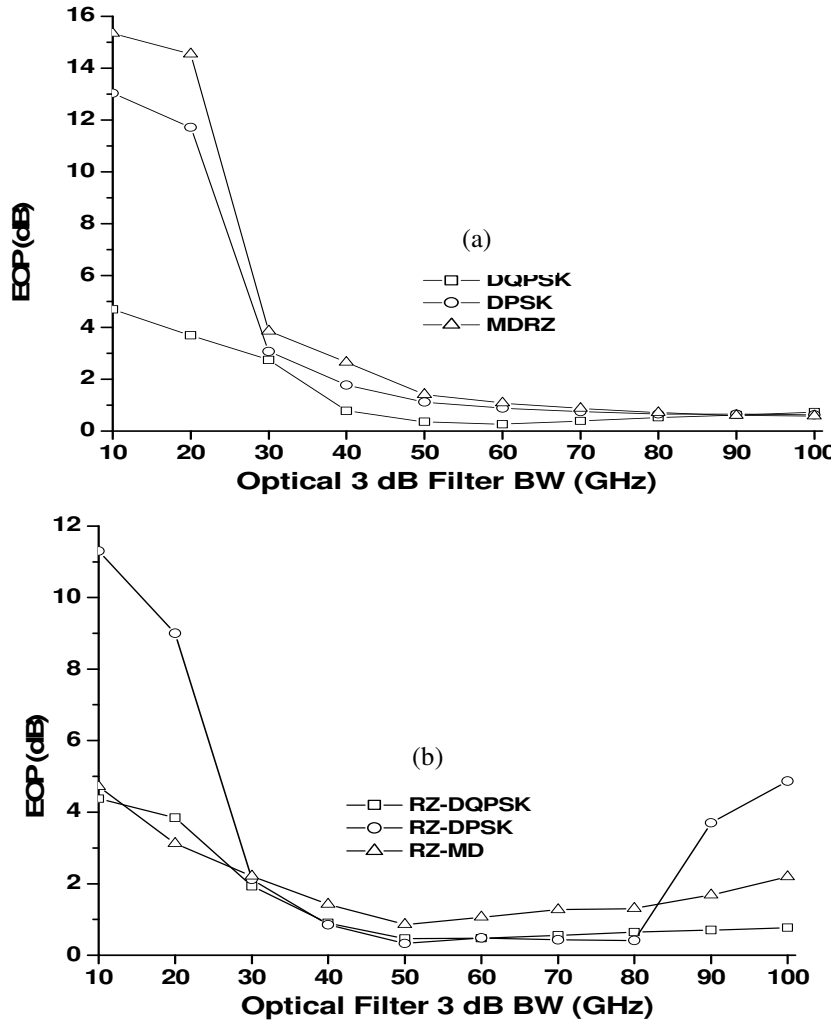

Figure 63. Numerical simulation of EOP after 500km transmission with varying 3-dB optical filter bandwidth (a) Single channel, (b) WDM transmission (ch#4)

Hence even though RZ signals have a broad spectrum than NRZ signals, fifty GHz channel spacing is still possible for RZ-DQPSK and MD-RZ signals. High robustness of DQPSK signals to reduce optical filter bandwidths lies in its better ISI tolerance.

Numerical simulation for 40 Gb/s signals has demonstrated that in this setup, RZ-DQPSK exhibits higher dispersion tolerance and less susceptible to nonlinear effects than RZ-DPSK and MD-RZ. Terminal filtering effect shows that MD-RZ and RZ-DQPSK can be employed in WDM systems with 50 GHz channel spacing because the optical filter with narrow bandwidth does not degrade system performance [64].

4.5 A Novel RZ-DQPSK Transmitter Design and Simulation Analysis

4.5.1 Motivation

This section presents a novel setup to generate a RZ-DQPSK signal which employs only two modulators as compared to three modulators in conventional parallel or serial setup configurations. The robustness of RZ-DQPSK signal generated by this technique is investigated using 8x40 Gb/s WDM systems with 50GHz separation over 500km SMF.

4.5.2 Simulation Setup

Up till now there are two conventional transmitter setups for RZ-DQPSK signal generation. First technique consists of parallel combination of two Mach-Zehnder modulators (MZM) followed by a RZ pulse carver (Figure 64a) to generate a RZ-DQPSK signal [63]. Another setup comprises (Figure 64b) of serial combination of MZM and a phase modulator (PM) followed by a RZ pulse carver [65], [61]. Both of these techniques use at least three modulators for the generation of RZ-DQPSK signal. Figure 64c presents

a proposed scheme for the generation of RZ-DQPSK signal using only one dual-arm Mach-Zehnder modulator and RZ pulse carver. Precoded data and clock signal is split into two paths and then added after introducing time delay to generate two RF signals to drive dual-arm modulator for the generation of RZ-DPSK signal.

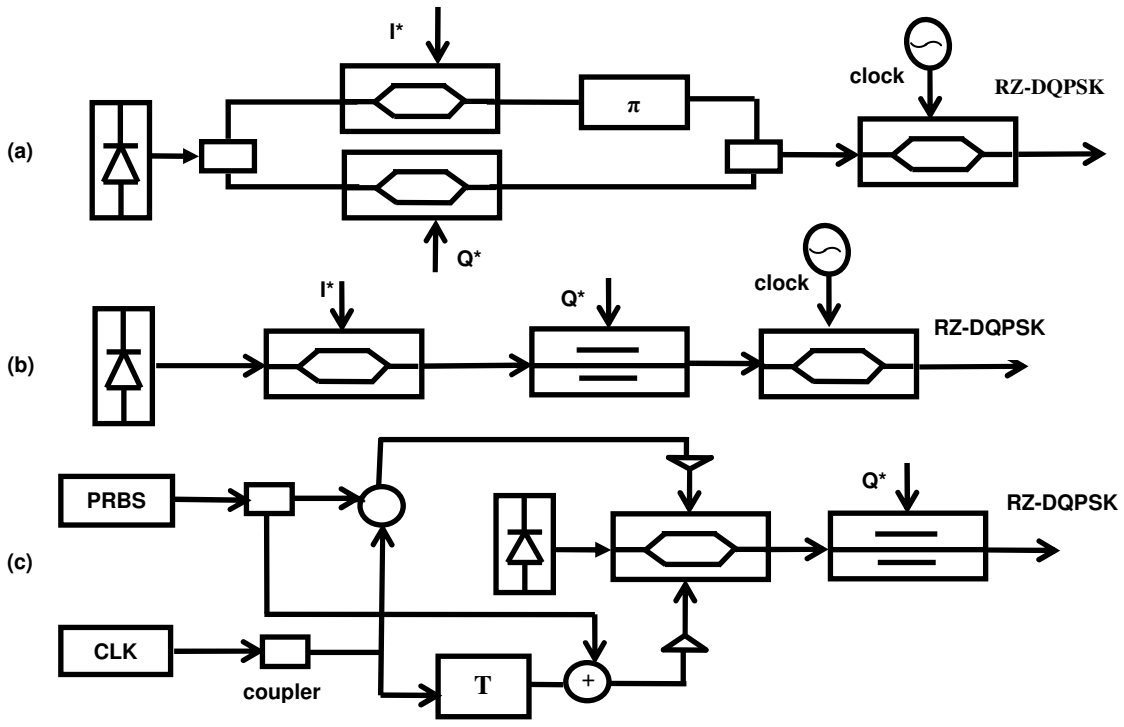

Figure 64. Configuration of RZ-DQPSK transmitter a) Parallel setup b) Serial Setup c) Proposed setup

Another 90 degree phase shift is introduced by phase modulator, which is connected in serial to generate RZ-DQPSK signal. RZ-DPSK signal by this technique is first presented in [66], this is the first time RZ-DQPSK signal is presented using this method and comparison is drawn with other schemes by numerical simulation. DQPSK signal carries two bits of information per symbol employing four states of optical phase. Time delay module in proposed scheme is set to one bit period, which in this case is 50ps as 40 Gb/s RZ-DQPSK signal has symbol rate of only 20 GHz. System performance is evaluated by

eye opening penalty. Numerical simulation has been performed with the VPI Transmission maker software. EOP penalty is calculated with respect to back-to-back transmission. The investigated system setup is similar as shown in Figure 60. Balanced detection is used for phase modulated signals at the receiver. Eight channels are considered with data rate of 40 Gb/s and 50 GHz channel spacing. The multiplexer and de-multiplexer both consist of third order band-pass Bessel filter with 3-dB bandwidth of 50 GHz. Each span has 100km of SSMF which is compensated by dispersion compensation fiber (DCF) by post compensation. The optical power launched into SMF is kept at 0 dBm per channel and noise figure (NF) of EDFA is kept at 4 dB. Loss of single mode fiber (SMF-28) and DCF is 0.25 and 0.45 dB/km, respectively. SSMF and DCF dispersion is 17 and -100ps/nm/km, effective core area is 80 and 40 μm^2, respectively. An optical pre-amplifier is set to provide +2 dBm optical power before optical detection.

4.5.3 Results and Discussion

Figure 65 presents eye diagrams of 40 Gb/s RZ-DQPSK signal generated by proposed technique.

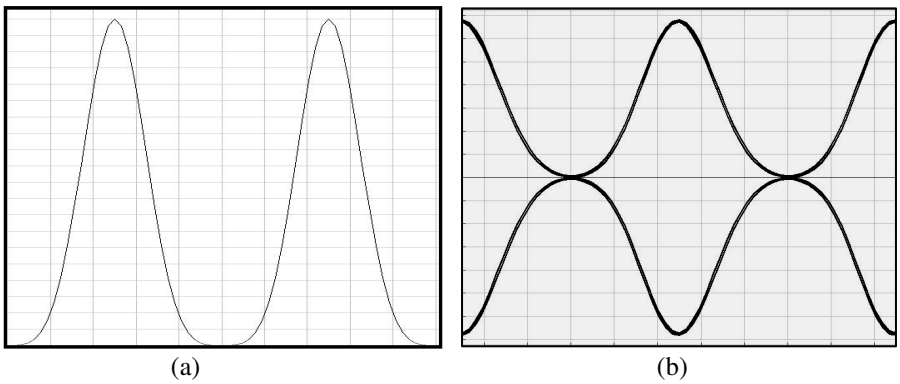

Figure 65. Eye diagrams of 40 Gb/s RZ-DQPSK signal a) at transmitter b) after demodulation

- Input Power

In Figure 66 the EOPs are plotted against average fiber input power per channel for all the three transmitter setups. Solid lines in graph represent SMF length of 500km and dotted lines represent SMF length of 100km. EOPs for serial and parallel setups are in agreement with each other. As expected EOPs shoot high as average power is increased and non-linear effects in fiber come into play at greater extent. Our setup exhibits similar performance for lower span length but for larger span length EOP is approximately 0.5 dB higher for proposed scheme.

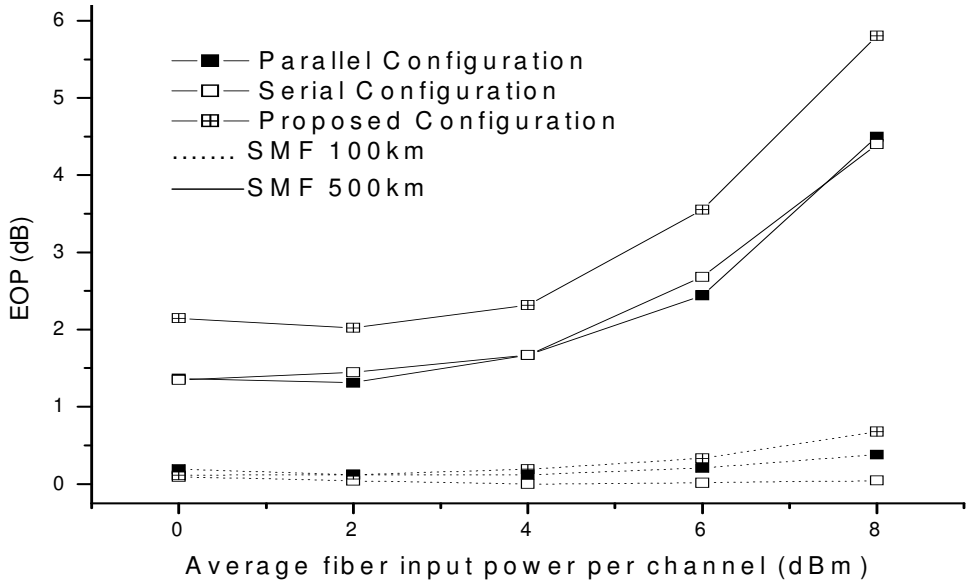

Figure 66. EOP versus average fiber input power per channel for 8x40 GB/s WDM transmission

- Residual Dispersion

Figure 67 shows residual dispersion plotted against EOP after WDM transmission over 500km SMF with 50GHz separation. DCF length is varied in each span to provide cumulative dispersion for 5 spans. If we choose EOP penalty of 2 dB as transmission threshold, parallel setup exhibits dispersion tolerance range of 145ps/nm, while serial

configuration and our proposed setup shows 140ps/nm and 125ps/nm of dispersion tolerance range. Figure 68 shows eye patterns after 10 spans of fiber totaling 1000km of transmission.

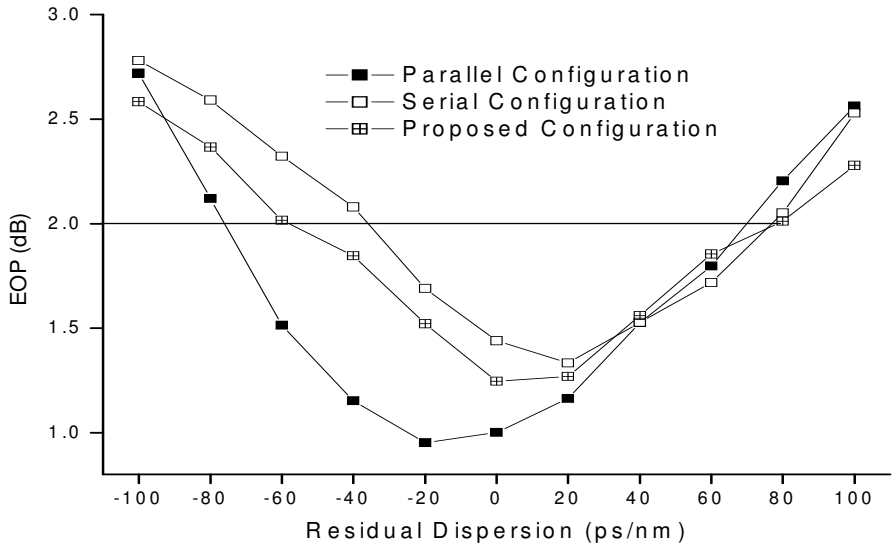

Figure 67. Simulated residual dispersion dependence of EOP after 500km SMF transmission

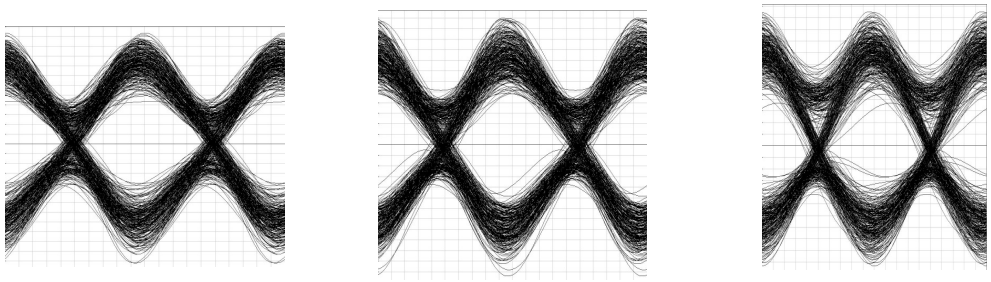

a) Parallel Setup b) Serial Setup c) Proposed Setup

Figure 68. Eye pattern for 8 x 40 Gb/s WDM transmission (50GHz spacing) after 1000km of SMF

In above section, a novel transmitter setup is presented to generate RZ-DQPSK signal, which require only one dual-arm Mach-Zehnder modulator and one phase modulator. This scheme can be cost effective since it reduces the number of modulators to two as compared to three in conventional setup. Simulation results are presented for RZ-DQPSK signal generation and WDM transmission with 0.8b/s/Hz spectral efficiency, which explain that performance of this proposed setup is in close agreement with other schemes.

Considering the tolerance to fiber nonlinearities and dispersion, no particular scheme outperforms the other two.

CHAPTER 5

CONCLUSION

In this research we made several contributions to research in advanced optical modulation formats for long-haul optical networks. We covered both intensity and phase modulated systems.

We have demonstrated a novel and cost effective method to generate MD-RZ signals by using only one single push-pull type Mach-Zehnder modulator. The duty cycle of the MD-RZ signals can be adjusted from 1 to 0.25 by changing the time delay of the two-arm driven electrical signals. The generated MD-RZ signals show high receiver sensitivity relative to MD-NRZ signals. Repeaterless transmission becomes very important for inaccessible terrestrial and sub-marine optical networks because drives the cost lower by increasing span length. We also have successfully demonstrated MD-RZ single channel repeaterless transmission over 300km SMF-28 with power penalty of 2.7 dB. WDM repeaterless transmission of eight MD-RZ equally spaced channels at 100GHz over 240km SMF-28 is also presented with power penalty of 2.4 dB. A numerical comparison has been drawn with other conventional MD-RZ transmitter schemes. Further, MDRZ signals are also compared with RZ-DPSK and RZ-DQPSK numerically. Experimental and simulation results indicate that the MD-RZ signal generated by our novel technique can take higher input power and can be transmitted over long SMF-28 without repeaters, and can be employed in WDM systems with 50 GHz channel spacing because the optical filter with narrow bandwidth does not degrade system performance.

We also studied DPSK and DQPSK modulation schemes in detail. These phase modulated systems have inherent 3-dB better receiver sensitivity with the use of balanced

receiver, which make them very attractive choice in this research context. In the deployment of high spectral-efficient WDM transmission systems, narrow optical filtering effects on such modulation formats are of key importance because these signals pass through various narrow optical filters at different stages. In this regard, design of Mach-Zehnder delay interferometer (MZ-DI) in DQPSK decoder becomes very significant since choice of optimal FSR helps us relieve some degradation due to strong optical filtering, and we can realize high bit rate and high spectral efficient WDM DQPSK transmission systems. We performed experimental and numerical study to show how FSR optimization effect DQPSK format with RZ and NRZ pulse shape. In this experiment, we used 100 Gb/s RZ-DQPSK signal and varied FSR of the MZ-DI going below and above normal 1-bit (50GHz FSR) delay operation using tight in-line filter configurations. We can observe that the performance with 55 GHz FSR (0.55 bit rate) is substantially better than the case with 44.5 GHz FSR (0.445 bit rate) measuring more than 6 dB difference of power penalty at 10^{-3}. This clearly shows that increasing FSR will substantially help the transmission even in the presence of narrow band optical filters, which in turn can help us achieve more SE high bit-rate WDM systems.

Wavelength offset tolerance is also studied for DPSK and DQPSK modulation formats experimentally for various transmitter designs employing phase or intensity modulators to produce required phase shift. In DQPSK transmitters, the phase shifts of π and $\pi/2$ can be achieved by cascading phase modulators or MZ modulators in any combination and sequence [61]. While DPSK signal by a PM has inherent chirp, MZ modulator can generate chirp-free DPSK signal with perfect π phase shift since it modulates the phase along the real axis of the complex optical field. It has been verified

with experiments that using an MZM as phase modulator is useful in imperfect conditions such as low driving voltage since it only affects residual intensity dips leaving perfect π phase shift intact [2]. Receiver penalties are greatly reduced in case of DPSK signals; 2.5dB decrease in power penalty is measured at 0.04nm offset when using intensity modulator as phase modulator. DQPSK format being inherently more sensitive to frequency and wavelength offset exhibit relatively less improvement, 0.5dB at 0.03nm offset, when one of the phase modulator is replaced by an intensity modulator. Additionally, numerical results are presented for penalties introduced due to non-optimal driving voltage and non-optimal delay at MZ-DI for phase coded formats.

Advanced modulation formats play an important role in the design of spectral-efficient WDM transport networks. In this research we have discussed generation, transmission and detection of some key modulation schemes focusing on duobinary, DPSK and DQPSK formats. These advanced modulation formats can be used with other recent technologies like electronic dispersion compensation (EDC), forward error correction (FEC) and receiver designs utilizing adaptive electronic post-processing and equalization to realize high spectral-efficient and cost effective WDM transmission networks. At 10 Gb/s data rates, electronic signal processing is already being used ranging from simple feed-forward equalizer (FFE) schemes to Maximum Likelihood Sequence Estimation (MLSE) [67]-[69]. Forward error correction has also become a standard feature of 10 Gb/s and 40 Gb/s commercial optical communication systems [70]. At the transmitters, controlled signal pre-distortion is becoming available at 10 Gb/s [71] and at the receiver side coherent detection is gaining a lot of renewed interest [72], [73]. In future, further experimental and numerical analysis can be performed for investigating end-to-end over-

all system performance for advanced modulation formats in the conjunction with some of the above mentioned technologies. Similarly we can investigate multi-level signals beyond two bits per symbol and other promising scheme like orthogonal frequency division multiplexing (OFDM). In OFDM, we utilize the orthogonality between the spectral profiles of each channel, and it can be very beneficial in future applications like optical wireless networks.

APPENDIX A

ACRONYMS

APRZ	Alternate Phase Return to Zero
ASE	Amplified Spontaneous Emission
AWG	Arrayed Waveguide Grating
BER	Bit Error Rate
BERT	Bit Error Rate Tester
CF RZDPSK	Chirp Free RZDPSK
CRZ	Chirped Return to Zero
CSRZ	Carrier Suppressed Return to Zero
DCF	Dispersion Compensating Fiber
DFB	Distributed Feedback
DFF	Dispersion-Flattened Fiber
DGD	Differential Group Delay
DM	Dispersion Management
DMF	Dispersion-Managed Fiber
DPSK	Differential Phase Shift Keying
DSF	Dispersion Shifted Fiber
EDFA	Erbium-Doped Fiber Amplifier
ESNL	Non Linear Schrodinger Equation
FEC	Forward Error Correction
FFT	Fast Fourier Transform
FWM	Four-Wave Mixing

GEF	Gain Equalizing Filter
GVD	Group-Velocity Dispersion
IMDD	Intensity Modulated Direct Detection
MZM	Mach-Zehnder Modulator
MZ-DI	Mach-Zenhder Delay Interferometer
NPSC	Nonlinear Phase Shift Compensation
NRZ	Non Return to Zero
OOK	On-Off keying
OPC	Optical Phase Conjugation
OSNR	Optical Signal to Noise Ratio
PMD	Polarisation Mode Dispersion
PC	Phase Conjugator
PRBS	Pseudo Random Bit Sequence
PSBT	Phase Shaped Binary Transmission
PSK	Phase Shift Keying
QPSK	Quadrature Phase Shift Keying
RF	Radio Frequency
RS	Reed Solomon
RZ	Return to Zero
SBS	Stimulated Brillouin Scattering
SMF	Single Mode Fiber
SNR	Signal to Noise Ratio
SPM	Self-Phase Modulation

SRS	Stimulated Raman Scattering
VSB	Vestigial Sideband
DWM	Wavelength-Division Multiplexing
WSS	Wide Sense Stationary
XPM	Cross-Phase Modulation

REFERENCES

[1]. Sen Zhang, "Advanced Optical Modulation Formats in high-speed Lightwave system," www.ittc.ku.edu/publications/documents consulted on 03/01/2008

[2]. Peter J. Winzer, and Rene-Jean Essiambre, "Advanced optical modulation formats," *Proceedings of the IEEE*, vol. 94, pp. 952-985, 2006.

[3]. A. Gnauck, G. Raybon, S. Chandrasekhar, J. Leuthold, C. Doerr, L. Stulz, A. Agarwal, S. Banerjee, D. Grosz, S. Hunsche, A. Kung, A. Marhelyuk, D. Maywar, M. Movassaghi, X. Liu, C. Xu, X. Wei, and D. Gill, "2.5 Tb/s 64 * 42.7 Gb/s Transmission Over 40*100 km NZDSF using RZ-DPSK Format and All-Raman- Amplified Spans," *OFC*, 2002. Paper FC2.

[4]. C. Xu, X. Liu, and X. Wei, "Ultra-Long Haul DWDM Transmission with Differential Phase Shift Keying Dispersion Managed Soliton," ECOC, vol. 1, September 2002.

[5]. J. Leibrich, C. Wree, and W. Rosenkranz, "CF-RZ-DPSK for Suppression of XPM on Dispersion-Managed Long-Haul Optical WDM Transmission on Standard Single-Mode Fiber," IEEE Photonics Technology Letters, vol. 14, pp. 155–157, February 2002.

[6]. I. P. Kaminow and T. L. Koch, Eds., *Optical Fiber Telecommunications* III A +B. New York: Academic, 1997.

[7]. G. P. Agrawal, *Fiber-Optic Communication Systems*, 3rd ed., New York: Wiley, 2002.

[8]. R. Ramaswami and K. Sivarajan, *Optical Networks: A Practical Perspective*. San Francisco, CA: Morgan Kaufmann, 2001.

[9]. L. G. Kazovsky, S. Benedetto, and A. E. Willner, *Optical Fiber Communication Systems*. Norwood, MA: Artech House, 1996.

[10]. K. Sato, S. Kuwahara, Y. Miyamoto, and N. Shimizu, "40Gb/s direct modulation of distributed feedback laser for very-shortreach optical links," *Electron. Lett.*, vol. 38, no. 15, pp. 816–817, 2002.

[11]. Y. Yu, R. Lewen, S. Irmscher, U. Westergren, and L. Thylen, "80 Gb/sETDM transmitter with a traveling-wave electroabsorption modulator," in *Proc. Eur. Conf. Optical Communication (ECOC)*, 2005, Paper OWE1.

[12]. Mahapatra and E. J. Murphy, "Electrooptic modulators," in Optical Fiber Telecommunications IV, I. Kaminow and T. Li, Eds. New York: Academic, 2002,pp. 258–294.

[13]. S. Song, "High-order four-wave mixing and its effect in WDM systems," *Optics Express*, vol. 7, pp. 166–171, August 2000.

[14]. R.M. Jopson and R. E. Tench, "Polarisation-independent phase conjugation of lightwave signals," *Electronics Letters*, vol. 29, pp. 2216–2217, December 1993.

[15]. H. Gnauck, R.M. Jopson, and R.M. Derosier, "10 Gb/s 360 km transmission over dispersive fiber using midsystem spectral inversion," *IEEE Photonics Technology Letters*, vol. 5, pp. 663–666, June 1993.

[16]. J. Herrera, F. Ramos, and J. Marti, "Nonlinear distortion generated by DSF-based optical-phase conjugators in analog optical systems," *IEEE Photonics Technology Letters*, vol. 20, pp. 1688–1693, September 2002.

[17]. G. J. Foschini and C. D. Poole, "Statistical theory of polarization dispersion in single mode fibers," *Journal of Lightwave Technology*, vol. 9, pp. 1439–1456, November 1991.

[18]. I. Kaminow and T. Li, eds., *Optical fiber communications* IV B. Academic Press, 2002.

[19]. M. Morisaki, H. Sugahara, T. Ito, and T. Ono, "2.56-Tb/s (64x42.7 Gb/s) WDM transmission over 6000 km using all-raman amplified inverse double-hybrid spans," *IEEE Photonics Technology Letters*, vol. 15, pp. 1615–1617, November 2003.

[20]. D. Bayart, P. Baniel, A. Bergonzo, J.-Y. Boniort, P. Bousselet, L. Gasca, D. Hamoir,F.Leplingard, A. L. Sauze, P. Nouchi, F. Roy, and P. Sillard, "Broadband optical fibre amplification over 17.7 THz range," *Electronics Letters*, vol. 36, pp. 1569–1571, August 2000.

[21]. K. Nakagawa, "Progress in optical amplifiers and the future of optical communication systems," in Proceedings of *Optical Amplifier and Applications (OAA'1999)*, 1999.

[22]. Y. Miyamoto, A. Hirano, K. Yonenaga, A. Sano, H. Toba, K. Murata, and O. Mitomi, "320 Gbit/s (8x40 Gb/s) WDM transmission over 367km with 120 km repeater spacing using carrier-suppressed return-to-zero format," *Electron. Letters*, vol. 35, pp. 20412042, Nov. 11, 1999

[23]. S. Bigo, Y. Frignac, G. Charlet,W. Idler, S. Borne, H. Gross, R. Dischler, W. Poehlmann, P. Tran, C. Simonneau, D. Bayart, G. Veith, A. Jourdan, and J. Hamide, "10.2 Tbit/s (256x42.7 Gbit/s PDM/WDM) transmission over 100 km teralight fiber with 1.28 bit/Hz spectral efficiency," Tech. Dig. of OFC01. PD23.

[24]. K. Yonenaga, Y. Miyamoto, H. Toba, K. Murata, M. Yonenayama, Y. Yamane, and H. Miyazawa, "320-Gbit/s, 100-km WDM repeater-less transmission using fully decoded 40 Gbit/s optical duobinary channels with dispersion tolerance of 380 ps/nm," Tech. Dig. ECOC 2000. Paper 2.2.4.

[25]. Y. Miyamoto, K. Yonenaga, A. Hirano, H. Toba, K. Murata, and H. Miyazawa, "Duobinary carrier-suppressed return-to-zero format and its application to 100 Ghzspaced 8x43-Gbit/s DWDM unrepeatered transmission over 163 km," Tech. Dig. OFC01. Paper TuU4.

[26]. R. Ohhira, D. Ogasahara, and T. Ono, "Novel RZ signal format with alternate-chirp for suppression of nonlinear degradation in 40 Gb/s based WDM," Tech. Dig. OFC01. WM2.

[27]. M. Nissov, J.-X. Cai, M. I. Hayee, A. N. Plilipetskii, S. G. Evangelides Jr, B. Pedersen, N. Ramanujam, C. R. Davidson, C. J. Chen, M. A. Mills, R. Menges, P. C. Corbett, C. Rivers, and N. S. Bergano, "30x20 Gbps transmission over trans-atrantic distance (6200 km) with 31% spectral efficiency," Tech. Dig. OFC00. PD30. SG15 Contribution, COM15-D.329, 2002.

[28]. Y. Miyamoto, K. Yonenaga, A. Hirano, and M. Tomizawa, "Nx40-Gbit/s DWDM transport system using novel return-to-zero formats with modulation bandwidth reduction," IEICE Trans. Commun., vol. E85-B, pp. 374385, 2002.

[29]. T. N. Nielsen, A. J. Stentz, K. Rottwitt, D. S. Vengsarkar, Z. J. Chen, P. B. Hansen, J. H. Park, K. S. Feder, T. A. Strasser, S. Cabot, S. Stulz, D. W. Peckham, L. Hsu, C. K. Kan, A. F. Judy, J. Sulhoff, S. Y. Park, L. E. Nelson, and L. Gruner-Nielsen, "3.28-Tbit/s (82x40 Gb/s) transmission over 3x100 km nonzero-dispersion fiber using dual Cand L-band hybrid Raman/erbium-doped inline amplifiers," Tech. Dig. OFC00, Mar. 2000. PD231.

[30]. Y. Zhu,W. S. Lee, C. Scahill, C. Fludger, D.Watley, M. Jones, J. Homan, B. Shaw, and A. Hadjifotiou, "1.28 Tbit/s (32x40 Gbit/s) transmission over 100 km with only 6 spans," Tech. Dig. *ECOC* 2000.

[31]. K. Fukuchi, T. Kasamatsu, M. Morie, R. Ohhira, T. Ito, K. Sekiya, D. Ogasahara, and T. Ono, "10.92-Tb/s (273x40-Gb/s) triple-band/ultradense WDM optical-repeatered transmission experiment," Tech. Dig. OFC01. PD24.

[32]. K. Yonenaga, A. Matsuura, S. Kuwahara, M. Yoneyama, Y. Miyamoto, K. Hagimoto, and K. Noguchi, "Dispersion-compensation-free 40-Gbit/sx4-channel WDM transmission experiment using zero-dispersion- flattened transmission line," Tech. Dig. OFC 1998, 1998. PD20.

[33]. Chris Xu, Xiang Liu, and Xing Wei, "Comparison of return-to-zero differential phase-shift keying and on-off keying in ling-haul dispersion managed transmission", *IEEE Photonics Technology Letters*, vol. 15, no. 4, pp. 617-619, April 2003

[34]. L. Boivin and G. J. Pendock, B "Receiver sensitivity for optically amplified RZ signals with arbitrary duty cycle," in *Proc. Optical Amplifiers and Their Applications (OAA)*, 1999, Paper ThB4.

[35]. P. J. Winzer and A. Kalmar, B, "Sensitivity enhancement of optical receivers by impulsive coding," *Journal of Lightwave Technology,* vol. 17, no. 2, pp. 171–177, Feb. 1999.

[36]. P. J. Winzer, M. Pfennigbauer, M. M. Strasser, and W. R. Leeb, B, "Optimum filter bandwidths for optically preamplified RZ and NRZ receivers," *Journal of Lightwave Technology*, vol. 19, no. 9, pp. 1263–1273, Sep. 2001.

[37]. W. Idler, A. Klekamp, R. Dischler, J. Lazaro, and A. Konczykowska, B "System performance and tolerances of 43 Gb/s ASK and DPSK modulation formats," in *Proc. Eur. Conf. Optical Communication (ECOC)*, 2003, Paper Th2.6.3.

[38]. A. Hirano, Y. Miyamoto, K. Yonenaga, A. Sano, and H. Toba, "40 Gbit/s l-band transmission experiment using SPM-tolerant carrier-suppressed RZ format," *Electronic Leters.*, vol. 35, no. 25,pp. 2213–2215, 1999.

[39]. D. Penninckx, M. Chbat, and J.-P. Thiery, "The phase-shaped binary transmission (PSBT): A new technique to transmit far beyond the chromatic dispersion limit," *IEEE Photon. Technol. Lett.*, vol. 9, no. 2, pp. 259–261, Feb. 1997.

[40]. J. B. Stark, J. E. Mazo, and R. Laroia, "Phased amplitude-shift signaling (PASS) codes: Increasing the spectral efficiency of DWDM transmission," in *Proc. Eur. Conf. Optical Communication (ECOC)*, 1998, pp. 373–374.

[41]. Hari Shankar, "Duobinary Modulation for Optical systems", http://www.inphi corp.com/products/whitepapers consulted on 11/01/2007

[42]. K. S. Cheng and Jan Conradi, "Reduction of pulse-to-pulse interaction using alternative RZ formats in 40Gb/s systems," *IEEE Photon. Technol. Lett.*, Vol. 14, No. 1, 2002: 98-100.

[43]. T. Franck, P. B. Hansen, T. N. Nielsen, and L. Eskildsen, "Duobinary transmitter with low intersymbol interference," *IEEE Photon. Technol. Lett.*, Vol. 10, No. 4, 1998: 597-599.

[44]. Y. Miyamoto, K. Yonenage, A. hirano, H. Toba, K. murata and H. Miyazawa, "100GHz spaced 8×43Gbit/s DWDM unrepeatered transmission over 163km using dobinary-carrier-suppressed return-to-zero format," *Electron. Lett.*, Vol. 37, No. 23, 2001: 1395-1396.

[45]. D. Breuer and K. Petermann, "Comparison of NRZ- and RZ-modulation format for 40Gb/s TDM standard-fiber systems," *IEEE Photon. Technol. Lett.*, Vol. 9, No. 3, 1997: 398-340.

[46]. J. Yu et al., "10Gb/s transmission over 200km conventional fiber without dispersion compensation using the bias control technique," *IEEE Photon. Technol. Lett.*, Vol. 14, No.12, 2002: 1746-1748.

[47]. J. Yu, "Generation of modified duobinary RZ signals by using one single dual-arm $LiNbO_3$ modulator", *IEEE Photon. Technol. Lett.*, Vol. 15, No. 10, 2003: 1455-1457.

[48]. R. J. S. Pedersen, B. F. Jorgensen, M. Nissov and He Yongqi, "10Gbit/s repeater-less transmission over 250km standard fiber", *Electron. Lett., Vol.* 32, No. 23, 1996: 2155-2156.

[49]. G. Grandpierre, O. Gautheron, L. Pierre, J. –P. Thiery and P. Kretzmeyer, "252km repeater-less 10Gb/s transmission demonstration", *IEEE Photonic Technology Letters* 1993, Vol. 5, No. 5, 531-533.

[50]. H. Maeda, G Funatsu, and A. Naka, "Ultra-long-span 500km 16_10 Gbit/s WDM unrepeatered transmission using RZ-DPSK format", *Electronic Letters*, Vol. 41, No. 1, 2005: 34-35

[51]. M. Haris, Jianjun Yu, and Gee-Kung Chang, " Repeaterless Transmission of 10Gbit/s MD-RZ Signal over 300km SMF-28 by Using Raman Amplification", *IEEE LEOS 2005*, pp. 479-480.

[52]. L Labrunie, P. Bousselet, V Faraci, N Tranvouez, G Sautereau-Martin, "4 x 10Gb/s WDM Unrepeatered Transmission over 525 Km with Third-Order Cascaded Pumping", *ECOC 2005,* pp. 71-72

[53]. M Du, L Nelson, D DiGiovanni, "Unrepeatered Transmission over 300km Non-Zero Dispersion-Shifted Fiber with Bi-Directionally Pumped Raman Amplification", *ECOC 2005,* pp. 75-76

[54]. M. Haris, Jianjun Yu, Gee-Kung Chang "8x10 Gbit/s WDM repeaterless transmission over 240km SMF using modified duobinary RZ signals" *CLEO 2006*, Long Beach, CA, 2006.

[55]. D. Penninckx, "Optical differential phase shift keying (DPSK) direct detection considered as a duobinary signal", *ECOC*, 2001, 456-457

[56]. M. Haris, Jianjun Yu, Gee-Kung Chang, "Analysis of Modified Duobinary RZ Signal Generation Techniques, Transmission and Characteristics" accepted *OECC*, Taiwan, 2006.

[57]. Yannick Keith Lize, "Free spectral range optimization of return-to-zero differential phase shift keyed demodulation in the presence of chromatic dispersion," *Optics Express* , Vol. 15, Issue 11, pp. 6817-6822, 2007

[58]. Christian Malouin, "DPSK Receiver Design-Optical filtering Considerations" *OFC* 2007, paper OThK1

[59]. A. Mikkelsen et al., "Partial DPSK with excellent filter tolerance and OSNR sensitivity," *Electron. Letters* , pp 1363-1364, 2006

[60]. A.H. Gnauck, P.J. Winzer, "Optical Phase-Shift-Keyed Transmission," *Journal of Lightwave Technology*, VOL. 23, NO. 1, January 2005, pp. 115-130.

[61]. Serbay, M., Wree, C., Rosenkranz, W., "Comparison of six different RZ-DQPSK transmitter set-ups regarding their tolerance towards fibre impairments in 8x40Gb/s WDM-systems," *IEEE LEOS* workshop on Advanced modulation formats, 2004, 00. 9-10

[62]. Hoon Kim, Peter J. Winzer, "Robustness to Laser Frequency Offset in Direct-Detection DPSK and DQPSK Systems*," Journal of Lightwave Technology*, VOL. 21, NO. 9, September 2003, pp. 1887-1891.

[63]. R. A. Griffin, "Optical Differential Quadrature Phase-Shift Key (oDQPSK) for High Capacity Optical Transmission", *OFC 2002*, Anaheim, USA

[64]. M. Haris, Jianjun Yu, Gee-Kung Chang, "Optimal RZ Modulation Format for 40 Gb/s Transmission Systems" accepted, *OECC* , Taiwan, 2006.

[65]. Serbay, M.; Wree, C.; Rosenkranz, "Implementation of differential precoder for high-speed optical DQPSK transmission" *Electronics Letters*, Volume 40, Issue 20, 2004 , 1288 – 1289

[66]. Yang J. Wen, Nirmalathas; Dong-Soo Lee; **"**RZ/CSRZ-DPSK and chirped NRZ signal generation using a single-stage dual-electrode Mach-Zehnder modulator," *IEEE Photonics Technology Letters*, Vol. 16, pp 2466-2468, 2004.

[67]. T. Nielsen and S. Chandrasekhar, "OFC 2004 workshop on optical and electronic mitigation of impairments," J. Lightw. Technol., vol. 23, no. 1, pp. 131–142, Jan. 2005.

[68]. D. Castagnozzi, B "Digital signal processing and electronic equalization (EE) of ISI," in Proc. Optical Fiber Communication Conf. (OFC), 2004, Paper WM6.

[69]. A. Fa¨rbert, S. Langenbach, N. Stojanovic, C. Dorschky, T. Kupfer, C. Schulien, J.-P. Elbers, H. Wernz, H. Griesser, and C. Glingener, "Performance of a 10.7-Gb/s receiver with digital equalizer using maximum likelihood sequence estimation," in Proc. Eur. Conf. Optical Communication (ECOC), 2004, Paper Th4.1.5.

[70]. T. Mizuochi, K. Kubo, H. Yoshida, H. Fujita, H. Tagami, M. Akita, and K. Motoshima, "Next generation FEC for optical transmission systems," in Proc. Optical Fiber Communication Conf. (OFC), 2003, Paper ThN1.

[71]. D. McGhan, C. Laperle, A. Savchenko, C. Li, G. Mak, and M. O'Sullivan, "5120 km RZ-DPSK transmission over G.652 fiber at 10 Gb/s with no optical dispersion compensation," in Proc. Optical Fiber Communication Conf. (OFC), 2005, Paper PDP27.

[72]. A. H. Gnauck, J. Sinsky, P. J. Winzer, and S. Chandrasekhar, "Linear microwave domain dispersion compensation of 10-Gb/s signals using heterodyne detection," in Proc. Optical Fiber Communication Conf. (OFC), 2005, Paper PDP31.

[73]. S. Tsukamoto, D.-S. Ly-Gagnon, K. Katoh, and K. Kikuchi, "Coherent demodulation of 40-Gbit/s polarization-multiplexed QPSK signals with 16-GHz spacing after 200-km transmission," in Proc. Optical Fiber Communication Conf. (OFC), 2005, Paper PDP29.